應用 GYC 部分區域穩定理論於新 Froude-Duffing 系統之廣義同步與控制，以 Bessel 函數為參數的 Rössler 系統之超渾沌，陰陽 Rössler 系統的渾沌及實用混合投影廣義同步

學生：徐瑜韓　　指導教授：戈正銘

摘要

本篇論文以相圖、龐卡萊映射圖、Lyapunov 指數、分歧圖等數值方法研究新 Froude-Duffing 系統的渾沌現象。更進一步使用 GYC 部分區域穩定理論來研究系統的廣義渾沌同步和渾沌控制。另外，將探討 Rössler 系統以 Bessel function 為參數所激發出的超渾沌行為。最後，對於陰 Rössler 系統的渾沌現象做歷史研究，並應用實用漸進穩定性理論和適應性控制法則來達成與陽 Rössler 系統的混合投影渾沌廣義同步。

Chaos Generalized Synchronization and Control of New Froude-Duffing System by GYC Partial Region Stability Theory Hyperchaos of Rössler System with Bessel Function Parameters, and Projective Yin-Yang Generalized Synchronization by Pragmatical Asymptotically Stability Theorem

Student: Ui-Han Hsu **Advisor: Zheng-Ming Ge**

ABSTRACT

In this thesis, the chaotic behavior in a new Froude-Duffing System is studied by phase portraits, time history, Poincaré maps, Lyapunov exponent and bifurcation diagrams. A new method, using GYC partial region stability theory, is studied for chaos synchronization and chaos control. Hyperchaos of a Rössler System with Bessel Function Parameters is studied. A new kind of chaotic generalized synchronization system, hybrid projective Yin-Yang generalized synchronization (HPYYGS), is obtained by pragmatical asymptotical stability theorem and adaptive control law. Numerical analyses, such as phase portraits and time histories can be provided to verify the effectiveness in all above studies.

誌謝

本篇論文得以順利完成，首先要感謝指導老師戈正銘兩年來不遺餘力的悉心教導。老師對於研究科學以及追求新知的熱誠，讓我了解到 ，從事研究工作，也如同在未知叢林中漫步、探索一樣，是那麼的有趣且值得的。同時也了解到學問如同生命一般是種長期而持續的累積過程，在此我要對老師致上我最高的敬意。

在交大兩年的碩士生涯中，我要感謝實驗室的所有學長特別是博士班的張晉銘、李仕宇學長，碩士班的李彥賢、許凱銘、何俊諺、江峻宇、陳聰文學長，不僅在我研究出現困難時給予我寶貴指導同時也跟我分享許多求學歷程讓我受益良多，在此也要感謝我的同學陳志銘與張育銘，在學業與研究進度上的討論與幫忙，讓我能順利的突破許多瓶頸。另外還要感謝學弟蔡尚恩、李泳厚、江振賓、王翔平幫忙處理繁瑣雜事，使我們的研究得以專心完成。此外我還要感謝在我求學路上所有教過我的老師，默默支持我的好朋友們，無法一一列名，在此一併致謝。

最後，感謝我的父親徐源蓬先生、母親邱瓊霞女士不計代價的為我付出跟栽培，讓我得以一路順利求學，攻讀碩士學位，感謝弟弟徐瑜聰、妹妹徐瑜鎂你們帶給家庭的愉樂氣氛，使我感覺到家的溫暖，在此也謝謝女友高芸蘋小姐對我的支持鼓勵與陪伴我度過不少生命中的重要時刻。最後僅以此論文獻給你們大家。

CONTENTS

LIST OF FIGURS

Chapter 1

Introduction

A large number of studies have shown that chaotic phenomena are observed in many physical nonlinear systems [1,2]. It was also reported that the chaos occurred in many nonlinear control systems [3,4]. Since chaos control was firstly achieved by Huber in 1989 [5], it has attracted a great deal of attention from various fields. Chaos is desirable in some systems, such as chemical reactions, power converters, biological systems, information processing, secure communications, etc. [6-13]. Numerous linear and nonlinear control methods have been employed in controlling chaos[14-22]. In the last few years, synchronization in chaotic dynamic system is a very interesting problem and has been widely studied [23-34]. Most of them are based on the exact knowledge of the system structure and all parameters. But in practice, some or all of the system parameters are uncertain. Additionally, these parameters change with time. Among many kinds of synchronizations, the generalized synchronization is investigated in this paper. It means that there exists a given functional relationship between the state vector **x** of the master and the state vector y of the slave $\mathbf{y} = G(\mathbf{x})$.

In Chinese philosophy[35-37], *Yin* and *Yang* are two fundamental opposites. In other words, just like there are two sides of a coin. *Yin* is the negative, historical or feminine principle in nature, and *yang* is the positive, contemporary or masculine principle in nature. There are many articles about Yang Rössler system have been reported [38-40]. In this thesis, we find there are rich chaotic dynamics in Yin Rössler system in the first time[41].

This thesis is organized as follows. In Chapter 2 and Chapter 3, a new strategy to achieve chaos generalized synchronization and chaos control by GYC partial region stability theory(Appendix A,B) is proposed [42-44]. Via using the GYC partial region

stability theory the new Lyapunov function is a simple linear homogeneous function of error states and the controllers are of lower degree than that of controllers by using traditional Lyapunov asymptotical stability theorem.

In Chapter 4, our study is devoted to a Rössler System with Bessel function parameters. Chaotic system features that it has complex dynamical behaviors and sensitive behavior of dependence on initial conditions. In recent years, there are many hyperchaotic systems have been reported [45-49]. The purpose of this work is to present a Rössler system, which is shown to be hyperchaos in a wide range of Bessel function parameters. It is found that both hyperchaos and chaos are abundant and give various applications, especially for secret communication. Numerical experiments such as phase portraits, bifurcation diagrams, Lyapunov exponent diagrams, parameter diagrams and Poincaré maps are shown.

In Chapter 5, the purpose is to introduce the Yin Rössler system and to investigate the chaotic behavior with *Yin* parameters by phase portrait, Lyapunov exponents and bifurcation diagrams in simulation results. We use positive, i.e. *Yang*, parameters for the Yang Rössler system, and negative, i.e. *Yin*, parameters for the Yin Rössler system.

In Chapter 6, pragmatical asymptotically stability theorem is proposed to achieve adaptive synchronization from Yin to Yang Rössler chaos. In current scheme of adaptive synchronization, traditional Lyapunov stability theorem and Barbalat lemma are used to prove that the error vector approaches zero as time approaches infinity, but the question is that why those estimated parameters also approach the uncertain values remains no answer[50-53]. In this article, pragmatical asymptotically stability theorem and an assumption of equal probability for ergodic initial conditions [54-55] are used to prove strictly that those estimated parameters approach the uncertain values. Moreover, traditional adaptive chaos synchronization in general is limited for

the same system.

Chapter 2

Chaos Generalized Synchronization of a New Froude-Duffing System by GYC Partial Region Stability Theory

2.1 Preliminaries

A new strategy via using GYC partial region stability theory is proposed to achieve chaos generalized synchronization. In this Chapter, two identical new Froude-Duffing systems are used as master system and slave system respectively. The Lyapunov function can be treated as a simple linear homogeneous function of error states by using the GYC partial region stability theory, and the controllers are in lower degree than that of traditional controllers, so less simulation error is introduced. Numerical simulations are given to verify the effectiveness of this strategy.

2.2 Generalized Chaos Synchronization Strategy

Consider the following unidirectional coupled chaotic systems

$$\begin{aligned} \dot{\mathbf{x}} &= \mathbf{f}(t, \mathbf{x}) \\ \dot{\mathbf{y}} &= \mathbf{h}(t, \mathbf{y}) + \mathbf{u} \end{aligned} \tag{2-1}$$

where $\mathbf{x} = [x_1, x_2, \cdots, x_n]^T \in R^n$, $\mathbf{y} = [y_1, y_2, \cdots, y_n]^T \in R^n$ denote the master state vector and slave state vector respectively, $\mathbf{f}$ and $\mathbf{h}$ are nonlinear vector functions, and $\mathbf{u} = [u_1, u_2, \cdots, u_n]^T \in R^n$ is a control input vector.

The generalized synchronization can be accomplished when $t \to \infty$, the limit of the error vector $\mathbf{e} = [e_1, e_2, \cdots, e_n]^T$ approaches zero:

$$\lim_{t \to \infty} \mathbf{e} = 0 \tag{2-2}$$

where

$$\mathbf{e} = \mathbf{G}(\mathbf{x}) - \mathbf{y} \tag{2-3}$$

$\boldsymbol{G}(\boldsymbol{x})$ is a given function of $\boldsymbol{x}$.

By using the partial region stability theory, the Lyapunov function is linear homogeneous function of error states. The controllers can be designed in lower degree.

2.3 Chaos of a New Froude-Duffing System

A new Froude-Duffing system is introduced. Froude equation [28] and Duffing equation are two typical nonlinear non-autonomous systems:

$$\begin{cases} \dfrac{dx_1}{dt} = x_2 \\ \dfrac{dx_2}{dt} = (a - bx_2^{\,2})x_2 + c\sin x_1 + d\cos \omega t \end{cases} \tag{2-4}$$

$$\begin{cases} \dfrac{dx_3}{dt} = x_4 \\ \dfrac{dx_4}{dt} = -x_3 - x_3^3 - fx_4 + g\sin \omega t \end{cases} \tag{2-5}$$

Exchanging cosωt in Eq. (2-4) with x_3x_4 and sinωt in Eq. (2-5) with x_1x_2, we obtain a new autonomous Froude-Duffing system:

$$\begin{cases} \dfrac{dx_1}{dt} = x_2 \\ \dfrac{dx_2}{dt} = (a - bx_2^{\,2})x_2 + c\sin x_1 + dx_3x_4 \\ \dfrac{dx_3}{dt} = x_4 \\ \dfrac{dx_4}{dt} = -x_3 - x_3^{\,3} - fx_4 + gx_1x_2 \end{cases} \tag{2-6}$$

where *a, b, c, d, g, f* are parameters. This system exhibits chaos when the parameters of system are $a = 0.35,\ b = 0.1,\ c = 1,\ d = 0.48,\ g = 0.25,\ f = 0.002$ and the initial states of system are $x_1(0) = 2, x_2(0) = 2.4, x_3(0) = 5,\ x_4(0) = 6$. Its phase portrait, time histories , Lyapunov exponents, bifurcation diagram, power spectram are shown in Fig2.1, Fig2.2, Fig2.3 and Fig2.4.

2.4 Numerical Simulationsll

Two Froude-Duffing systems with unidirectional coupling are given:

$$\begin{cases} \dfrac{dx_1}{dt} = x_2 \\ \dfrac{dx_2}{dt} = (a - bx_2^{\,2})x_2 + c\sin x_1 + dx_3x_4 \\ \dfrac{dx_3}{dt} = x_4 \\ \dfrac{dx_4}{dt} = -x_3 - x_3^{\,3} - fx_4 + gx_1x_2 \end{cases} \tag{2-7}$$

$$\begin{cases} \dfrac{dy_1}{dt} = y_2 + u_1 \\ \dfrac{dy_2}{dt} = (a - by_2^{\,2})y_2 + c\sin y_1 + dy_3y_4 + u_2 \\ \dfrac{dy_3}{dt} = y_4 + u_3 \\ \dfrac{dy_4}{dt} = -y_3 - y_3^{\,3} - fy_4 + gy_1y_2 + u_4 \end{cases} \tag{2-8}$$

where Eq.(2-7)is the master, Eq,(2-8) is the slave.

CASE I. The generalized synchronization error function is

$$e_i = x_i - y_i + 80, \qquad i = 1,\ 2,\ 3,\ 4 \tag{2-9}$$

The addition of the constant 80 makes the error dynamics always happens in the first quadrant. Our goal is $y_i = x_i + 80$, i.e.

$$\lim_{t\to\infty} e_i = \lim_{t\to\infty}(x_i - y_i + 80) = 0, \qquad i = 1,\ 2,\ 3,\ 4 \tag{2-10}$$

$$\dot{e}_i = \dot{x}_i - \dot{y}_i, \qquad i = 1,\ 2,\ 3,\ 4 \tag{2-11}$$

By Eq.(2-7),(2-8),the error dynamics becomes

$$\begin{cases} \dot{e}_1 = \dot{x}_1 - \dot{y}_1 = x_2 - y_2 - u_1 \\ \dot{e}_2 = \dot{x}_2 - \dot{y}_2 = (a - bx_2^{\,2})x_2 + c\sin x_1 + dx_3x_4 - \left((a - by_2^{\,2})y_2 + c\sin y_1 + dy_3y_4\right) - u_2 \\ \dot{e}_3 = \dot{x}_3 - \dot{y}_3 = x_4 - y_4 - u_3 \\ \dot{e}_4 = \dot{x}_4 - \dot{y}_4 = -x_3 - x_3^{\,3} - fx_4 + gx_1x_2 - \left(-y_3 - y_3^{\,3} - fy_4 + gy_1y_2 + u_4\right) - u_4 \end{cases} \tag{2-12}$$

Let initial states be $(x_{10}, x_{20}, x_{30}, x_{40})$= (2, 2.4, 5, 6), $(y_{10}, y_{20}, y_{30}, y_{40})$= (3, 3.2, 6.8, 5.5) and system parameters $a = 0.35,\ b = 0.1,\ c = 1,\ d = 0.48,\ g = 0.25,\ f = 0.002$, we find that the error dynamic always exists in first quadrant as shown in Fig. 2.5. By GYC partial region asymptotical stability theorem, one can choose a Lyapunov function in the form of a positive definite function in first quadrant:

$$V = e_1 + e_2 + e_3 + e_4 \tag{2-13}$$

By Eq.(2-11),its time derivative is

$$\begin{aligned}\dot{V} &= \dot{e}_1 + \dot{e}_2 + \dot{e}_3 + \dot{e}_4 \\ &= \left(x_2 - y_2 - u_1\right) \\ &\quad + \left((a - bx_2^{\,2})x_2 + c\sin x_1 + dx_3x_4 - \left((a - by_2^{\,2})y_2 + c\sin y_1 + dy_3y_4\right) - u_2\right) \\ &\quad + \left(x_4 - y_4 - u_3\right) \\ &\quad + \left(-x_3 - x_3^{\,3} - fx_4 + gx_1x_2 - \left(-y_3 - y_3^{\,3} - fy_4 + gy_1y_2 + u_4\right) - u_4\right)\end{aligned} \tag{2-14}$$

Choose

$$\begin{cases} u_1 = x_2 - y_2 + e_1 \\ u_2 = (a - bx_2^{\,2})x_2 + c\sin x_1 + dx_3x_4 - \left((a - by_2^{\,2})y_2 + c\sin y_1 + dy_3y_4\right) + e_2 \\ u_3 = x_4 - y_4 + e_3 \\ u_4 = -x_3 - x_3^{\,3} - fx_4 + gx_1x_2 - \left(-y_3 - y_3^{\,3} - fy_4 + gy_1y_2\right) + e_4 \end{cases} \tag{2-15}$$

We obtain

$$\dot{V} = -e_1 - e_2 - e_3 - e_4 < 0 \tag{2-16}$$

which is negative definite function in the first quadrant. Four state errors versus time and time histories of states are shown in Fig. 2.6 and Fig. 2.7.

CASE II. The generalized synchronization error function is

$$e_i = x_i - y_i + F\sin\omega t + 80, \qquad i = 1,\ 2,\ 3,\ 4 \tag{2-17}$$

Our goal is $y = x + F\sin\omega t + 80$, i.e.

$$\lim_{t\to\infty} e_i = \lim_{t\to\infty}(x_i - y_i + F\sin\omega t + 80) = 0, \qquad i = 1,\ 2,\ 3,\ 4 \tag{2-18}$$

$$\dot{e}_i = \dot{x}_i - \dot{y}_i + F\omega\cos\omega t, \qquad i = 1,\ 2,\ 3,\ 4 \tag{2-19}$$

The error dynamics becomes

$$\begin{cases} \dot{e}_1 = x_2 + F\omega\cos\omega t - y_2 - u_1 \\ \dot{e}_2 = (a - bx_2^{\,2})x_2 + c\sin x_1 + dx_3x_4 - \left((a - by_2^{\,2})y_2 + c\sin y_1 + dy_3y_4\right) + F\omega\cos\omega t - u_2 \\ \dot{e}_3 = x_4 + F\omega\cos\omega t - y_4 - u_3 \\ \dot{e}_4 = -x_3 - x_3^{\,3} - fx_4 + gx_1x_2 - \left(-y_3 - y_3^{\,3} - fy_4 + gy_1y_2 + u_4\right) + F\omega\cos\omega t - u_4 \end{cases} \tag{2-20}$$

Let initial states be $(x_{10}, x_{20}, x_{30}, x_{40}) = (2,\ 2.4,\ 5,\ 6)$, $(y_{10}, y_{20}, y_{30}, y_{40}) = (3,\ 3.2,\ 6.8,\ 5.5)$ and system parameters $a = 0.35,\ b = 0.1,\ c = 1,\ d = 0.48,\ g = 0.25,\ f = 0.002,$ $F = 3$ and $\omega = 0.3$, we find the error dynamics always exists in first quadrant as shown in Fig. 2.8. By GYC partial region asymptotical stability theorem, one can choose a Lyapunov function in the form of a positive definite function in first quadrant:

$$V = e_1 + e_2 + e_3 + e_4 \tag{2-21}$$

By Eq.(2-18),its time derivative is

$$\begin{aligned} \dot{V} = {} & \left(x_2 + F\omega\cos\omega t - y_2 - u_1\right) + (a - bx_2^{\,2})x_2 + c\sin x_1 + dx_3x_4 \\ & - \left((a - by_2^{\,2})y_2 + c\sin y_1 + dy_3y_4\right) + F\omega\cos\omega t - u_2 \\ & + \left(x_4 + F\omega\cos\omega t - y_4 - u_3\right) - x_3 - x_3^{\,3} - fx_4 + gx_1x_2 \\ & - \left(-y_3 - y_3^{\,3} - fy_4 + gy_1y_2 + u_4\right) + F\omega\cos\omega t - u_4 \end{aligned} \tag{2-22}$$

Choose

$$\begin{cases} u_1 = x_2 + F\omega\cos\omega t - y_2 + e_1 \\ u_2 = (a - bx_2^{\,2})x_2 + c\sin x_1 + dx_3x_4 - \left((a - by_2^{\,2})y_2 + c\sin y_1 + dy_3y_4\right) \\ \qquad + F\omega\cos\omega t + e_2 \\ u_3 = x_4 + F\omega\cos\omega t - y_4 + e_3 \\ u_4 = -x_3 - x_3^{\,3} - fx_4 + gx_1x_2 - \left(-y_3 - y_3^{\,3} - fy_4 + gy_1y_2\right) \\ \qquad + F\omega\cos\omega t + e_4 \end{cases} \tag{2-23}$$

We obtain

$$\dot{V} = -e_1 - e_2 - e_3 - e_4 < 0 \tag{2-24}$$

which is negative definite function in first quadrant. Four state errors versus time and time histories of states are shown in Fig. 2.9 and Fig. 2.10.

CASE III. The generalized synchronization error function is

$$e_i = x_i \sin x_i - y_i + 80, \qquad i = 1,\ 2,\ 3,\ 4 \tag{2-25}$$

Our goal is $y_i = x_i \sin x_i + 80$, i.e.

$$\lim_{t\to\infty} e_i = \lim_{t\to\infty}(x_i \sin x_i - y_i + 80) = 0, \qquad i = 1,2,3,4 \tag{2-26}$$

$$\dot{e}_i = \dot{x}_i \sin x_i + x_i \dot{x}_i \cos x_i - \dot{y}_i, \qquad i = 1,\ 2,\ 3,\ 4 \tag{2-27}$$

The error dynamics become

$$\begin{cases} \dot{e}_1 = x_2 \sin x_1 + x_1 x_2 \cos x_1 - y_2 - u_1 \\ \dot{e}_2 = \left((a - bx_2^{\,2})x_2 + c\sin x_1 + dx_3 x_4\right)\sin x_2 + \left((a - bx_2^{\,2})x_2 + c\sin x_1 + dx_3 x_4\right)x_2 \cos x_2 \\ \qquad -\left((a - by_2^{\,2})y_2 + c\sin y_1 + dy_3 y_4\right) - u_2 \\ \dot{e}_3 = x_4 \sin x_3 + x_3 x_4 \cos x_3 - y_4 - u_3 \\ \dot{e}_4 = \left(-x_3 - x_3^{\,3} - fx_4 + gx_1 x_2\right)\sin x_4 + \left(-x_3 - x_3^{\,3} - fx_4 + gx_1 x_2\right)x_4 \cos x_4 \\ \qquad -\left(-y_3 - y_3^{\,3} - fy_4 + gy_1 y_2\right) - u_4 \end{cases} \tag{2-28}$$

Let initial states be $(x_{10}, x_{20}, x_{30}, x_{40}) = (2,\ 2.4,\ 5,\ 6)$, $(y_{10}, y_{20}, y_{30}, y_{40}) = (3,\ 3.2,\ 6.8,\ 5.5)$ and system parameters $a = 0.35,\ b = 0.1,\ c = 1,\ d = 0.48,\ g = 0.25,\ f = 0.002$, we find the error dynamics always exists in first quadrant as shown in Fig. 2.11. By GYC partial region asymptotical stability theorem, one can choose a Lyapunov function in the form of a positive definite function in first quadrant:

$$V = e_1 + e_2 + e_3 + e_4 \tag{2-29}$$

Its time derivative is

$$\begin{aligned}\dot{V} &= \left(x_2 \sin x_1 + x_1 x_2 \cos x_1 - y_2 - u_1\right) + \left((a - bx_2{}^2)x_2 + c \sin x_1 + dx_3 x_4\right) \sin x_2 \\ &+ \left((a - bx_2{}^2)x_2 + c \sin x_1 + dx_3 x_4\right) x_2 \cos x_2 - \left((a - by_2{}^2)y_2 + c \sin y_1 + dy_3 y_4\right) - u_2 \\ &+ \left(x_4 \sin x_3 + x_3 x_4 \cos x_3 - y_4 - u_3\right) + \left(-x_3 - x_3{}^3 - fx_4 + gx_1 x_2\right) \sin x_4 \\ &+ \left(-x_3 - x_3{}^3 - fx_4 + gx_1 x_2\right) x_4 \cos x_4 - \left(-y_3 - y_3{}^3 - fy_4 + gy_1 y_2\right) - u_4\end{aligned} \tag{2-30}$$

Choose

$$\begin{cases} u_1 = x_2 \sin x_1 + x_1 x_2 \cos x_1 - y_2 + e_1 \\ u_2 = \left((a - bx_2{}^2)x_2 + c \sin x_1 + dx_3 x_4\right) \sin x_2 + \left((a - bx_2{}^2)x_2 + c \sin x_1 + dx_3 x_4\right) x_2 \cos x_2 \\ \quad - \left((a - by_2{}^2)y_2 + c \sin y_1 + dy_3 y_4\right) + e_2 \\ u_3 = x_4 \sin x_3 + x_3 x_4 \cos x_3 - y_4 + e_3 \\ u_4 = \left(-x_3 - x_3{}^3 - fx_4 + gx_1 x_2\right) \sin x_4 + \left(-x_3 - x_3{}^3 - fx_4 + gx_1 x_2\right) x_4 \cos x_4 \\ \quad - \left(-y_3 - y_3{}^3 - fy_4 + gy_1 y_2\right) + e_4 \end{cases} \tag{2-31}$$

We obtain

$$\dot{V} = -e_1 - e_2 - e_3 - e_4 < 0 \tag{2-32}$$

which is negative definite function in first quadrant. Four state errors versus time and time histories of states are shown in Fig. 2.12 and Fig. 2.13.

CASE IV. The generalized synchronization error function is

$$e_i = x_i^2 - y_i + z_i^2 + 80, \qquad i = 1,\ 2,\ 3,\ 4 \tag{2-33}$$

$z = \begin{bmatrix} z_1 & z_2 & z_3 & z_4 \end{bmatrix}^T$ is the state vector of generalized Lorenz system.

The goal system for synchronization is generalized Lorenz system and initial states is (1, 1, 1, 1), system parameters $a_1 = 1,\ b_1 = 26,\ c_1 = 0.7,\ d_1 = 1.5$.

$$\begin{cases} \dot{z}_1 = a_1\left(z_2 - z_1\right) + d_1 z_4 \\ \dot{z}_2 = b_1 z_2 - z_1 z_3 - z_2 \\ \dot{z}_3 = z_1 z_2 - c_1 z_3 \\ \dot{z}_4 = -z_1 - a_1 z_4 \end{cases} \tag{2-34}$$

We have

$$\lim_{t\to\infty} e_i = \lim_{t\to\infty}(x_i^2 - y + z_i^2 + 80) = 0, \qquad i = 1,\ 2,\ 3,\ 4 \tag{2-35}$$

$$\dot{e}_i = 2x_i\dot{x}_i - \dot{y}_i + 2z_i\dot{z}_i, \qquad i = 1,\ 2,\ 3,\ 4 \tag{2-36}$$

The error dynamics becomes

$$\begin{cases} \dot{e}_1 = 2x_1x_2 - y_2 + 2z_1\left(a_1\left(z_2 - z_1\right) + d_1z_4\right) - u_1 \\ \dot{e}_2 = 2x_2\left((a - bx_2{}^2)x_2 + c\sin x_1 + dx_3x_4\right) - \left((a - by_2{}^2)y_2 + c\sin y_1 + dy_3y_4\right) \\ \qquad + 2z_2\left(b_1z_2 - z_1z_3 - z_2\right) - u_2 \\ \dot{e}_3 = 2x_3x_4 - y_4 + 2z_3\left(z_1z_2 - c_1z_3\right) - u_3 \\ \dot{e}_4 = 2x_4\left(-x_3 - x_3{}^3 - fx_4 + gx_1x_2\right) - \left(-y_3 - y_3{}^3 - fy_4 + gy_1y_2 + u_4\right) \\ \qquad + 2z_4\left(-z_1 - a_1z_4\right) - u_4 \end{cases} \tag{2-37}$$

Let initial states be $(x_{10}, x_{20}, x_{30}, x_{40})$= (2, 2.4, 5, 6), $(y_{10}, y_{20}, y_{30}, y_{40})$= (3, 3.2, 6.8, 5.5) and system parameters $a = 0.35,\ b = 0.1,\ c = 1,\ d = 0.48,\ g = 0.25,\ f = 0.002$, we find the error dynamics always exists in first quadrant as shown in Fig. 2.14. By GYC partial region asymptotical stability theorem, one can choose a Lyapunov function in the form of a positive definite function in first quadrant:

$$V = e_1 + e_2 + e_3 + e_4 \tag{2-38}$$

Its time derivative is

$$\begin{aligned} \dot{V} = {} & \left(2x_1x_2 - y_2 + 2z_1\left(a_1\left(z_2 - z_1\right) + d_1z_4\right) - u_1\right) + 2x_2\left((a - bx_2{}^2)x_2 + c\sin x_1 + dx_3x_4\right) \\ & - \left((a - by_2{}^2)y_2 + c\sin y_1 + dy_3y_4\right) + 2z_2\left(b_1z_2 - z_1z_3 - z_2\right) - u_2 \\ & + \left(2x_3x_4 - y_4 + 2z_3\left(z_1z_2 - c_1z_3\right) - u_3\right) + 2x_4\left(-x_3 - x_3{}^3 - fx_4 + gx_1x_2\right) \\ & - \left(-y_3 - y_3{}^3 - fy_4 + gy_1y_2\right) + 2z_4\left(-z_1 - a_1z_4\right) - u_4 \end{aligned} \tag{2-39}$$

Choose

$$\begin{cases} u_1 = 2x_1x_2 - y_2 + 2z_1\left(a_1\left(z_2 - z_1\right) + d_1z_4\right) + e_1 \\ u_2 = 2x_2\left((a - bx_2{}^2)x_2 + c\sin x_1 + dx_3x_4\right) - \left((a - by_2{}^2)y_2 + c\sin y_1 + dy_3y_4\right) \\ \qquad + 2z_2\left(b_1z_2 - z_1z_3 - z_2\right) + e_2 \\ u_3 = 2x_3x_4 - y_4 + 2z_3\left(z_1z_2 - c_1z_3\right) + e_3 \\ u_4 = 2x_4\left(-x_3 - x_3{}^3 - fx_4 + gx_1x_2\right) - \left(-y_3 - y_3{}^3 - fy_4 + gy_1y_2\right) \\ \qquad + 2z_4\left(-z_1 - a_1z_4\right) + e_4 \end{cases} \tag{2-40}$$

We obtain

$$\dot{V} = -e_1 - e_2 - e_3 - e_4 < 0 \tag{2-41}$$

which is negative definite function in first quadrant. Four state errors versus time and time histories of states are shown in Fig. 2.15 and Fig. 2.16.

2.5 Summary

In this Chapter, a new strategy by using GYC partial region stability theory is proposed to achieve chaos generalized synchronization. By using the GYC partial region stability theory, the Lyapunov function is only a linear homogeneous function of error states and the controllers are of lower degree than that of controllers by using traditional Lyapunov asymptotical stability theorem. The lower degree controllers are more simple and introduce less simulation error. The new Froude-Duffing system and generalized Lorenz system are used in simulation examples which verify the effectiveness of the proposed scheme.

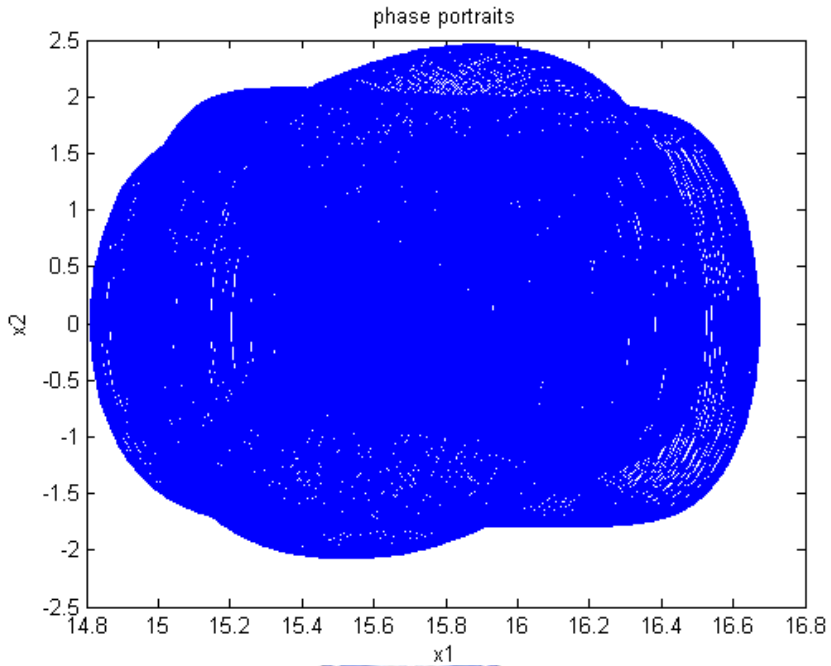

(a)

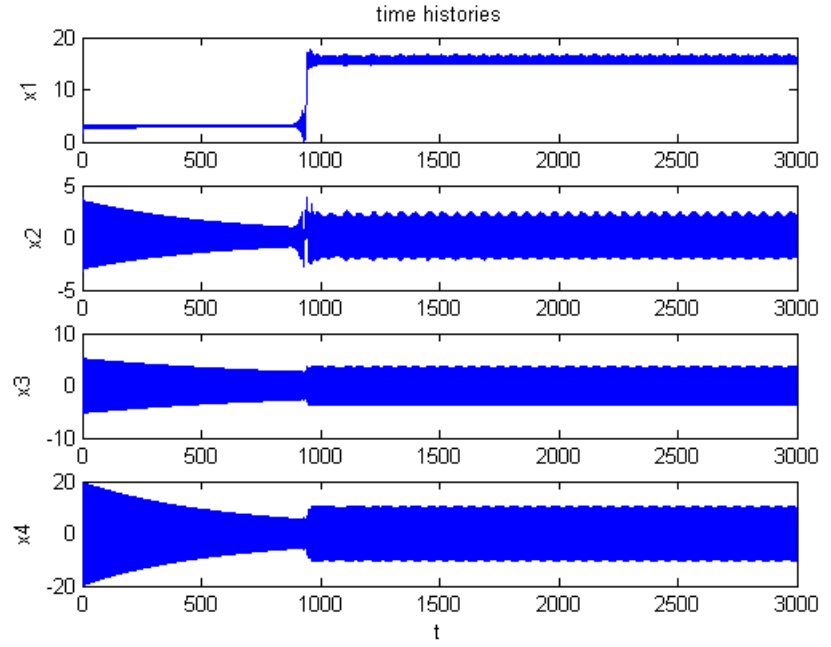

(b)

Fig. 2.1 Chaos of a new Froude-Duffing system: (a) Phase portrait (b) Time histories.

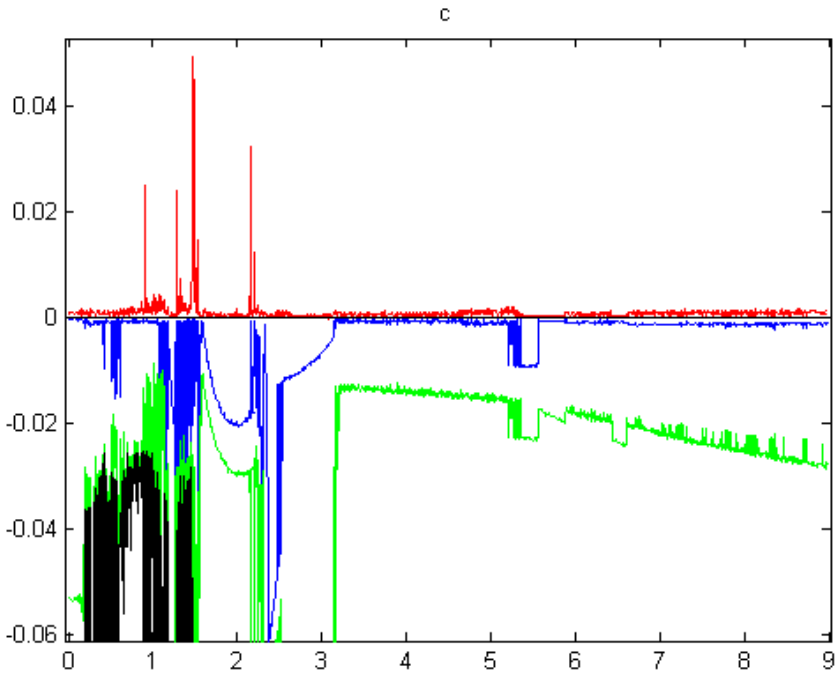

Fig. 2.2 The Lyapunov exponents for a new Froude-Duffing system.

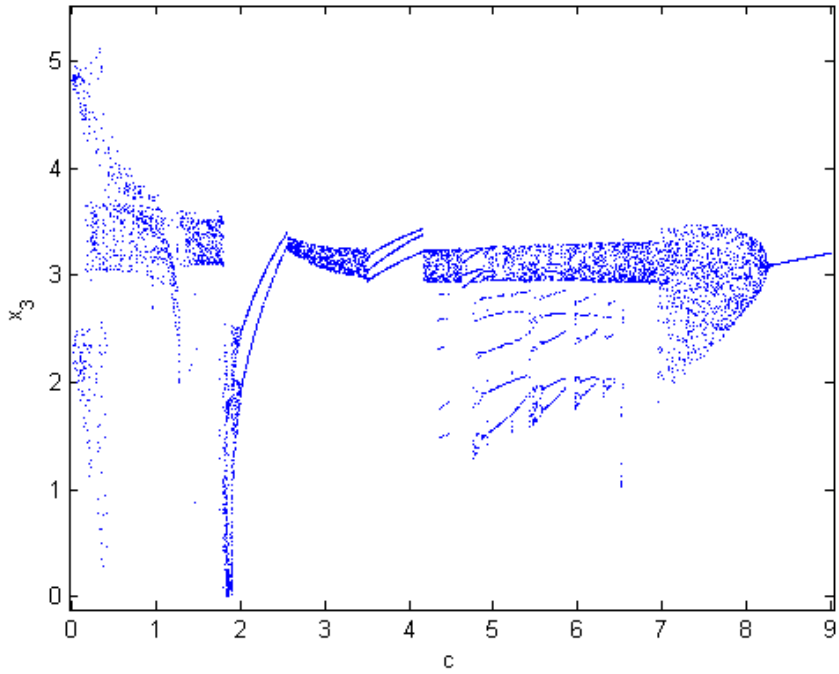

Fig. 2.3 The bifurcation diagram for a new Froude-Duffing system.

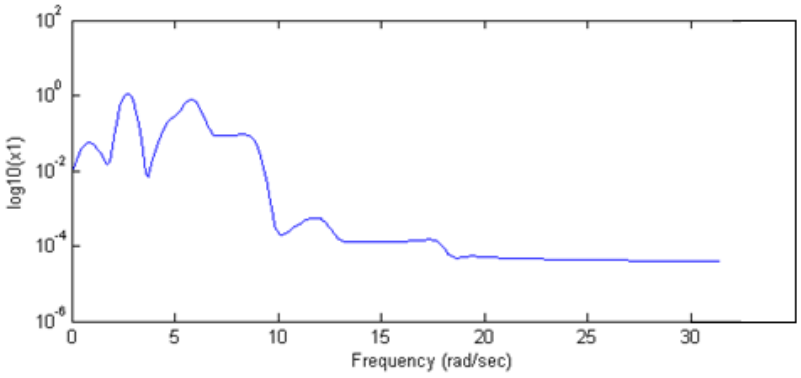

Fig. 2.4 The Power spectra for a new Froude-Duffing system.

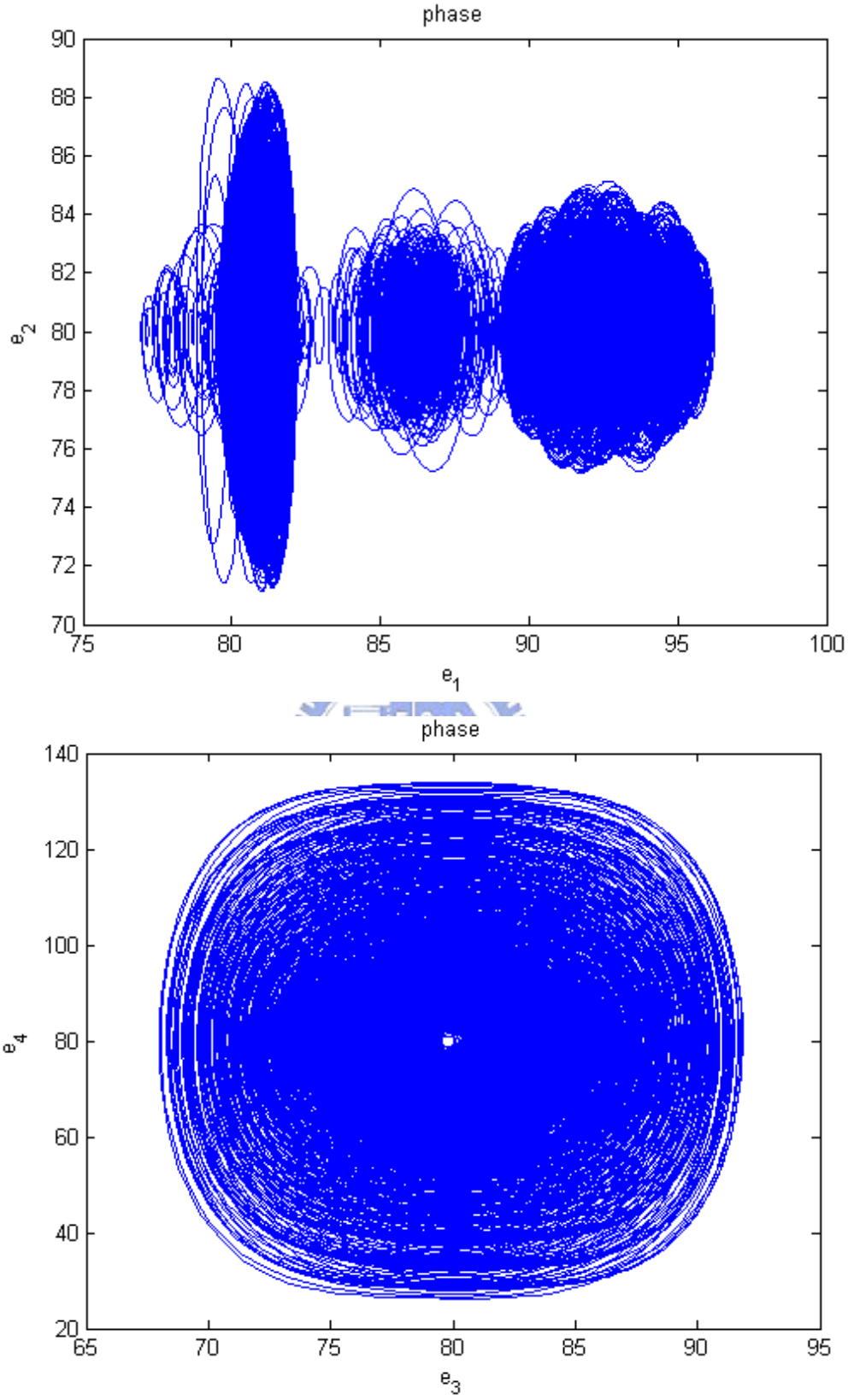

Fig. 2.5 Phase portraits of error dynamics for Case I.

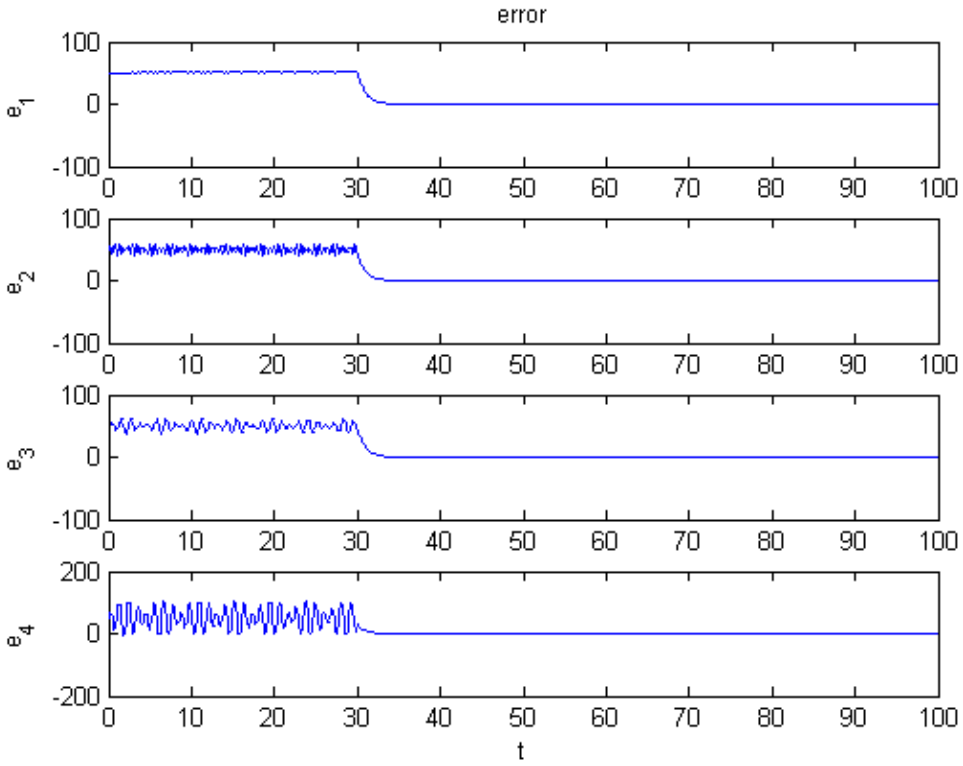

Fig. 2.6 Time histories of errors for Case I.

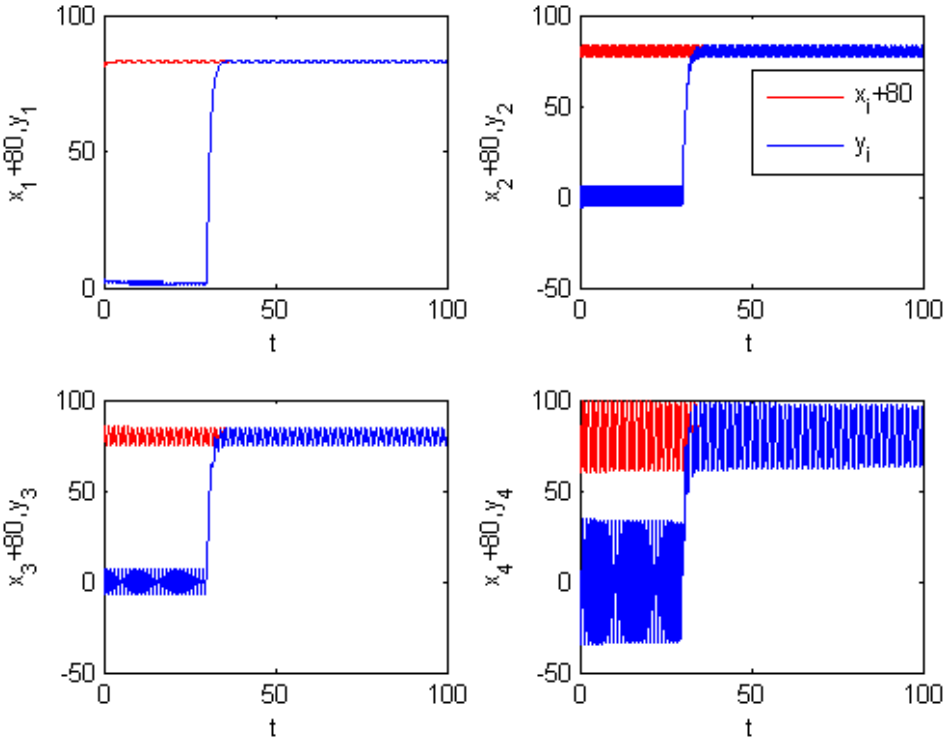

Fig. 2.7 Time histories of $x_i + 80$ and y_i for Case I.

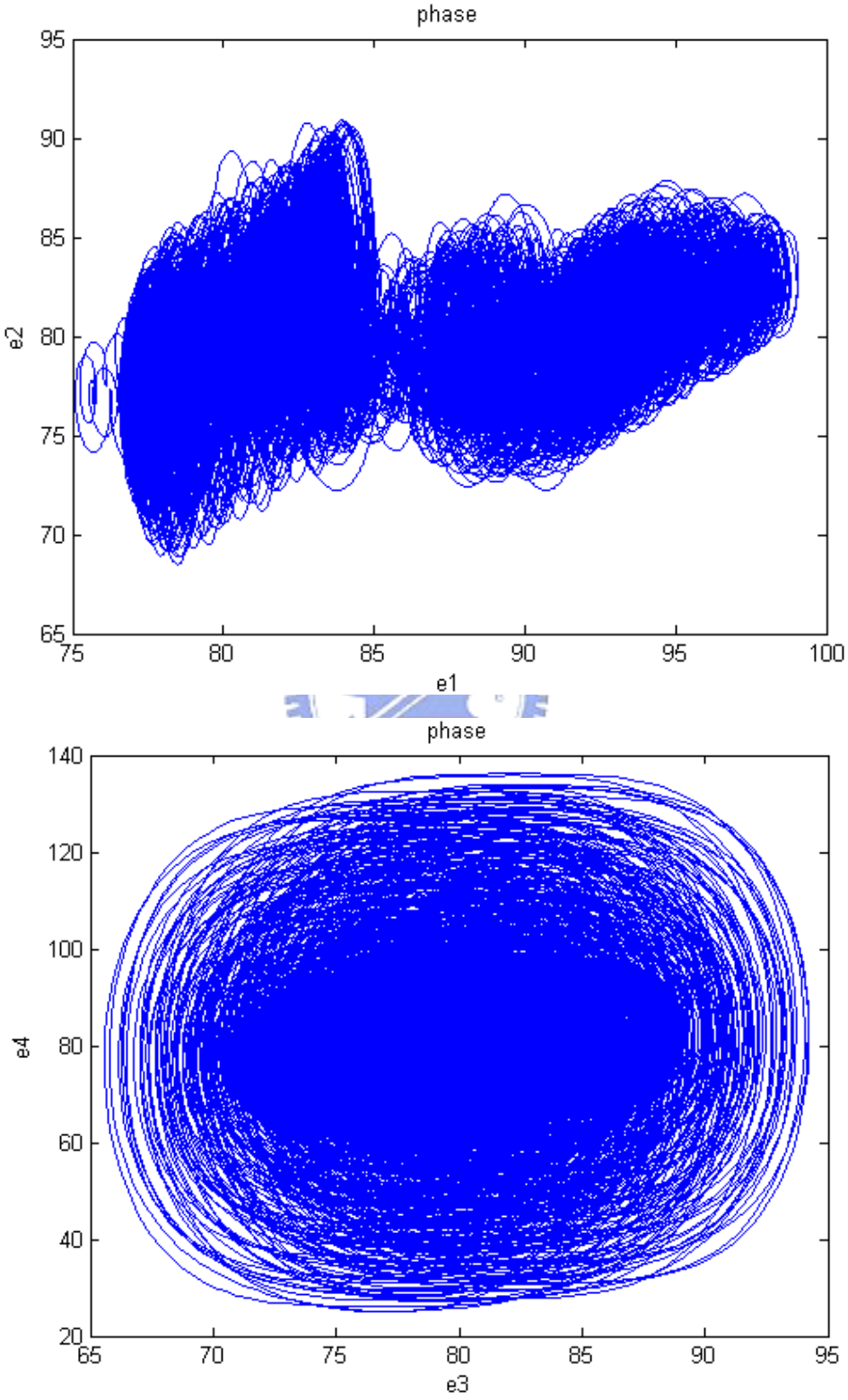

Fig. 2.8 Phase portraits of error dynamics for Case II.

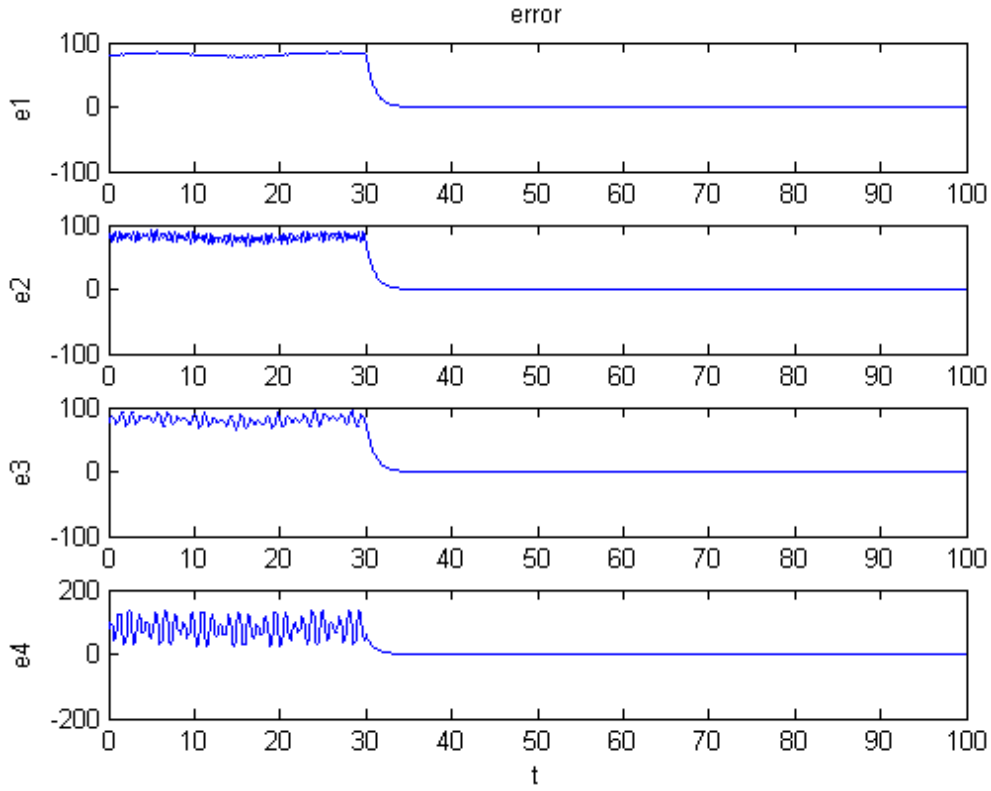

Fig. 2.9 Time histories of errors for Case II.

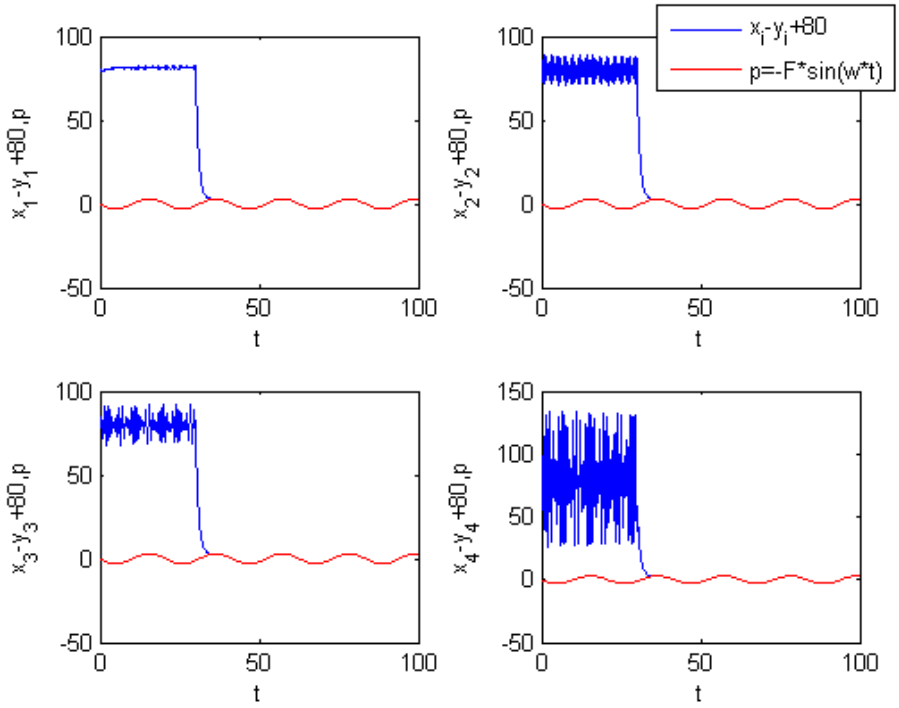

Fig. 2.10 Time histories of $x_i - y_i + 80$ and $-F\sin\omega t$ for Case II.

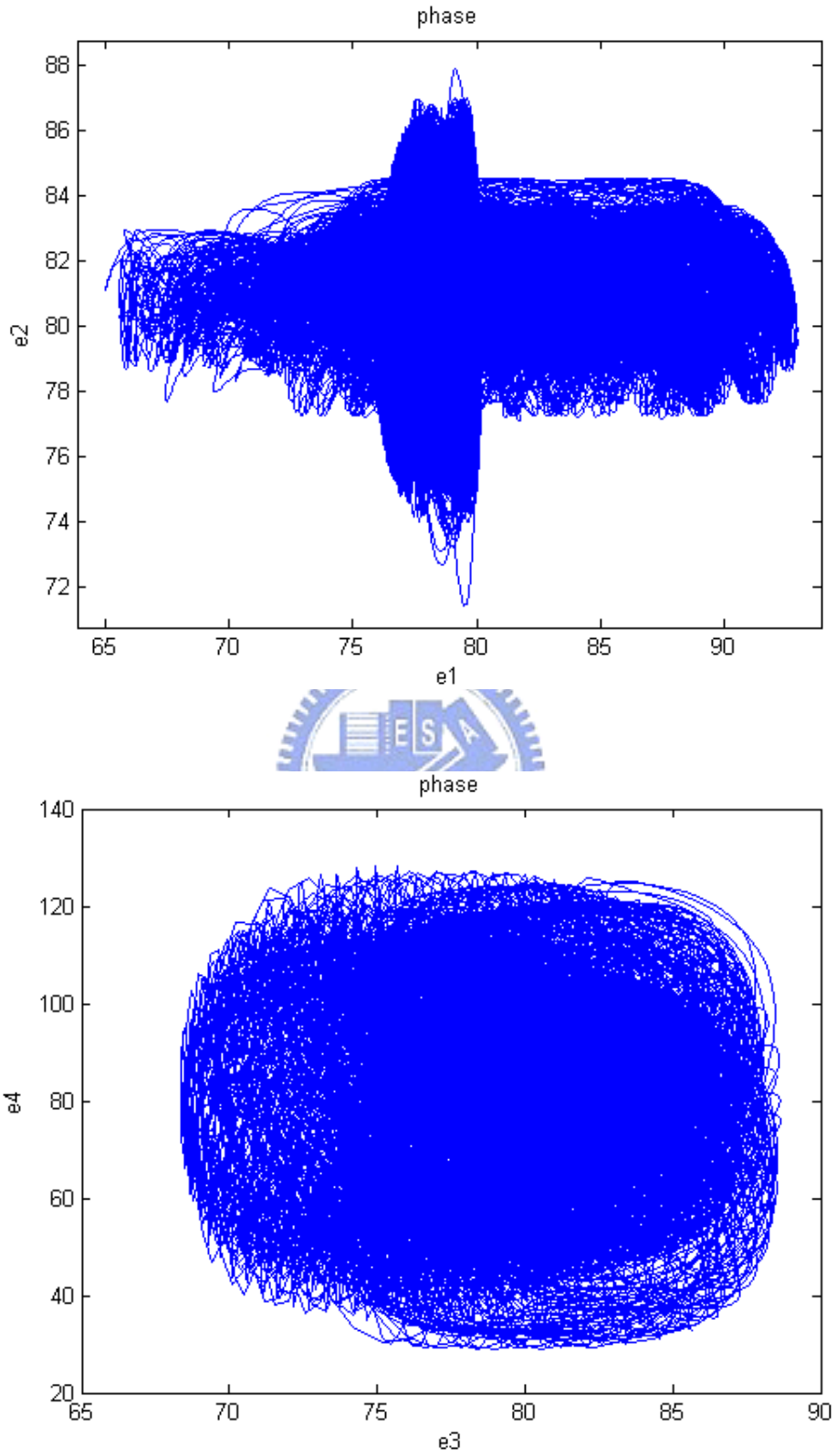

Fig. 2.11 Phase portraits of error dynamics for Case III.

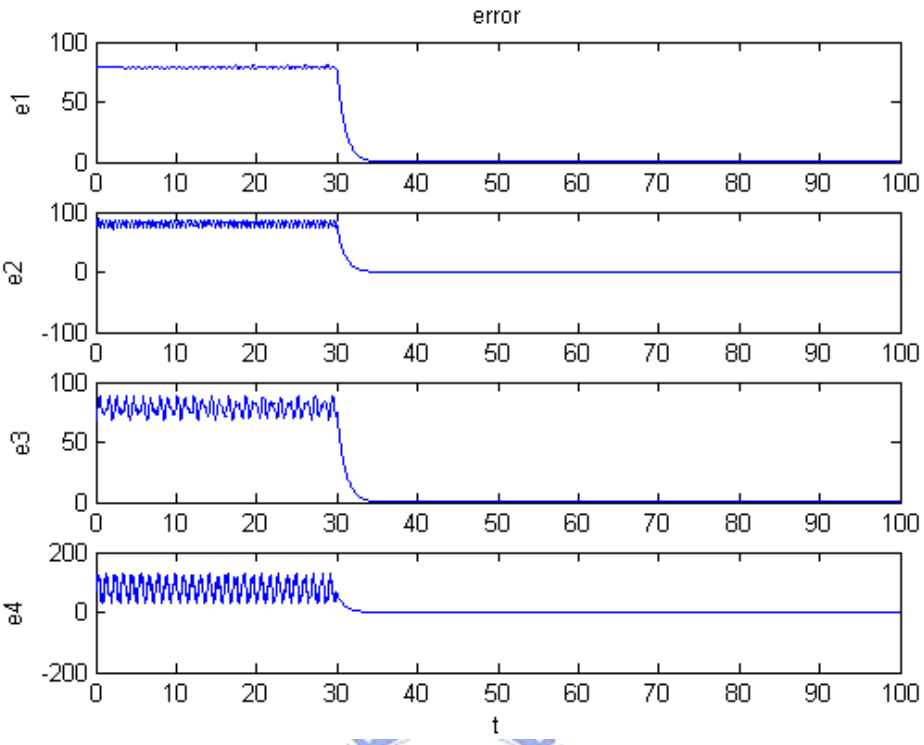

Fig. 2.12 Time histories of errors for Case III.

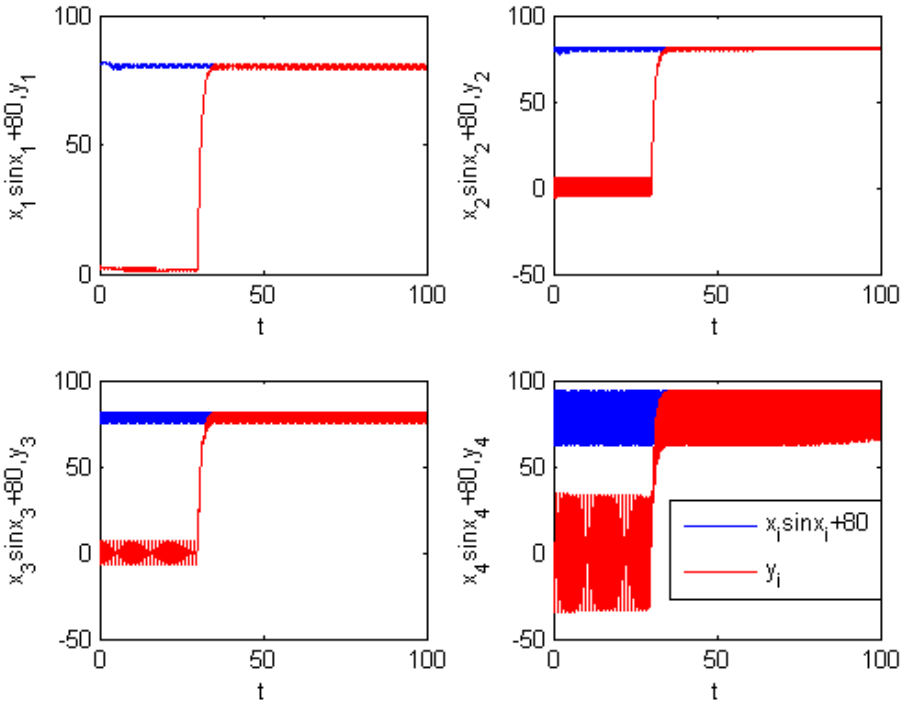

Fig. 2.13 Time histories of $x_i \sin x_i + 80$ and y_i for Case III.

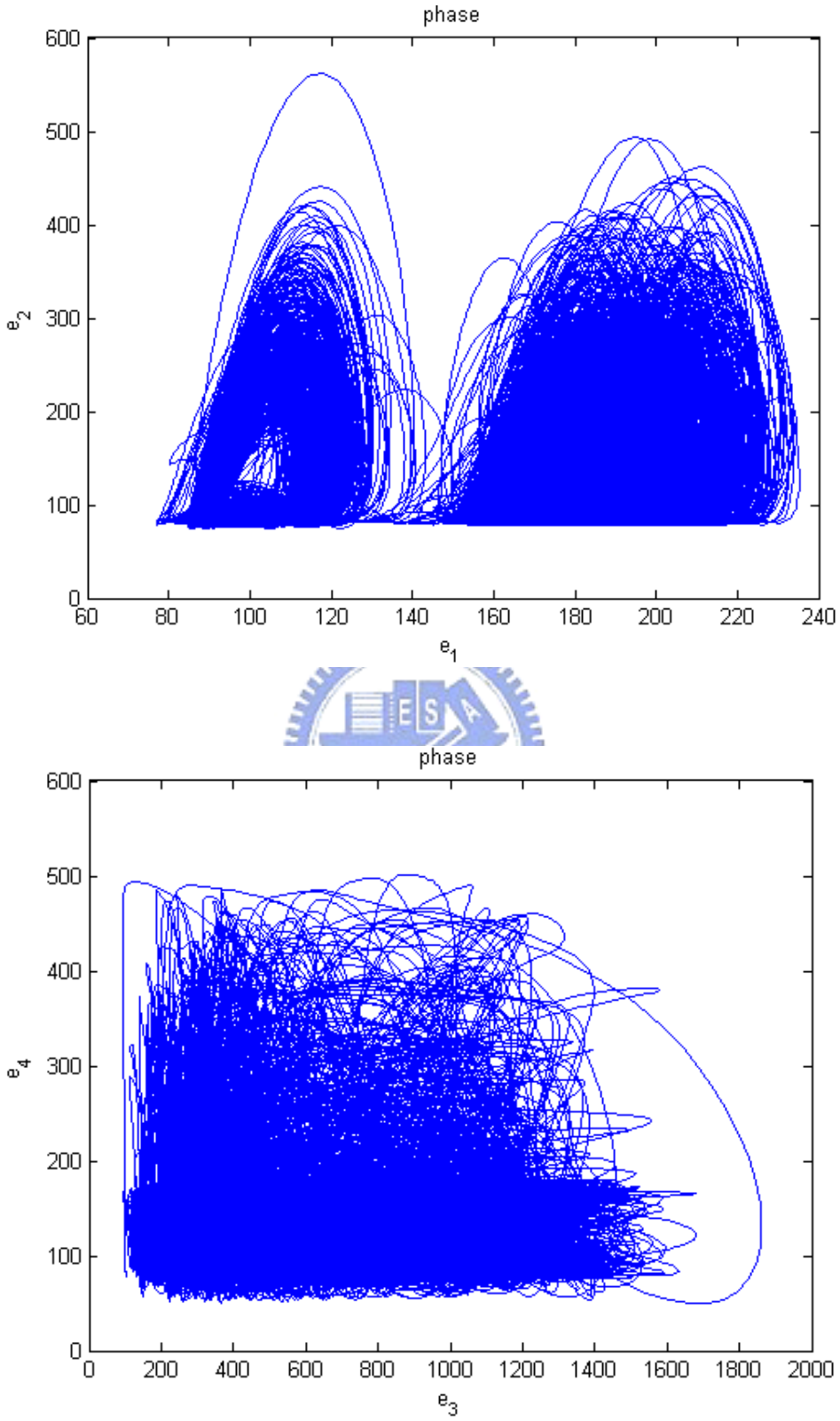

Fig. 2.14Phase portrait of error dynamics for Case IV.

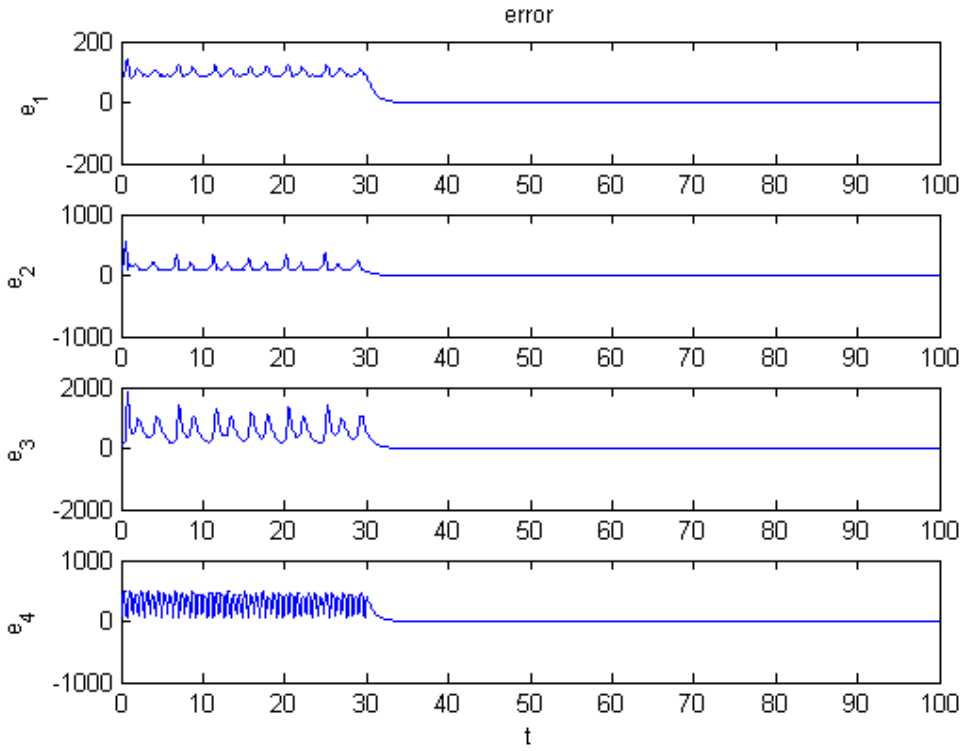

Fig. 2.15 Time histories of errors for Case IV.

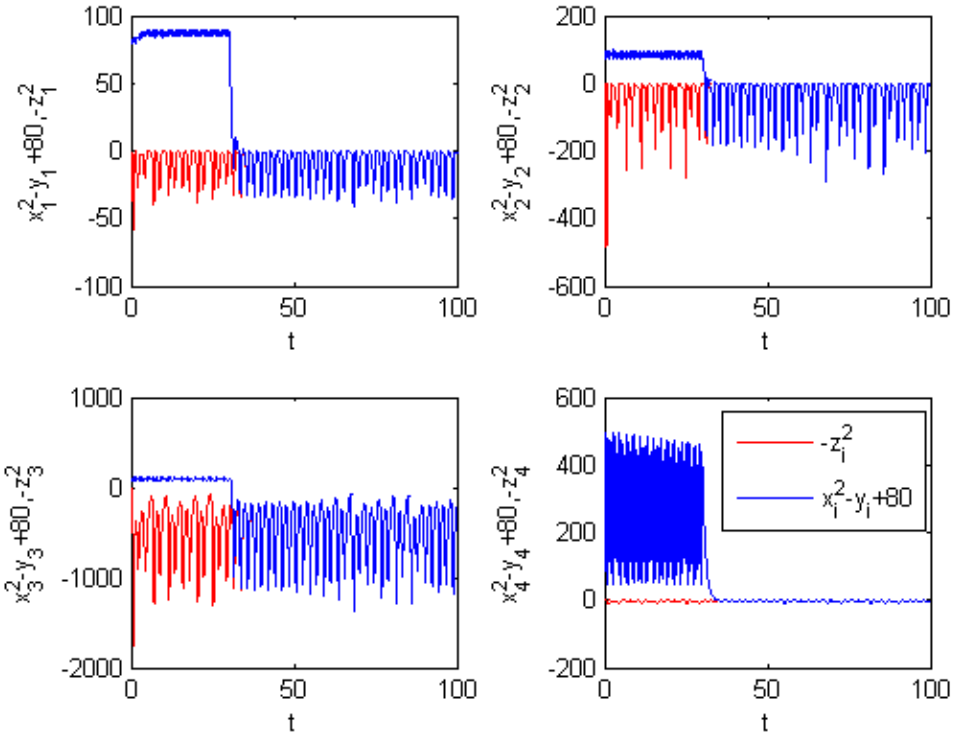

Fig. 2.16 Time histories of $x_i^2 - y_i^2 + 80$ and $-z_i^2$ for Case IV.

Chapter 3

Chaos Control of a New Froude-Duffing System by GYC Partial Region Stability Theory

3.1 Preliminaries

A new strategy via using GYC partial region stability theory is proposed to control the chaos of a new Froude-Duffing System to fixed point, to a given regular motion and to chaos of any given system. The Lyapunov function can be treated as a simple linear homogeneous function of error states by using the GYC partial region stability theory, controllers are in lower degree and simpler than traditional ones, so cause less simulation error. Numerical simulations are given to verify the effectiveness of this strategy.

3.2 Chaos Control Scheme

Consider the following chaotic systems

$$\dot{\mathbf{x}} = \mathbf{f}(t, \mathbf{x}) \tag{3-1}$$

where $\mathbf{x} = [x_1, x_2, \cdots, x_n]^T \in R^n$ is a the state vector, $\mathbf{f} : R_+ \times R^n \to R^n$ is a vector function.

The goal system which can be either chaotic or regular, is

$$\dot{\mathbf{y}} = \mathbf{g}(t, \mathbf{y}) \tag{3-2}$$

where $\mathbf{y} = [y_1, y_2, \cdots, y_n]^T \in R^n$ is a state vector, $\mathbf{g} : R_+ \times R^n \to R^n$ is a vector function.

In order to make the chaotic state $\mathbf{x}$ approaching the goal state $\mathbf{y}$, define error $\mathbf{e} = \mathbf{x} - \mathbf{y}$ as the state error. The chaos control is accomplished in the sense that :

$$\lim_{t\to\infty}\mathbf{e}=\lim_{t\to\infty}(\mathbf{x}-\mathbf{y})=0 \tag{3-3}$$

In this Chapter, we will use examples in which the error dynamics always happens in the first quadrant of coordinate system and use GYC partial region stability theory which is enclosed in Appendix. The Lyapunov function is a simple linear homogeneous function of error states and the controllers are simpler because they are in lower degree than that of traditional controllers and give less simulation error. Furthermore, the chaos of a new Froude-Duffing system is controlled to a fixed point, to a given regular motion and to the chaos of a generalized Lorenz system. This strategy enlarges the effective scope of traditional chaos control which is limited to control the chaos of only one given system.

3.3 Numerical Simulations

In this Section a new Froude-Duffing system in Eq.(2-6)

$$\begin{cases}\dfrac{dx_1}{dt}=x_2\\ \dfrac{dx_2}{dt}=(a-bx_2{}^2)x_2+c\sin x_1+dx_3x_4\\ \dfrac{dx_3}{dt}=x_4\\ \dfrac{dx_4}{dt}=-x_3-x_3{}^3-fx_4+gx_1x_2\end{cases} \tag{3-4}$$

is studied where *a, b, c, d, g, f* are parameters. This system exhibits chaos when the parameters of system are $a=0.35,\ b=0.1,\ c=1,\ d=0.48,\ g=0.25,\ f=0.002$ and the initial states of system are $x_1(0)=2, x_2(0)=2.4, x_3(0)=5,\ x_4(0)=6$.

Another translated chaotic system is given as

$$\begin{cases} \dfrac{dx_1}{dt} = x_2 - 50 \\ \dfrac{dx_2}{dt} = \left[a - b(x_2 - 50)^2 \right](x_2 - 50) + c\sin(x_1 - 50) + d(x_3 - 50)(x_4 - 50) \\ \dfrac{dx_3}{dt} = x_4 - 50 \\ \dfrac{dx_4}{dt} = -(x_3 - 50) - (x_3 - 50)^3 - f(x_4 - 50) + g(x_1 - 50)(x_2 - 50) \end{cases} \tag{3-5}$$

This is the same Froude-Duffing system of which the old origin is translated to $(x_1, x_2, x_3, x_4) = (50, 50, 50, 50)$ and the chaotic motion happens always in the first quadrant of coordinate system (x_1, x_2, x_3, x_4), as shown in Fig.3.1, with initial conditions $x_1(0) = 52, x_2(0) = 52.4, x_3(0) = 55, x_4(0) = 56$ and parameters $a = 0.35,\ b = 0.1,\ c = 1,\ d = 0.48,\ g = 0.25,\ f = 0.002$.

In order to lead (x_1, x_2, x_3, x_4) to the goal, we add control terms u_1, u_2, u_3, u_4 to each equation of Eq. (3-5), respectively.

$$\begin{cases} \dfrac{dx_1}{dt} = x_2 - 50 + u_1 \\ \dfrac{dx_2}{dt} = \left[a - b(x_2 - 50)^2 \right](x_2 - 50) + c\sin(x_1 - 50) + d(x_3 - 50)(x_4 - 50) + u_2 \\ \dfrac{dx_3}{dt} = x_4 - 50 + u_3 \\ \dfrac{dx_4}{dt} = -(x_3 - 50) - (x_3 - 50)^3 - f(x_4 - 50) + g(x_1 - 50)(x_2 - 50) + u_4 \end{cases} \tag{3-6}$$

CASE I. Control the chaotic motion to zero.

In this case we will control the chaotic motion of Froude-Duffing system (3-7) to zero. The goal is $\mathbf{y} = 0$. The state error is $\mathbf{e} = \mathbf{x} - \mathbf{y} = \mathbf{x}$ and error dynamics becomes

$$\begin{cases} \dot{e}_1 = \dot{x}_1 = (x_2 - 50) + u_1 \\ \dot{e}_2 = \dot{x}_2 = \left[a - b(x_2 - 50)^2 \right](x_2 - 50) + c\sin(x_1 - 50) + d(x_3 - 50)(x_4 - 50) + u_2 \\ \dot{e}_3 = \dot{x}_3 = (x_4 - 50) + u_3 \\ \dot{e}_4 = \dot{x}_4 = -(x_3 - 50) - (x_3 - 50)^3 - f(x_4 - 50) + g(x_1 - 50)(x_2 - 50) + u_4 \end{cases} \quad (3\text{-}7)$$

In Fig.3.2, the error dynamics always exists in first quadrant.

By GYC partial region stability, choose a Lyapunov function in the form of a positive definite function in first quadrant as:

$$V = e_1 + e_2 + e_3 + e_4 \quad (3\text{-}8)$$

Its time derivative through error dynamics (3-9) is

$$\begin{aligned} \dot{V} &= \dot{e}_1 + \dot{e}_2 + \dot{e}_3 + \dot{e}_4 \\ &= (x_2 - 50) + u_1 + \left[a - b(x_2 - 50)^2 \right](x_2 - 50) + c\sin(x_1 - 50) \\ &\quad + d(x_3 - 50)(x_4 - 50) + u_2 + x_4 - 50 + u_3 \\ &\quad - (x_3 - 50) - (x_3 - 50)^3 - f(x_4 - 50) + g(x_1 - 50)(x_2 - 50) + u_4 \end{aligned} \quad (3\text{-}9)$$

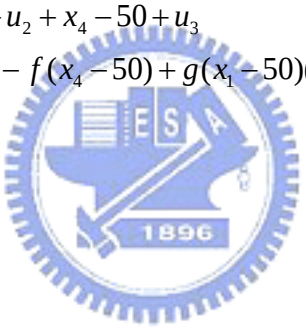

Choose

$$\begin{cases} u_1 = -\left(x_2 - 50\right) - e_1 \\ u_2 = -\left\{ \left[a - b(x_2 - 50)^2 \right](x_2 - 50) + c\sin(x_1 - 50) + d(x_3 - 50)(x_4 - 50) \right\} - e_2 \\ u_3 = -\left(x_4 - 50\right) - e_3 \\ u_4 = -\left(-(x_3 - 50) - (x_3 - 50)^3 - f(x_4 - 50) + g(x_1 - 50)(x_2 - 50) \right) - e_4 \end{cases} \quad (3\text{-}10)$$

We obtain

$$\dot{V} = -e_1 - e_2 - e_3 - e_4 < 0$$

which is negative definite function in first quadrant. By GYC partial region asymptotical stability theorem, **e** approaches zero. The numerical results are shown in Fig.3.3 After 100 sec, e_1, e_2, e_3 and e_4 approach zero.

CASE II. Control the chaotic motions to a four different sine functions of time.

In this case we will control the chaotic motion of the new Froude-Duffing system (3-7) to four different sine functions of time. The goal motion is $y_i = n\sin\omega_i t \quad (i = 1,2,3,4)$. The error are defined as

$$e_i = x_i - y_i = x_i - n\sin\omega_i t \qquad i = 1,2,3,4 \tag{3-11}$$

$$\lim_{t\to\infty} e_i = \lim_{t\to\infty}(x_i - n\sin\omega_i t) = 0 \qquad i = 1,2,3,4$$

is demanded.

From(3-13)

$$\dot{e}_i = \dot{x}_i - n\omega_i \cos\omega_i t \quad (i = 1,2,3,4)$$

where $n = 3$, $\omega_1 = 0.3$, $\omega_2 = 0.4$, $\omega_3 = 0.5$, $\omega_4 = 0.6$. The error dynamics is

$$\begin{cases} \dot{e}_1 = \dot{x}_1 - n\omega_1 \cos\omega_1 t \\ \dot{e}_2 = \dot{x}_2 - n\omega_2 \cos\omega_2 t \\ \dot{e}_3 = \dot{x}_3 - n\omega_3 \cos\omega_3 t \\ \dot{e}_4 = \dot{x}_4 - n\omega_4 \cos\omega_4 t \end{cases} \tag{3-12}$$

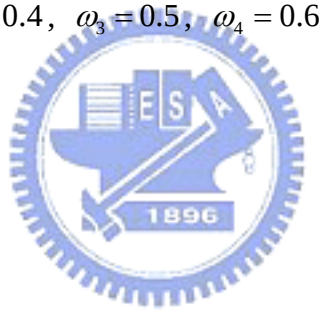

It always exists in first quadrant as shown in Fig.3.4.

By GYC partial region stability, one can easily choose a Lyapunov function in the form of a positive definite function in first quadrant as:

$$V = e_1 + e_2 + e_3 + e_4$$

Its time derivative is

$$\begin{aligned} \dot{V} &= \dot{e}_1 + \dot{e}_2 + \dot{e}_3 + \dot{e}_4 \\ &= (x_2 - 50) - n\omega_1 \cos\omega_1 t + u_1 + \left[a - b(x_2 - 50)^2\right](x_2 - k) + c\sin(x_1 - 50) \\ &\quad + d(x_3 - 50)(x_4 - 50) - n\omega_2 \cos\omega_2 t + u_2 + (x_4 - 50) - n\omega_3 \cos\omega_3 t + u_3 \\ &\quad - (x_3 - 50) - (x_3 - 50)^3 - f(x_4 - 50) + g(x_1 - 50)(x_2 - 50) - n\omega_4 \cos\omega_4 t + u_4 \end{aligned} \tag{3-13}$$

Choose

$$\begin{cases} u_1 = -\left((x_2 - 50) - n\omega_1 \cos\omega_1 t\right) - e_1 \\ u_2 = -\left(\left(a - b(x_2 - 50)^2\right)(x_2 - k) + c\sin(x_1 - 50) + d(x_3 - 50)(x_4 - 50) - n\omega_2 \cos\omega_2 t\right) - e_2 \\ u_3 = -\left((x_4 - 50) - n\omega_3 \cos\omega_3 t\right) - e_3 \\ u_4 = -\left(-(x_3 - 50) - (x_3 - 50)^3 - f(x_4 - 50) + g(x_1 - 50)(x_2 - 50) - n\omega_4 \cos\omega_4 t\right) - e_4 \end{cases} \quad (3\text{-}14)$$

$\dot{V}$ becomes

$$\dot{V} = -e_1 - e_2 - e_3 - e_4 < 0$$

which is a negative definite function in first quadrant. The numerical results are shown in Fig.3.5 and Fig. 3.6. After 100 sec., the errors approach zero and the chaotic trajectories approach to four sine functions of time.

CASE III. Control the chaotic motion to chaotic motion of generalized Lorenz system.

In this case we will control chaotic motion of Froude-Duffing system (3-5) to that of generalized Lorenz system. The goal system is generalized Lorenz system:

$$\begin{cases} \dot{z}_1 = a_1(z_2 - z_1) + d_1 z_4 \\ \dot{z}_2 = b_1 z_2 - z_1 z_3 - z_2 \\ \dot{z}_3 = z_1 z_2 - c_1 z_3 \\ \dot{z}_4 = -z_1 - a_1 z_4 \end{cases} \quad (3\text{-}15)$$

The error equation is $\mathbf{e = x - z}$. Our goal is $\lim_{t\to\infty} \mathbf{e} = 0$. The error dynamics become

$$\begin{cases} \dot{e}_1 = \dot{x}_1 - \dot{z}_1 = (x_2 - 50) - \left(a_1(z_2 - z_1) + d_1 z_4\right) + u_1 \\ \dot{e}_2 = \dot{x}_2 - \dot{z}_2 = \left[a - b(x_2 - 50)^2\right](x_2 - 50) + c\sin(x_1 - 50) + d(x_3 - 50)(x_4 - 50) \\ \qquad\qquad - \left(b_1 z_2 - z_1 z_3 - z_2\right) + u_2 \\ \dot{e}_3 = \dot{x}_3 - \dot{z}_3 = (x_4 - 50) - (z_1 z_2 - c_1 z_3) + u_3 \\ \dot{e}_4 = \dot{x}_4 - \dot{z}_4 = -(x_3 - 50) - (x_3 - 50)^3 - f(x_4 - 50) + g(x_1 - 50)(x_2 - 50) - \left(-z_1 - a_1 z_4\right) + u_4 \end{cases} \quad (3\text{-}16)$$

The error dynamics always exists in first quadrant as shown in Fig.3.7.

By GYC partial region stability, one can easily choose a Lyapunov function in the form of a positive definite function in first quadrant as:

$$V = e_1 + e_2 + e_3 + e_4$$

Its time derivative is

$$\begin{aligned}\dot{V} &= \dot{e}_1 + \dot{e}_2 + \dot{e}_3 + \dot{e}_4 \\ &= (x_2 - 50) - \left(a_1(z_2 - z_1) + d_1 z_4\right) + u_1\left[a - b(x_2 - 50)^2\right](x_2 - 50) \\ &\quad + c\sin(x_1 - 50) + d(x_3 - 50)(x_4 - 50) - \left(b_1 z_2 - z_1 z_3 - z_2\right) + u_2 \\ &\quad + (x_4 - 50) - (z_1 z_2 - c_1 z_3) + u_3 - (x_3 - 50) - (x_3 - 50)^3 - f(x_4 - 50) \\ &\quad + g(x_1 - 50)(x_2 - 50) - \left(-z_1 - a_1 z_4\right) + u_4\end{aligned} \tag{3-17}$$

Choose

$$\begin{cases} u_1 = -\left((x_2 - 50) - \left(a_1(z_2 - z_1) + d_1 z_4\right)\right) - e_1 \\ u_2 = -\left[a - b(x_2 - 50)^2\right](x_2 - 50) - c\sin(x_1 - 50) - d(x_3 - 50)(x_4 - 50) \\ \qquad + \left(b_1 z_2 - z_1 z_3 - z_2\right) - e_2 \\ u_3 = -\left((x_4 - 50) - (z_1 z_2 - c_1 z_3)\right) - e_3 \\ u_4 = -\left(-(x_3 - 50) - (x_3 - 50)^3 - f(x_4 - 50) + g(x_1 - 50)(x_2 - 50) - \left(-z_1 - a_1 z_4\right)\right) - e_4 \end{cases} \tag{3-18}$$

$\dot{V}$ becomes

$$\dot{V} = -e_1 - e_2 - e_3 - e_4 < 0$$

which is negative definite function in first quadrant. The numerical results are shown in Fig.3.8 and Fig. 3.9, where $a_1 = 1$, $b_1 = 26$, $c_1 = 0.7$, $d_1 = 1.5$. After 100 sec., the errors approach zero and the chaotic trajectories of Froude-Duffing system approach to that of the generalized Lorenz system.

3.4 Summary

In this Chapter, a new strategy by using partial region stability theory is proposed to achieve chaos control. By using the GYC partial region stability theory, the controllers are of lower degree than that of controllers by using traditional Lyapunov asymptotical stability theorem. The simple linear homogeneous function of error states and the lower order controllers are much more simple and introduce less simulation error. Besides, the strategy enlarges the effective scope of traditional chaos control which is limited to control the chaos of only one given system .To control the chaos of a new Froude-Duffing system to that of a generalized Lorenz system are used as one of three simulation examples which verify the effectiveness of the proposed scheme.

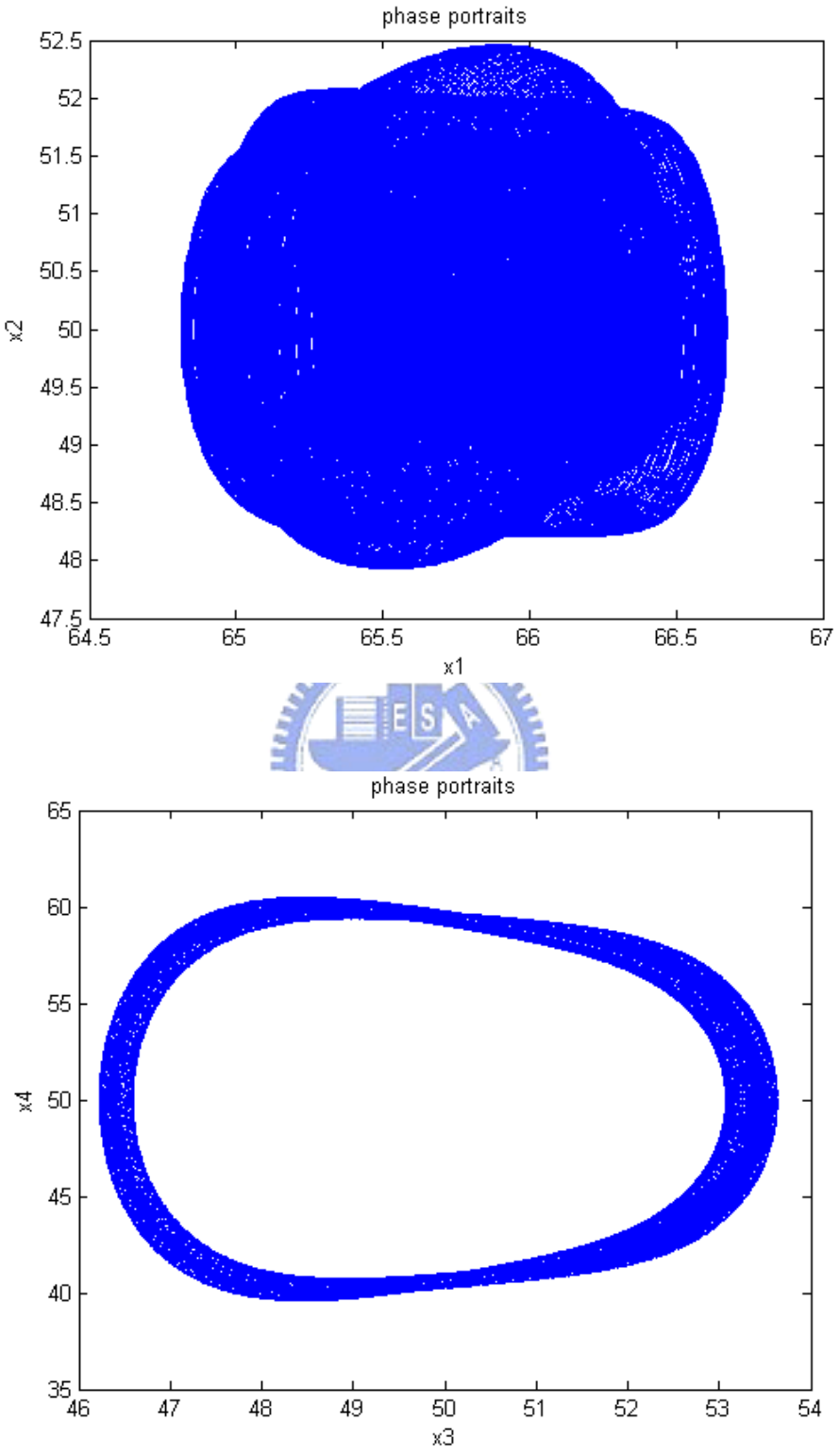

Fig. 3.1 Chaotic phase portraits for a new Froude-Duffing system in the first quadrant.

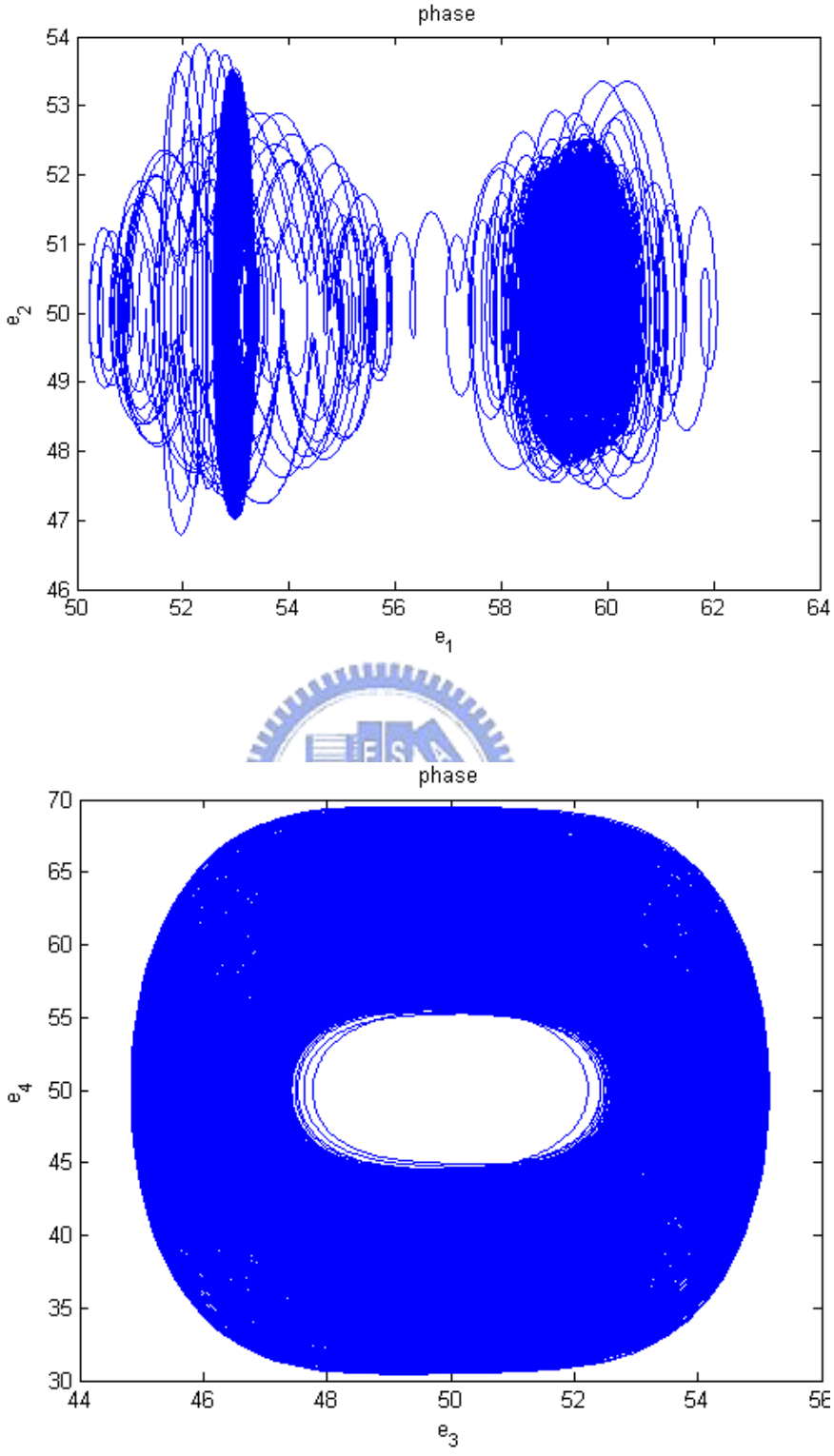

Fig. 3.2 Phase portraits of error dynamics for Case I.

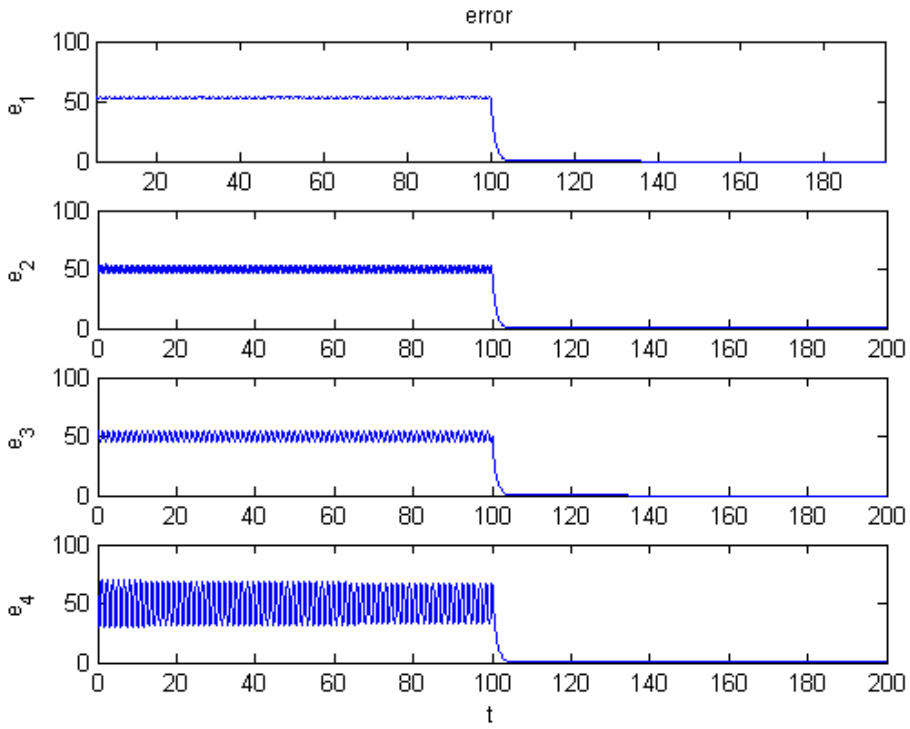

Fig. 3.3 Time histories of errors for Case I.

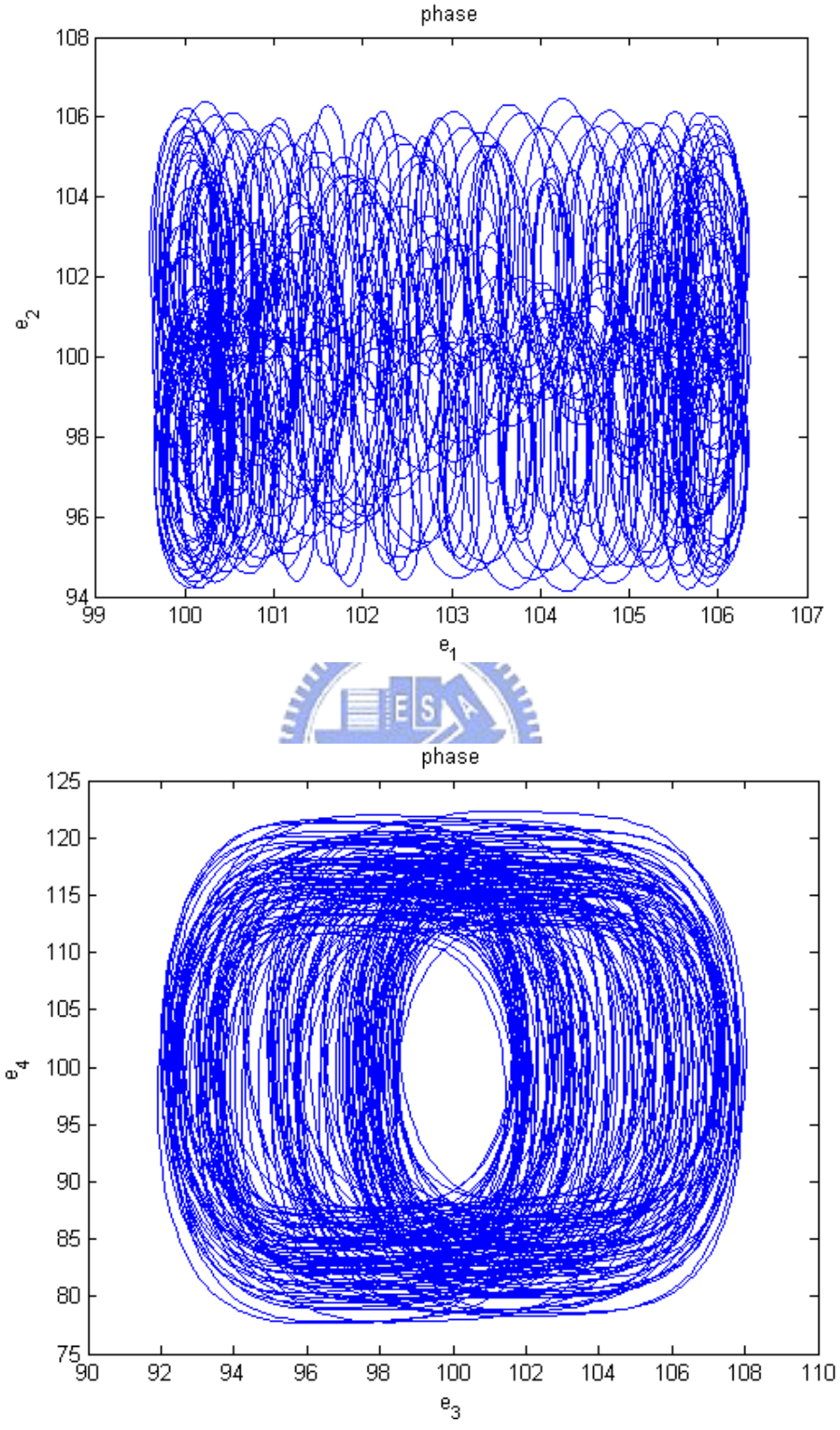

Fig. 3.4 Phase portraits of error dynamics for Case II.

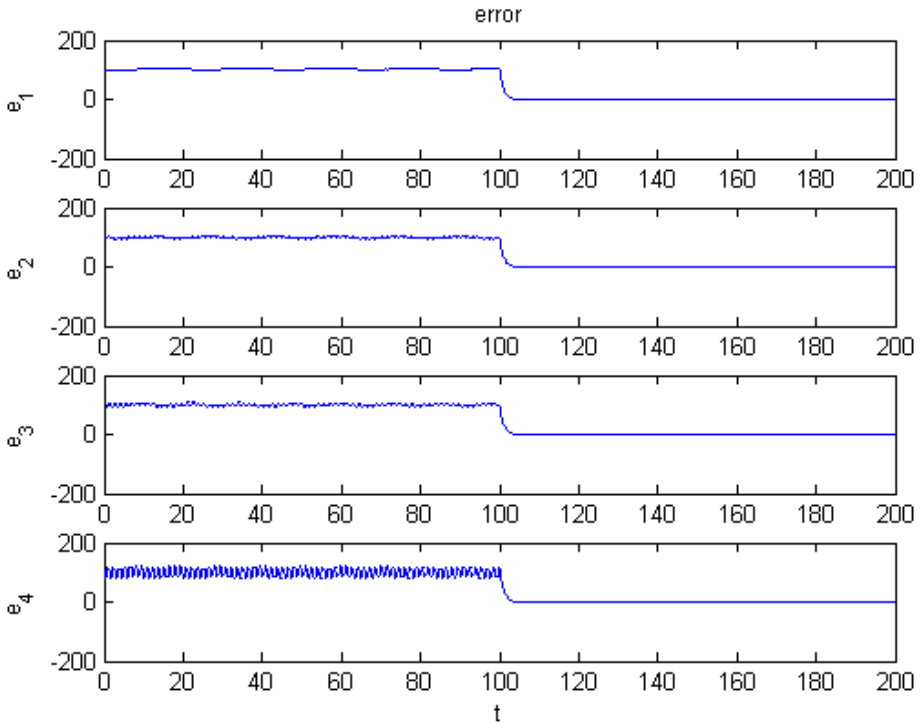

Fig. 3.5 Time histories of errors for Case II.

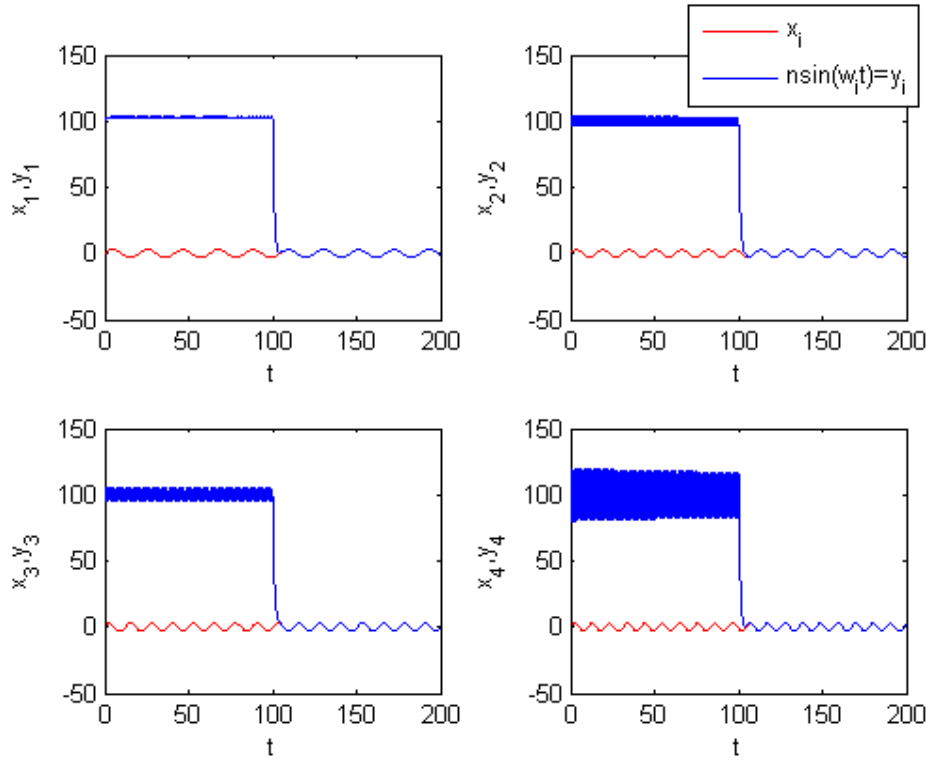

Fig. 3.6 Time histories of x_1, x_2, $x_{3,}x_4$ and y_1, y_2, $y_{3,}$ y_4 for Case II.

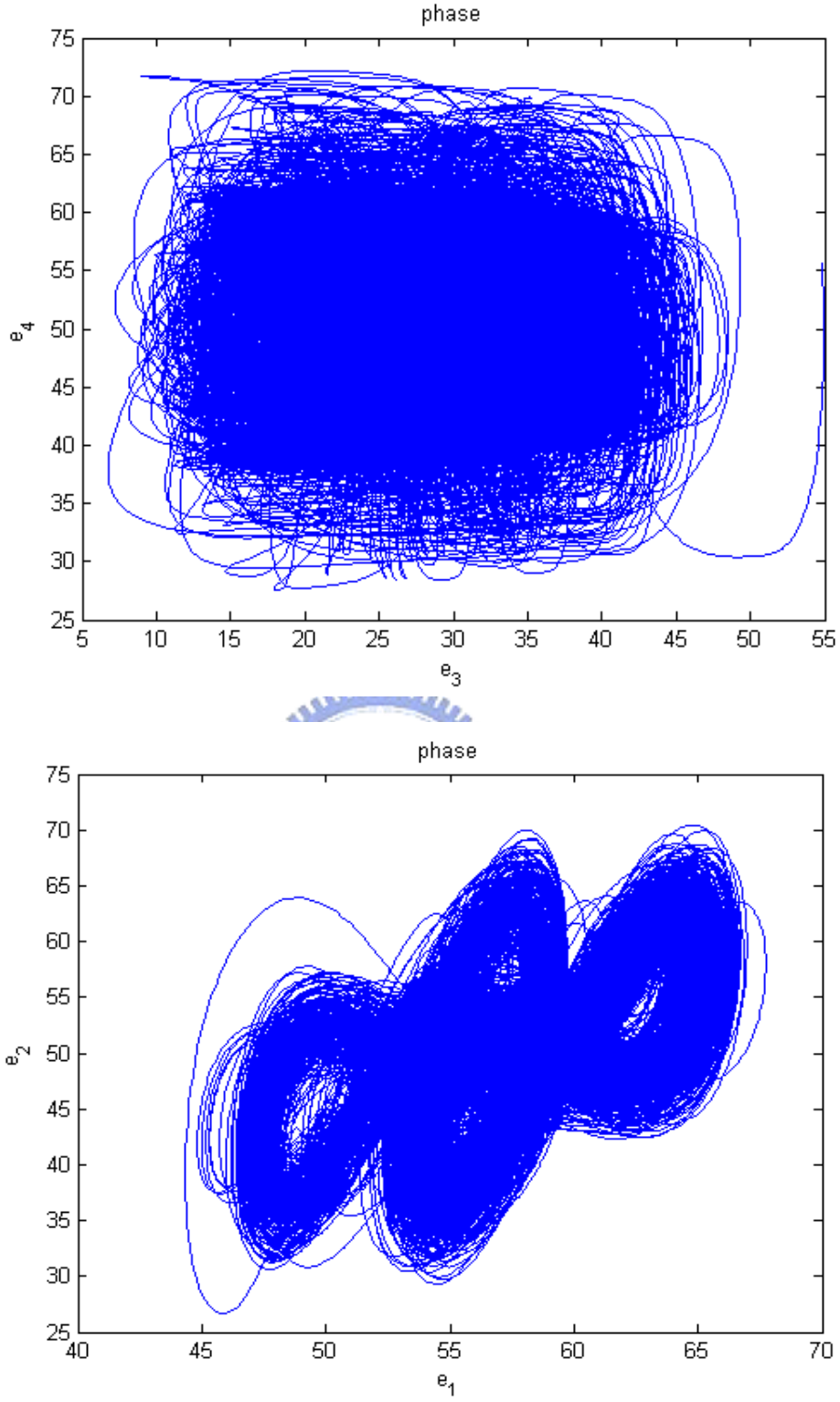

Fig. 3.7 Phase portraits of error dynamics for Case III.

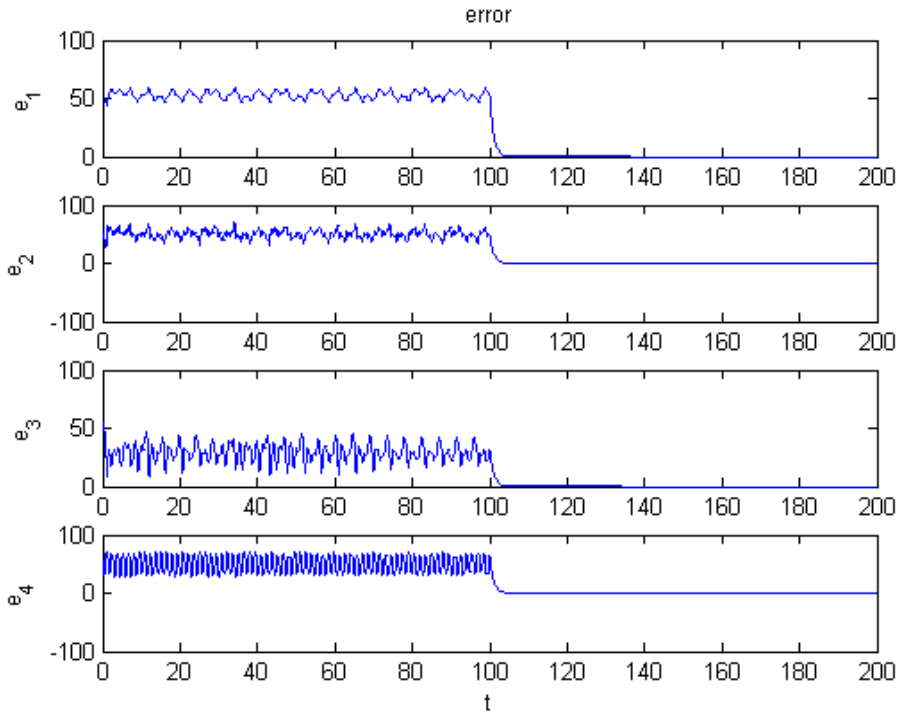

Fig. 3.8 Time histories of errors for Case III.

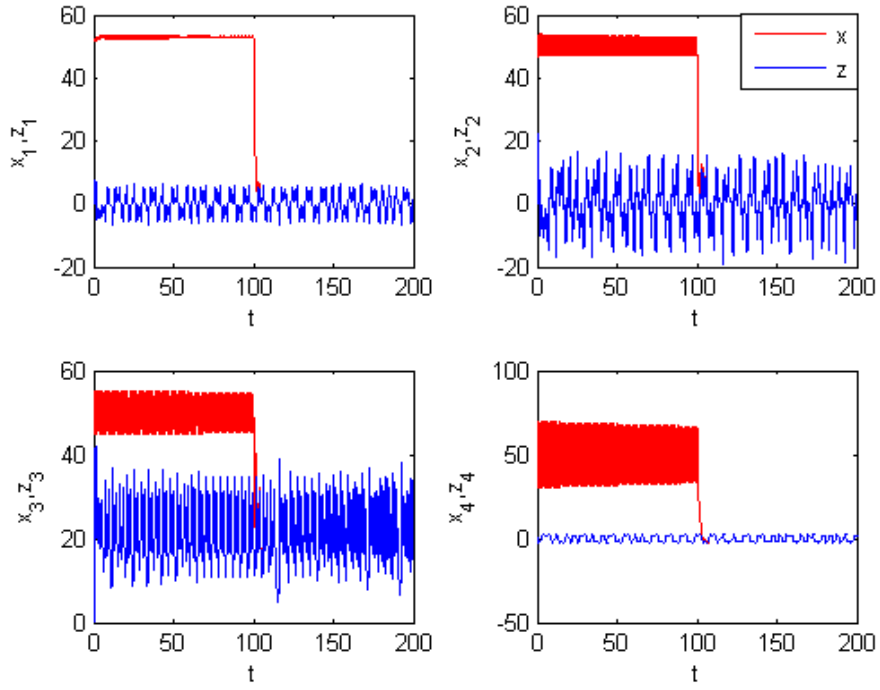

Fig. 3.9 Time histories of x_1, x_2, x_3, x_4 and z_1, z_2, z_3, z_4 for Case III.

Chapter 4

Hyperchaos of a Rössler System with Bessel Function Parameters

4.1 Preliminaries

In this Chapter, our study is devoted to a Rössler System with Bessel function parameters. The chaotic behaviors is studied numerically by time histories of states, phase portraits, bifurcation diagram, parameter diagram, Lyapunov exponent diagram and Poincaré maps. It is found that both hyperchaos and chaos are abundant and give various applications, especially for secret communication exist.

4.2 Chaos of Rössler System with Bessel Function Parameters

The Rössler system with Bessel function parameters is:

$$\begin{cases} \dfrac{dx}{dt} = -(y+z) \\ \dfrac{dy}{dt} = x + ay \\ \dfrac{dz}{dt} = b + xz - cz \end{cases} \tag{4-1}$$

with parameters $a(t)$ $b(t)$, $c(t)$ as given functions of time. It is a nonautonomous system, which is equivalent to a four-dimensional autonomous system. a, b, c are given as：

$$\begin{cases} a(t) = k_1 \\ b(t) = k_2 b_1 + 0.2 \\ c(t) = b_2 + k_3 \end{cases} \tag{4-2}$$

where k_1, k_2, k_3 are constant parameters, and

$$b_1 = Y_0(t+0.5) = \lim_{\mu \to 0} \frac{\cos \mu\pi J_\mu(t+0.5) - J_\mu(t+0.5)}{\sin \mu\pi} \tag{4-3}$$

$$b_2 = J_1 = \sum_{n=0}^{\infty} \frac{(-1)^n}{n!\Gamma(n+2)} (\frac{t}{2})^{2n+1} \tag{4-4}$$

where Y_0 is Bessel function of the second type , J_μ is Bessel function of the first kind and Γ is Gamma function. The time histories of $b(t) = k_2 b_1 + 0.2$, $c(t) = b_2 + k_3$ with $k_2 = 0.6$, $k_3 = 10$ are show in Figs 4.1 and 4.2. The numerical simulations are carried out by MATLAB using the fractional operator in the Simulink environment.

4.3 Numerical Simulations

This system exhibits chaos when the parameters of system (4-1) are $k_1 = 0.15$, $k_2 = 0.6$, $k_3 = 10$ and the initial condition is $(x, y, z) = (0.3,\ 0.1,\ 0.5)$. The time history of three states, phase portraits, Poincaré maps, and bifurcation diagrams of the system are shown in Fig. 4.3~Fig. 4.8. When the parameters are $k_1 = 0.06$, $k_2 = 0.6$, $k_3 = 10$, the motion becomes period 1. The time histories of three states, phase portraits and Poincaré maps of the system are shown in Fig. 4.9~Fig. 4.12.

Lyapunov exponents and parametric diagram are also given to certify the existence of hyperchaos. Let us assume Lyapunov exponents λ_i $(i = 1, 2, 3, 4)$ satisfying $\lambda_1 > \lambda_2 > \lambda_3$, and $\lambda_4 = 0$. Then the dynamics of system (4-1) can be characterized as follows:

(1) When $\lambda_{1,2,3} < 0$ and $\lambda_4 = 0$, system (4-1) is periodic.

(2) When $\lambda_1 > 0,\ \lambda_{2,3} < 0$, and $\lambda_4 = 0$, system (4-1) exhibits chaotic motion.

(3) When $\lambda_{1,2} > 0,\ \lambda_3 < 0$, and $\lambda_4 = 0$, system (4-1) exhibits hyperchaotic motion.

Three cases are studied as follows.

Case I

Fix k_2, k_3, vary k_1. The Lyapunov exponents of the system (4-1) for $k_2 = 0.6$, and $k_3 = 10$ are shown in Fig. 4.13 and Fig. 4.14. The parametric diagram of system (4-1) for varying k_1 and k_2 with $k_3 = 10$ is shown in Fig. 3.15. The white area corresponds to periodic motion. By simulation, system is periodic when $0.01 \le k_1 \le 0.1$. The blue area corresponds to chaotic motion. And the green area corresponds to hyperchaotic motion which is identified by the existence of two positive Lyapunov exponents, as clearly shown in Fig. 4.13 and Fig. 4.14. As k_1 varies in $0.1 \le k_1 \le 0.35$, the system displays complex behavior, with an interweaving between chaotic and hyperchaotic motions. The hyperchaotic motion is quite abundant.

Case II

Fix $k_3 = 10$, and vary k_1, k_2. Some typical values of k_1 and k_2 that generate hyperchaos with two positive Lyapunov exponents are shown in Tables $1 \sim 3$, respectively. Comparing Table $1 \sim 3$, a notable phenomenon appears when k_1 increases. As k_1 increases, the value of Lyapunov exponent λ_2 becomes larger. It means that larger k_1 can arouse hyperchaotic motion. In other words, hyperchaos is aroused with enlarged Bessel function of first kind.

Table 1 Typical values of parameter k_2 that generate hyperchaos for $k_1 = 0.1$ and $k_3 = 10$.

k_2	λ_1	λ_2	λ_3	λ_4
0.500	0.00634	0.00065	-9.830902	0
0.544	0.00730	0.00069	-9.831895	0
0.580	0.00783	0.00069	-9.832725	0
0.620	0.00969	0.00067	-9.834285	0
0.700	0.00549	0.00062	-9.829993	0
0.760	0.00741	0.00038	-9.831599	0
0.856	0.00692	0.00026	9.831332	0

Table 2 Typical values of parameter k_2 that generate hyperchaos for $k_1 = 0.2$ and $k_3 = 10$.

k_2	λ_1	λ_2	λ_3	λ_4
1.104	0.10918	0.00095	-9.703637	0
1.152	0.11056	0.00071	-9.699163	0
1.176	0.10769	0.00067	-9.695142	0
1.204	0.11382	0.00077	-9.707276	0
1.232	0.10929	0.00194	-9.698110	0
1.292	0.11663	0.00039	-9.704187	0

Table 3 Typical values of parameter k_2 that generate hyperchaos for $k_1 = 0.3$ and $k_3 = 10$.

k_2	λ_1	λ_2	λ_3	λ_4
0.504	0.17391	0.00052	-9.227365	0
0.536	0.17959	0.00015	-9.192967	0
0.544	0.17410	0.00060	-9.196768	0
0.652	0.17324	0.00106	-9.219144	0
0.732	0.17996	0.00142	-9.215868	0

Case III

Fix $k_1 = 0.15$, $k_2 = 0.6$ and vary k_3. Fig. 4.18 and Fig. 4.19 shows the Lyapunov exponents as a function of k_3 to classify the chaotic or hyperchaotic motions. With increasing k_3, the motion of system (2-2) becomes hyperchaotic when $k_3 \le 10.3$ and $k_3 \ge 10.4$;and chaotic motions occur with $10.3 \le k_3 \le 10.4$. In this case, periodic motion has not be found.

4.4 Summary

Rössler system with Bessel function parameters is studied firstly. The results are verified by time histories of states, phase portraits, Poincaré maps, bifurcation diagram, Lyapunov exponents and parametric diagram. Abundant hyperchaos is found for this system, which gives potential in various applications, particularly in secret communication.

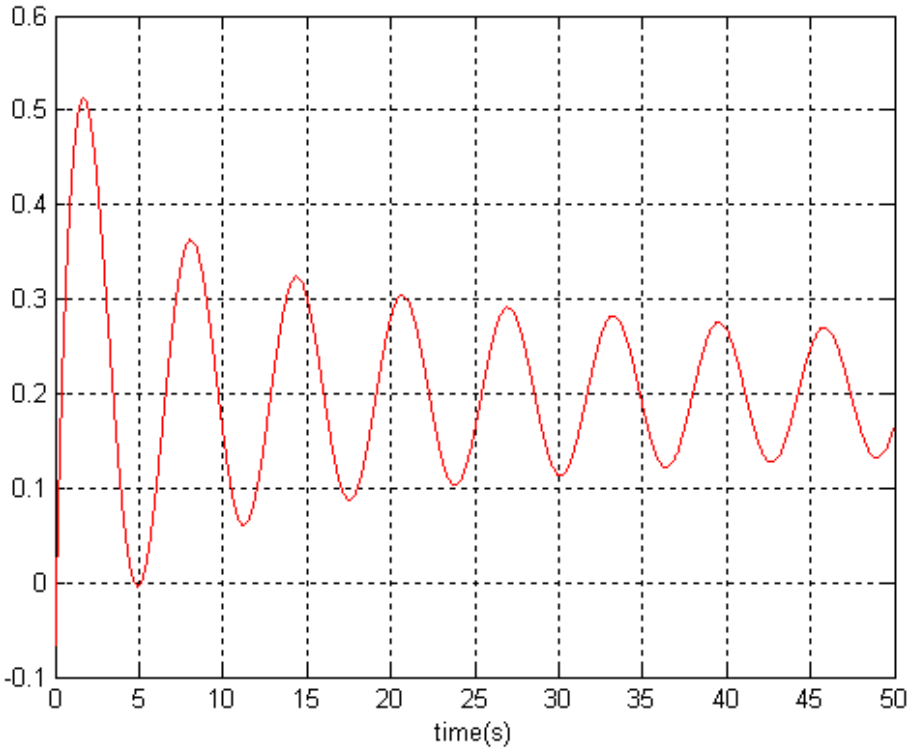

Fig. 4.1 The time history $b(t)$ with $k_2 = 0.6$.

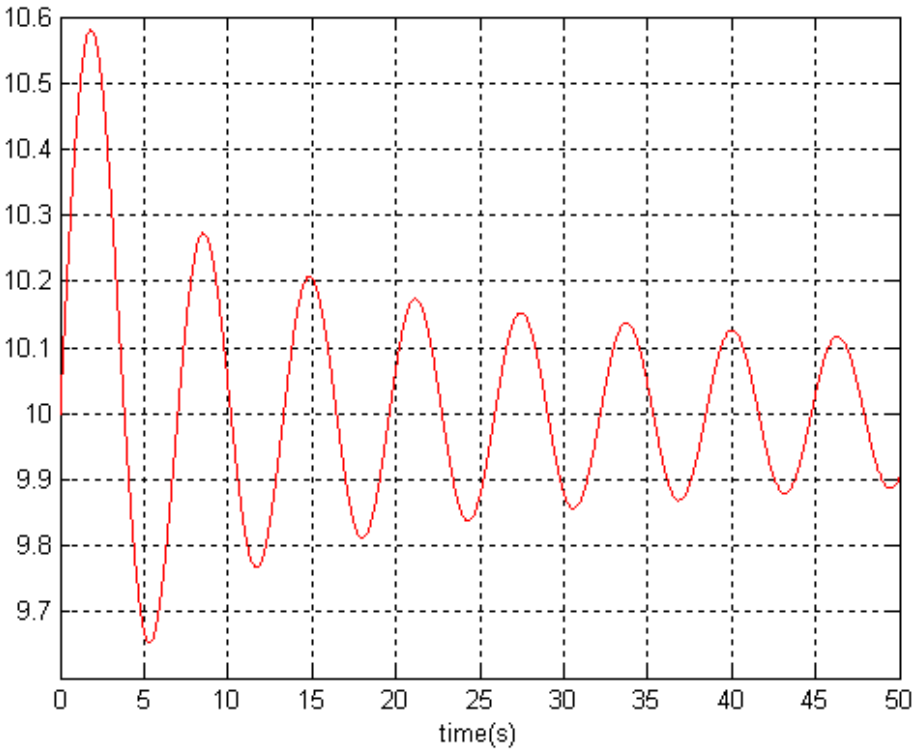

Fig. 4.2 The time history $c(t)$ with $k_3 = 10$.

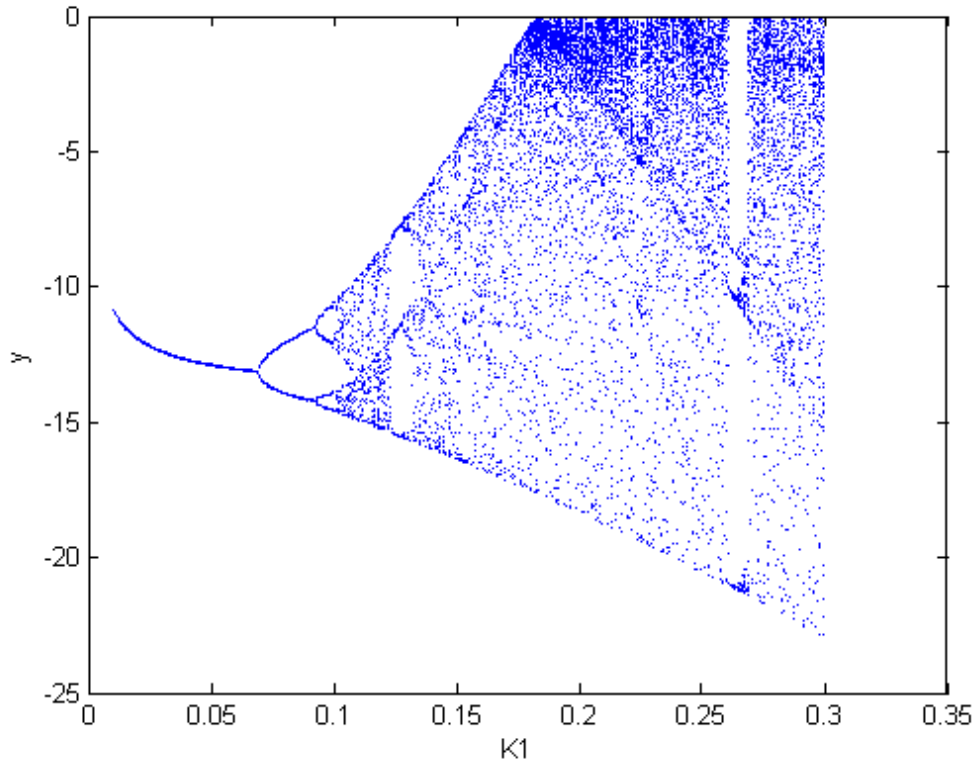

Fig. 4.3 The bifurcation diagram with $k_2 = 0.6$, $k_3 = 10$.

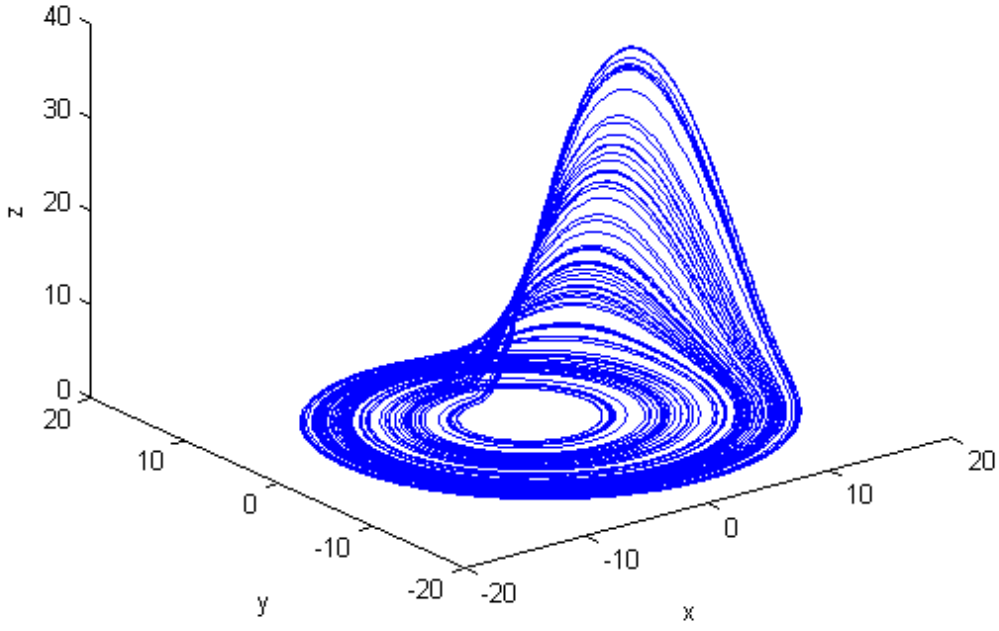

Fig. 4.4 The phase portrait of x, y, z states.

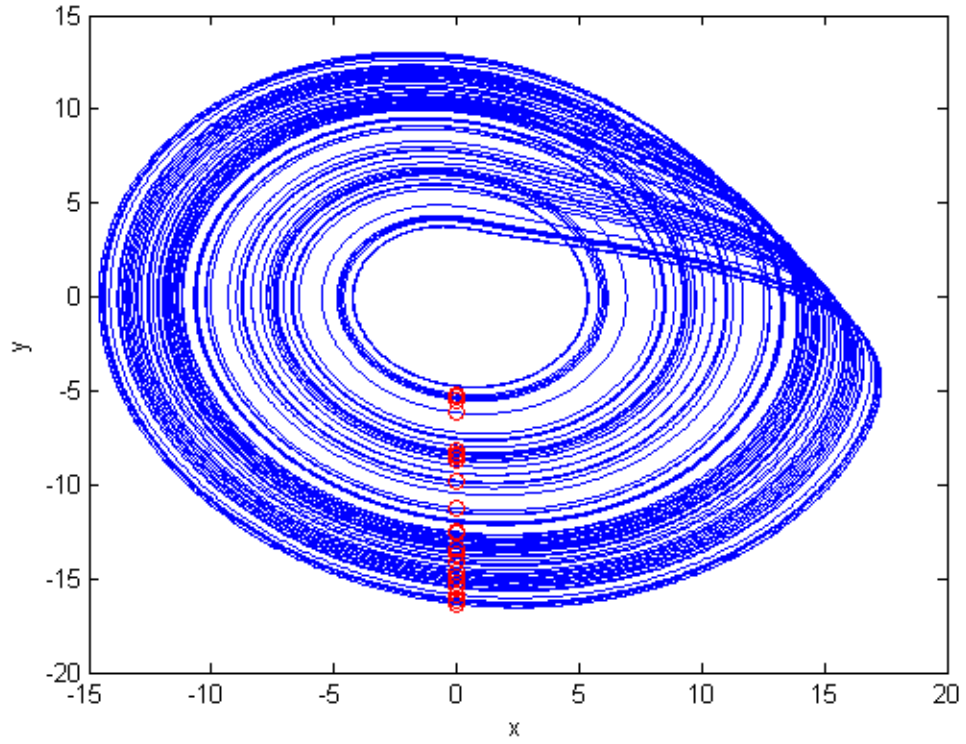

Fig. 4.5 The phase portrait and Poincaré maps of x_1, x_2 states.

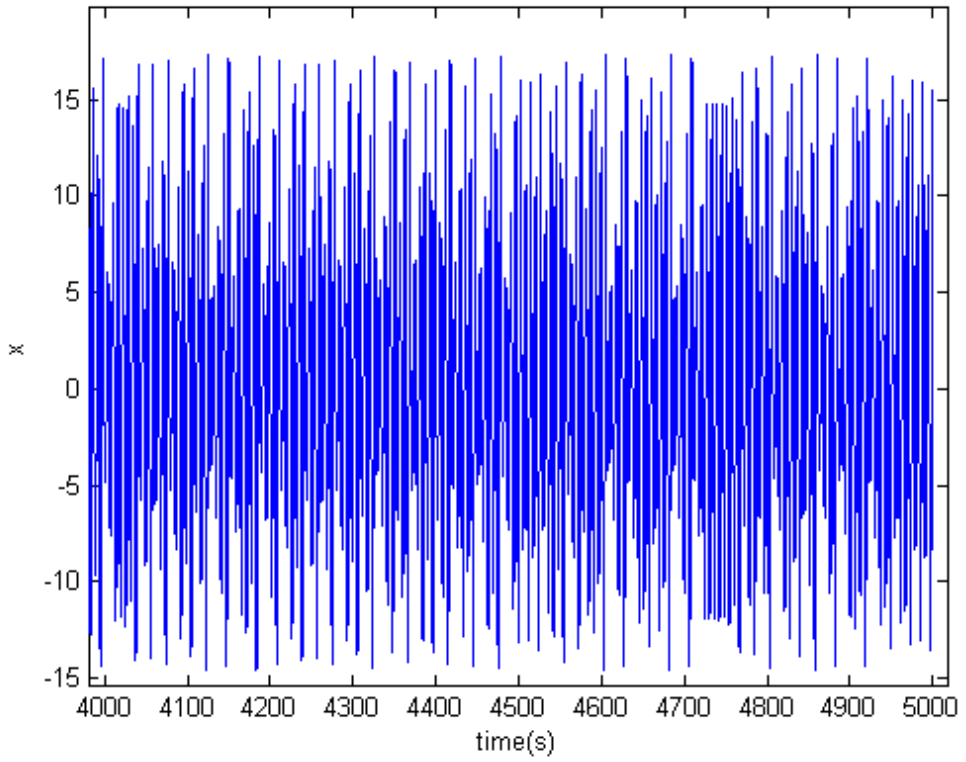

Fig. 4.6 The time histories of the state x.

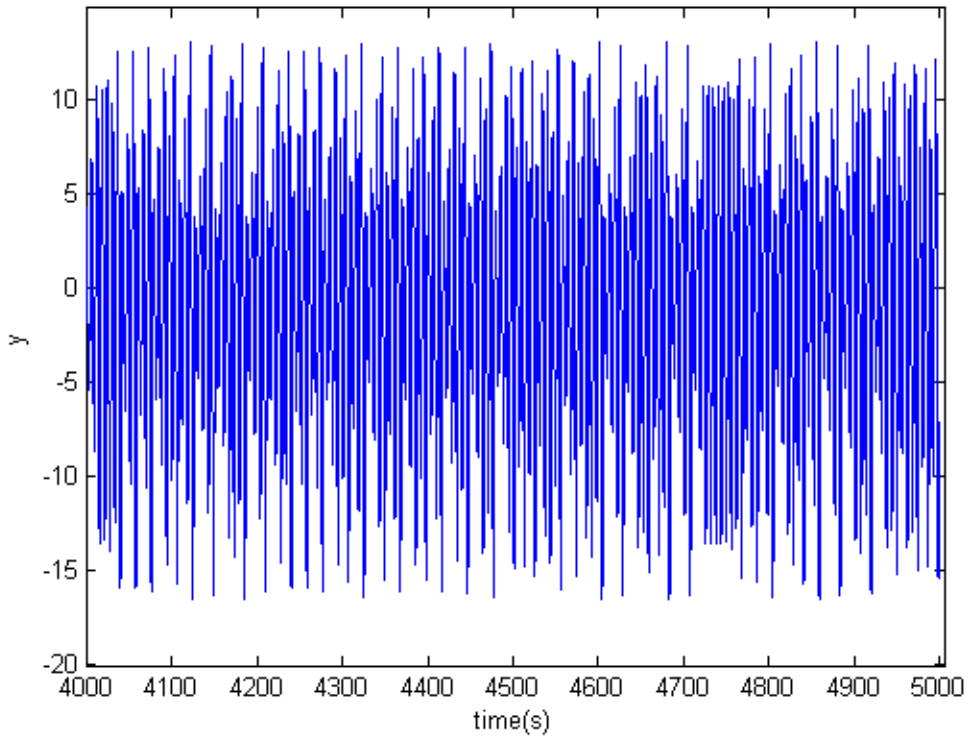

Fig. 4.7 The time histories of the state y.

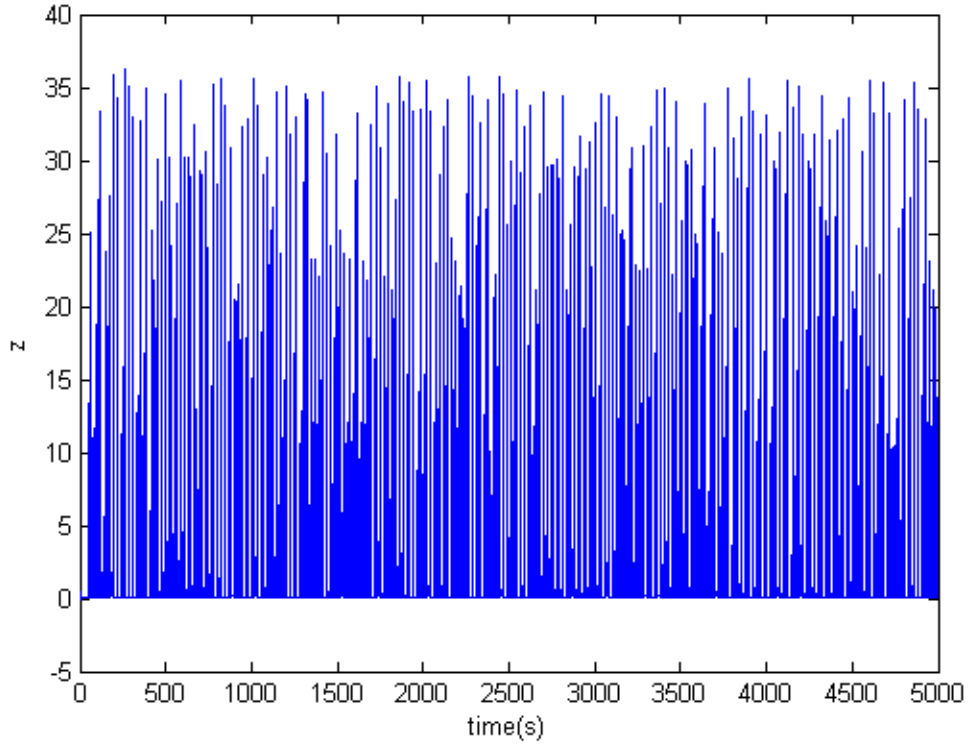

Fig. 4.8 The time histories of the state z.

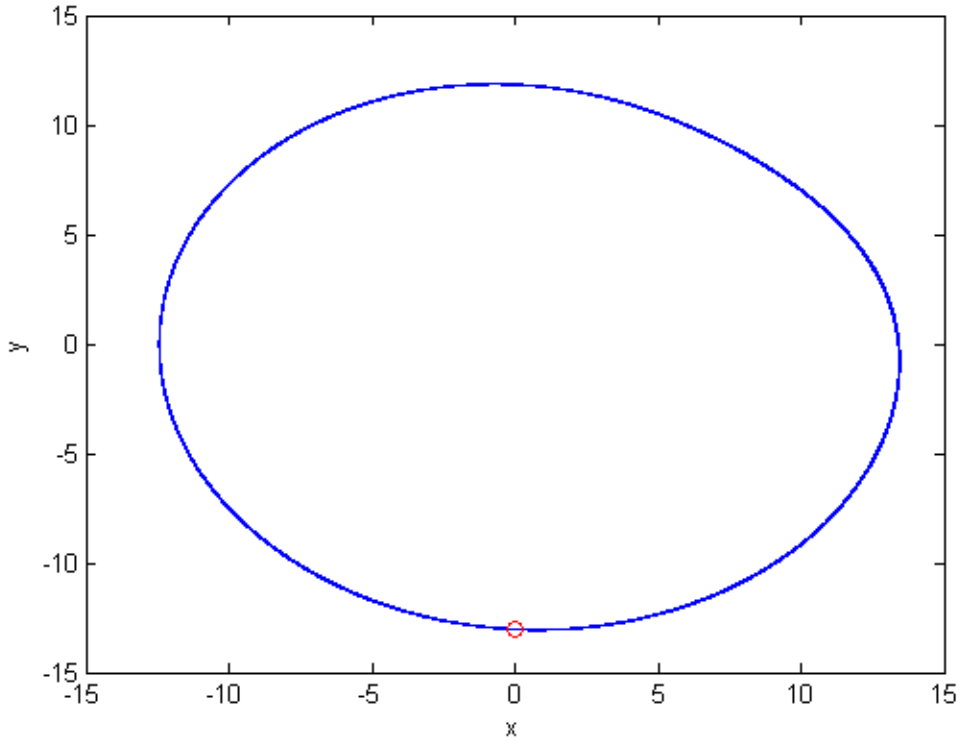

Fig. 4.9 The phase portrait and Poincaré map of x, y states.

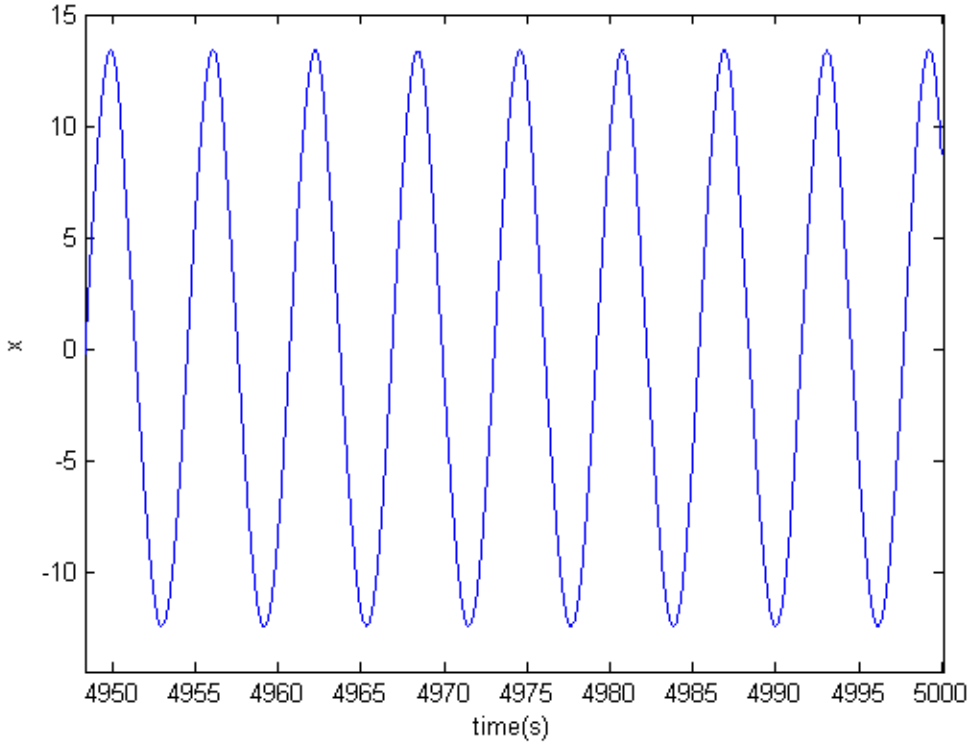

Fig. 4.10 The time history of the state x.

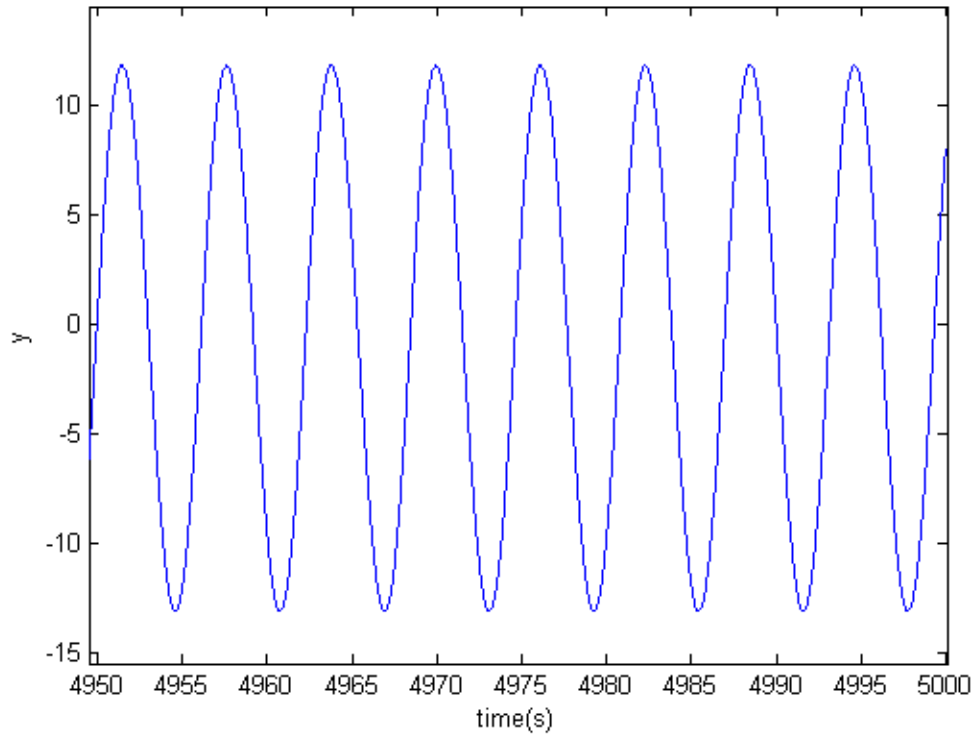

Fig. 4.11 The time history of the state y.

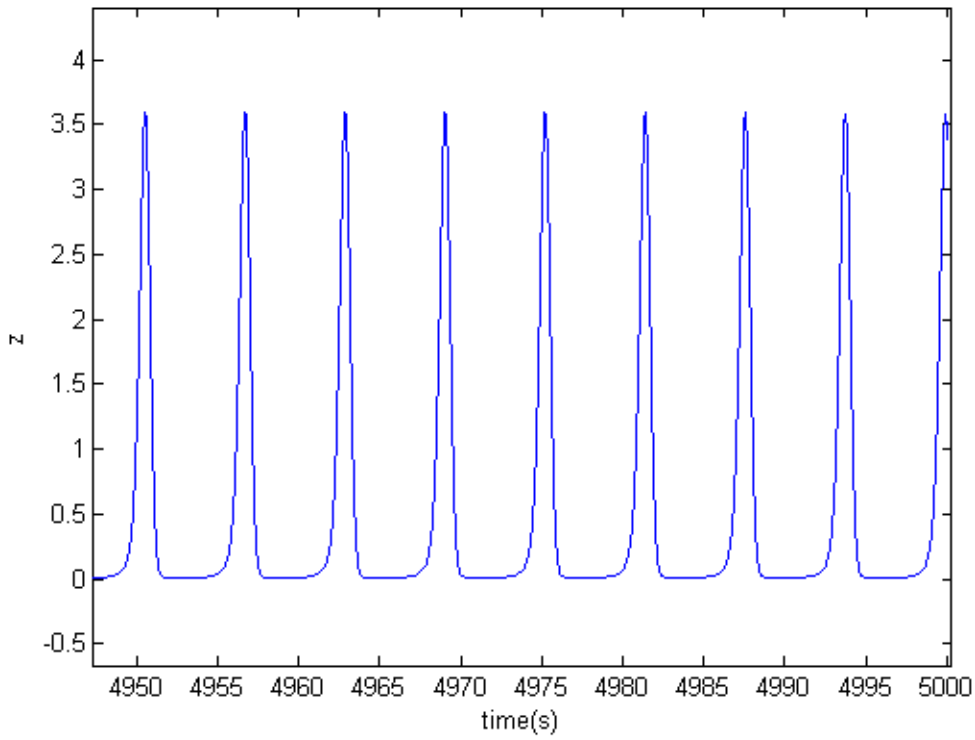

Fig. 4.12 The time history of the state z.

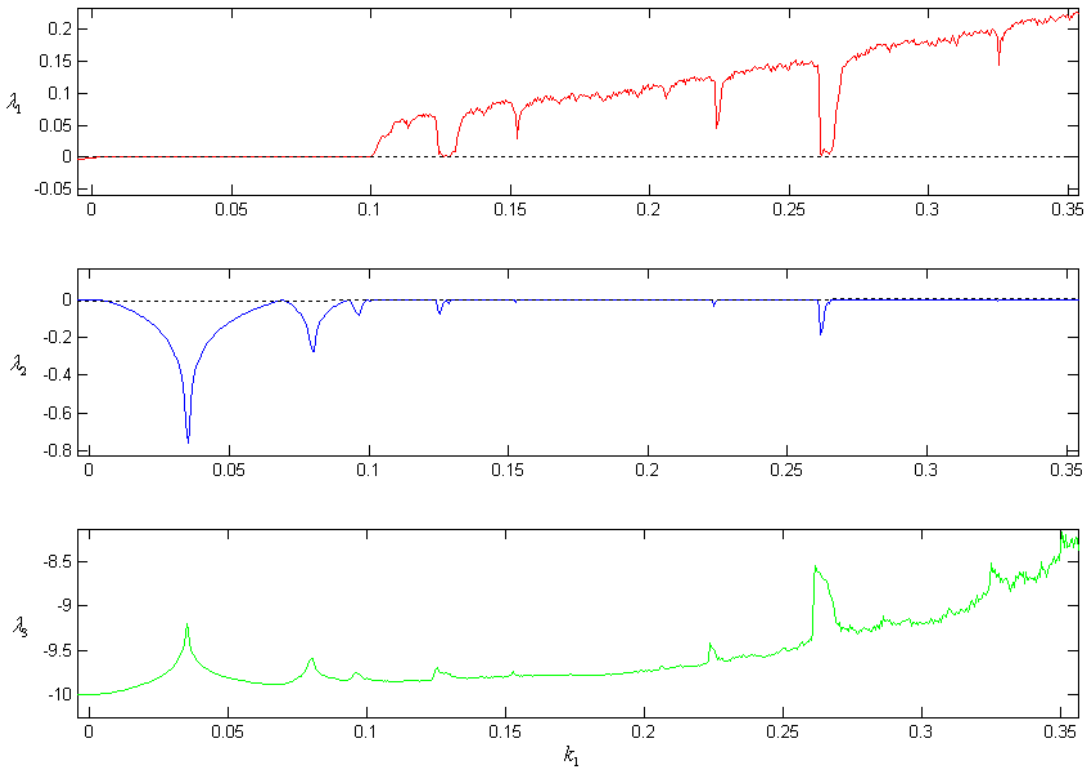

Fig. 4.13 Lyapunov exponents of system (2-2) for varying k_1.

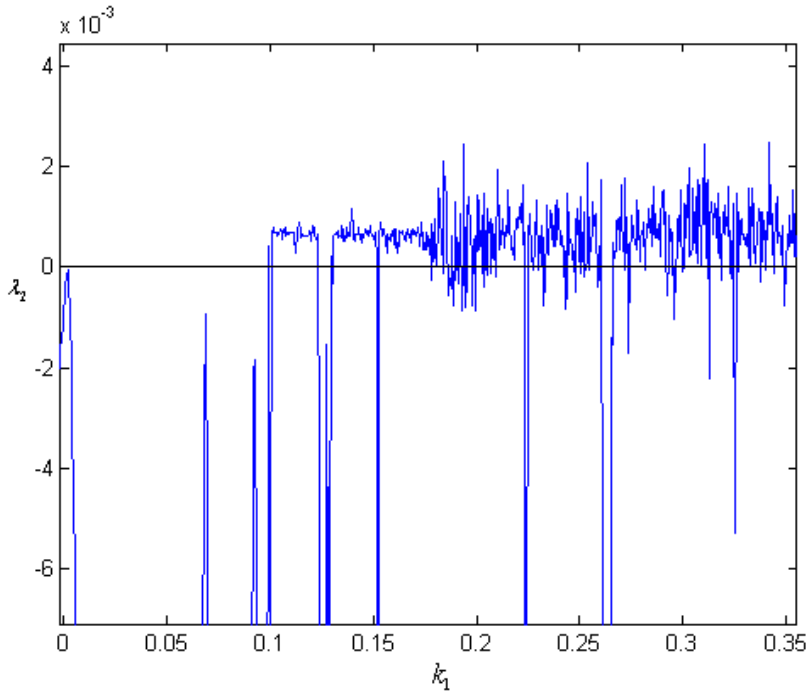

Fig. 4.14 Enlarged figure for λ_2 versus k_1.

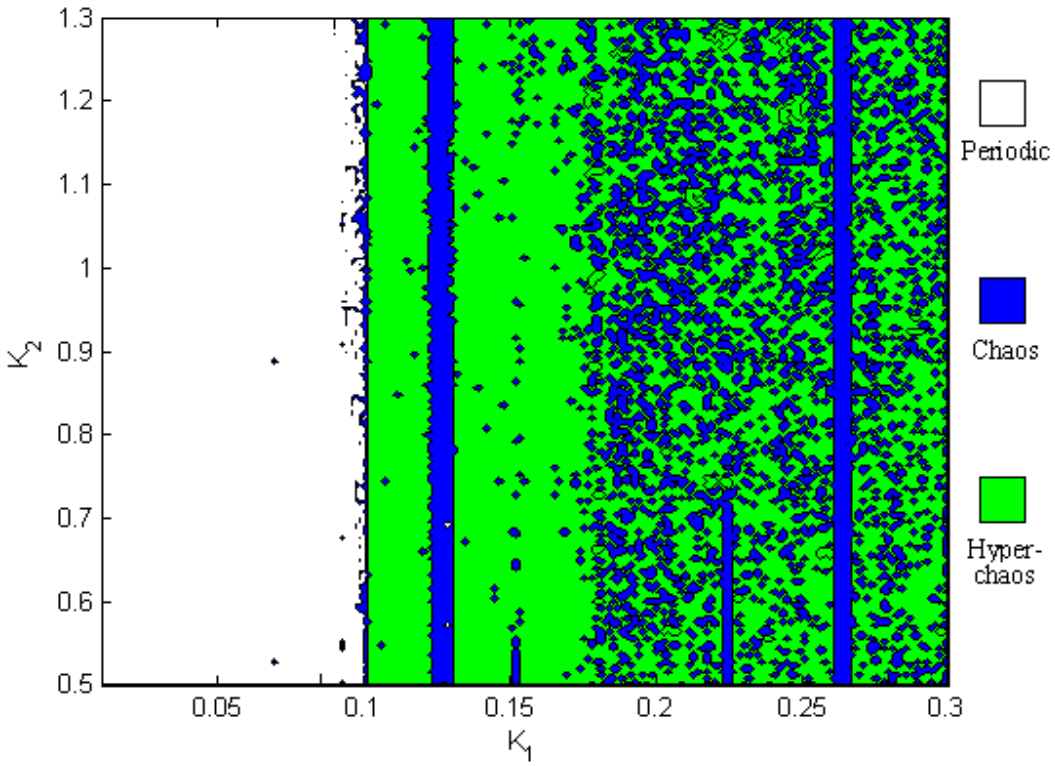

Fig. 4.15The parametric diagram of system (4-2) for varying k_1 and k_2 with $k_3 = 10$.

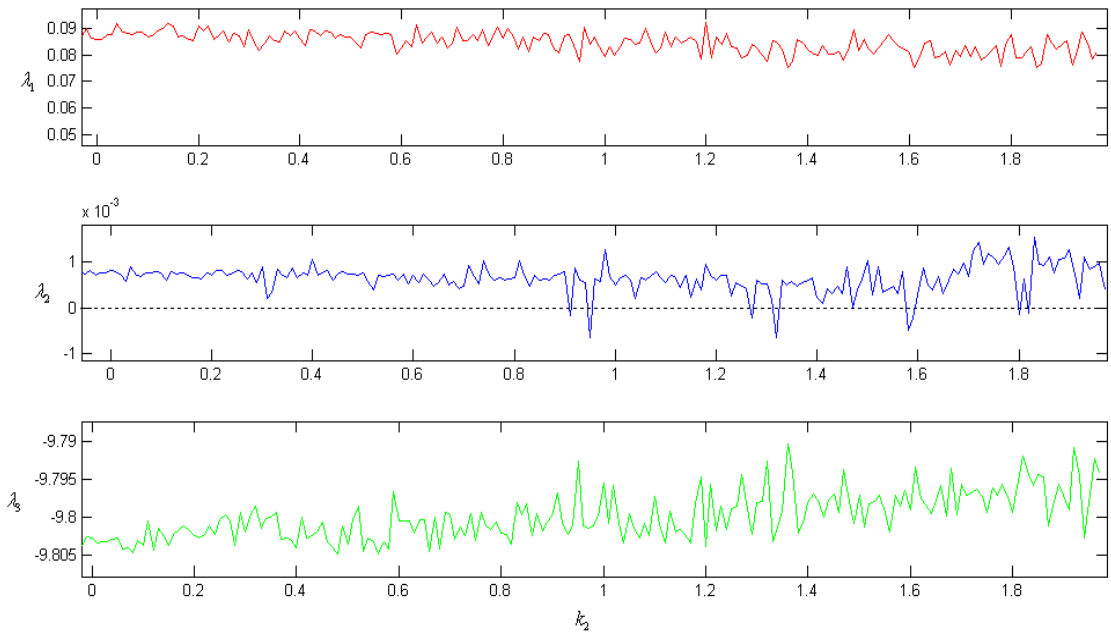

Fig. 4.16 Lyapunov exponents of system (2-2) for varying k_2.

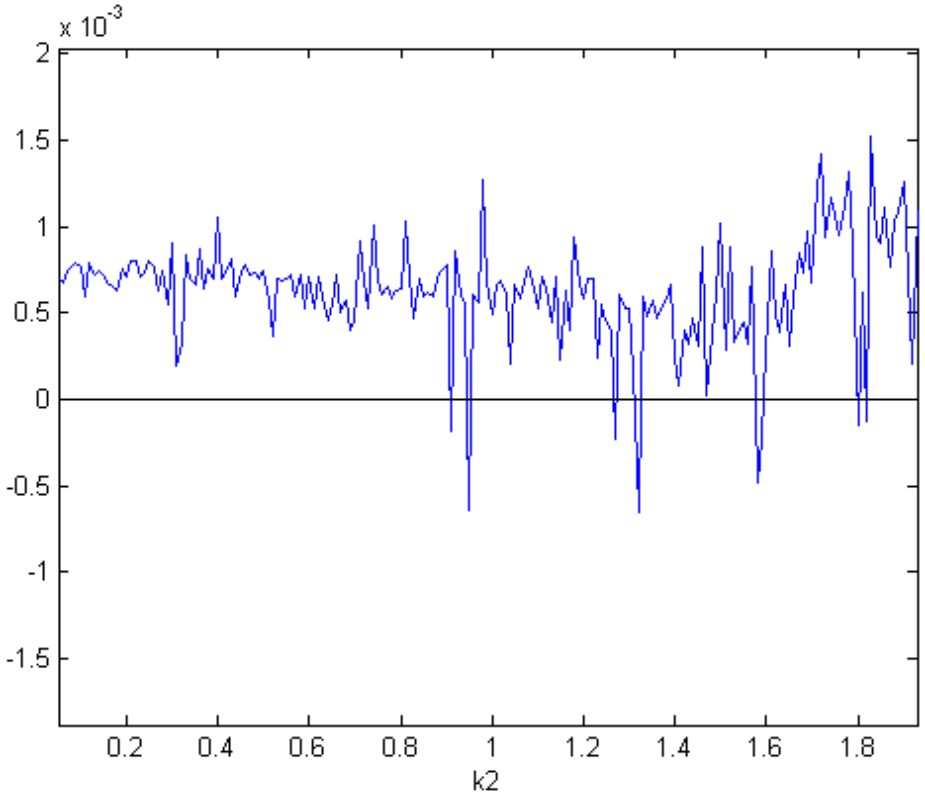

Fig. 4.17 Enlarged figure for λ_2 versus k_2.

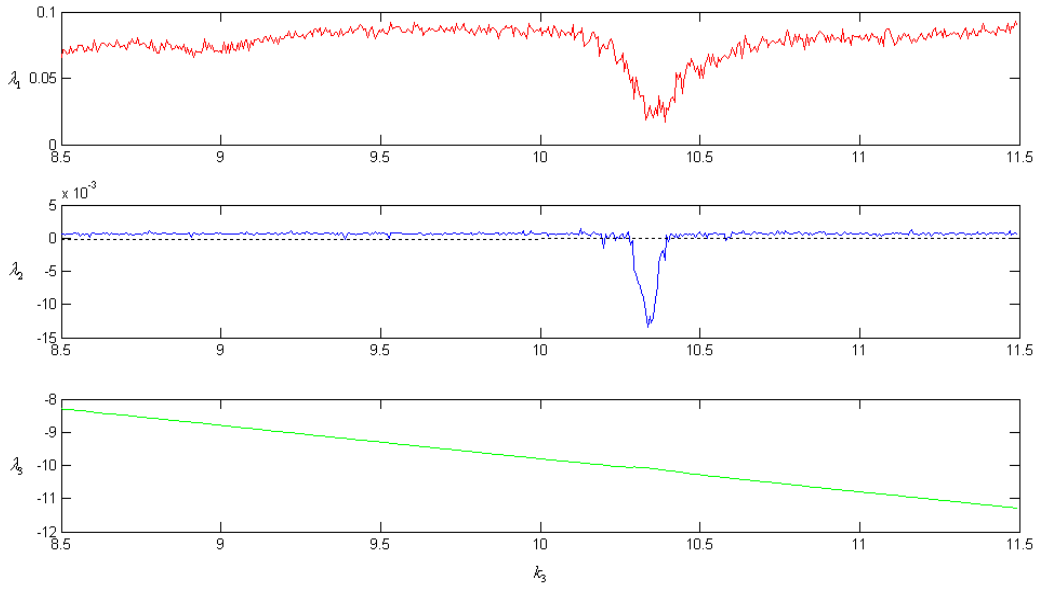

Fig. 4.18 Lyapunov exponents of system (2-2) for varying k_3, with $k_1 = 0.15$ and $k_2 = 0.6$

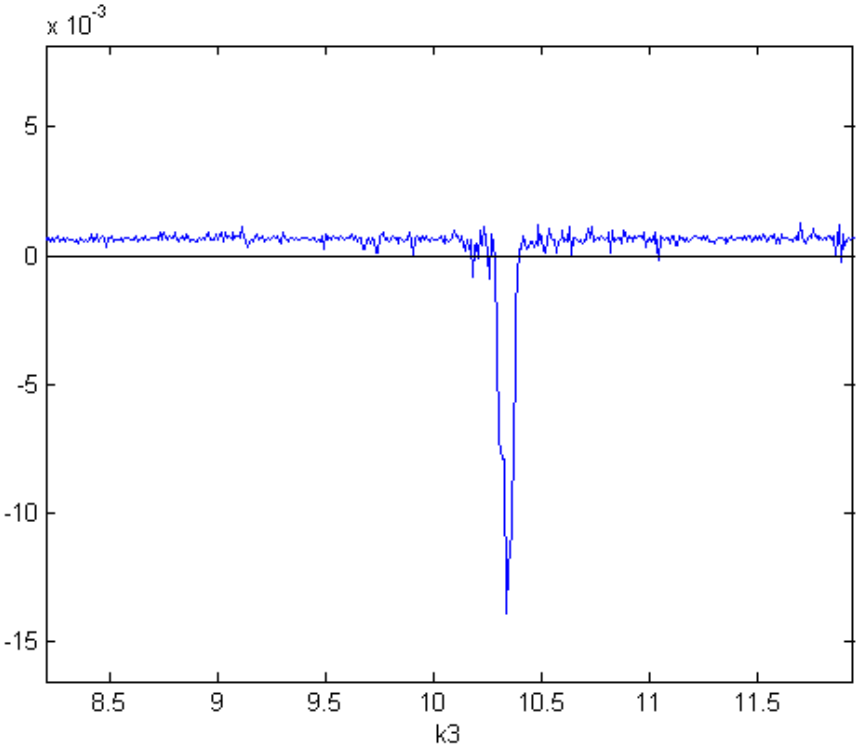

Fig. 4.19 Enlarged figure for λ_2 versus k_3.

Chapter 5

Yin Chaos of a Rössler System

5.1 Preliminaries

In this Chapter, our study is devoted to show the behavior of Yin Rössler system firstly. Simulation results are shown that chaos of Yin Rössler system is appeared when using "*Yin*" parameters. The history of Rössler system is discussed in the first time. To the best of our knowledge, all studies of Rössler system are devoted to Yang Rössler system, there are no articles in making an inquiry about the history of Rössler system up to now. Consequently, the Yin chaos of Rössler system with "*Yin* parameters" is introduced in this Chapter and the behavior of Yin Rössler system is investigated by Lyapunov exponents, Poincaré maps, phase portraits and bifurcation diagram.

5.2 Yang Rössler system

Before introducing the Yin Rössler equation, the Yang Rössler system can be recalled as follow:

$$\begin{cases} \dfrac{dx_1(t)}{dt} = -(x_2(t) + x_3(t)) \\ \dfrac{dx_2(t)}{dt} = x_1(t) + ax_2(t) \\ \dfrac{dx_3(t)}{dt} = b + x_1(t)x_3(t) - cx_3(t) \end{cases} \tag{5-1}$$

when initial condition $x_1(0) = 0.3, x_2(0) = 0.1, x_3(0) = 0.5$ and parameters *a=0.15*, *b=0.2* and *c=10*,chaos of the Yang Rössler system is appeared. The chaotic behavior of Eq. (5-1) is shown in Fig. 5.1~ Fig. 5.3.

5.3 Yin Rössler system

Yin Rössler equations are:

$$\begin{cases} \dfrac{dx_1(-t)}{d(-t)} = -(x_2(-t) + x_3(-t)) \\ \dfrac{dx_2(-t)}{d(-t)} = x_1(-t) + ax_2(-t) \\ \dfrac{dx_3(-t)}{d(-t)} = b + x_1(-t)x_3(-t) - cx_3(-t) \end{cases} \tag{5-2}$$

It is clear that in the left hand sides, the derivative are taken with the back-time. It means Eq. (5-2) aims to find out the Yin behavior of the Rössler system and to comprehend the relation between history and presence. The simulation results are arranged in Table 1:

Table 1 Dynamic behaviors of Yin Rössler system for different signs of parameters

a	b	c	states
-	+	+	Approach to infinity
+	-	+	Approach to infinity
+	+	-	periodic
-	-	+	Approach to infinity
-	+	-	Approach to infinity
-	-	-	Chaos and periodic

Table 1 shows the dynamic behaviors of Yin Rössler system for different signs of parameters. An interesting phenomenon is discovered. When initial condition $x_1(0) = 0.3, x_2(0) = 0.1, x_3(0) = 0.5$ and parameters *a=-0.15, b=-0.2* and *c=-10,*chaos of the Yin Rössler system appears. Therefore, we call these parameters *Yin* parameters. In Chinese philosophy, *Yin* is the negative, past or feminine principle in nature, while *yang* is the positive, present or masculine principle in nature. *Yin* and *Yang* are two fundamental opposites in Chinese philosophy. Consequently, the positive value of parameters, *a=0.15, b=0.2* and *c=10,* in Yang Rössler system can be called *Yang* parameters. The chaotic behavior of Eq. (5-2) is shown in Fig.5.4-Fig. 5.8.

5.4 Other simulation results

In order to research the difference and similarity between Yang and Yin Rössler system, the bifurcation and Lyapunov exponents are used. The simulation results are divided into three parts:

Part1: parameter a is varied and b, c are fixed:

Table 2 Range of parameter a of Yang Rössler system

0.01~0.101	Periodic trajectory
0.101~0.124	Chaos
0.124~0.129	Periodic trajectory
0.129~0.16	Chaos

Table 3 Range of parameter a of Yin Rössler system

-0.01~-0.101	Periodic trajectory
-0.101~-0.125	Chaos
-0.125~-0.129	Periodic trajectory
-0.129~-0.16	Chaos

Table 2 and 3 show different dynamics in the different ranges of parameter a of Yang and Yin Rössler system. In Table 2, the behaviors of Yang Rössler system vary with parameter a, become either chaotic or periodic. When $0.01 \le a \le 0.101$ or $0.124 \le a \le 0.129$, Yang Rössler system is going to become periodic. When $0.101 \le a \le 0.124$ or $0.129 \le a \le 0.16$, chaos appears. Table 3 shows that when parameter When $-0.101 \le a \le -0.125$ or $-0.129 \le a \le -0.16$,the chaotic behavior is shown in Yin Rössler system. When parameter $-0.01 \le a \le -0.101$ and

$-0.125 \le a \le -0.129$, the behaviors of Yin Rössler system are periodic trajectories. Comparing Table 2 and 3, it can be found that there are only chaos and periodic motion in both Yang Rössler system and Yin Rössler system. Bifurcation diagram and Lyapunov exponents are shown in Fig. 5.9and Fig. 5.10.

Part2: parameter b is varied and a, c are fixed:

Table 4 Range of parameter b of Yang Rössler system

0.01~0.47	Chaos
0.47~0.553	Periodic trajectory
0.553~1.078	Chaos
1.078~3.000	Periodic trajectory

Table 5 Range of parameter b of Yin Rössler system

-0.01~-0.462	Chaos
-0.462~-0.555	Periodic trajectory
-0.555~-1.08	Chaos
-1.08~-3.000	Periodic trajectory

Table 4 and 5 show that the behaviors of Yang and Yin Rössler system are similar but not the same. When parameter of b is -1.36, in Yin Rössler system period 2 obviously turns into period 4 .But this phenomenon is not very obvious in Yang Rössler system. Bifurcation diagram and Lyapunov exponents are shown in Fig. 5.11 and Fig. 5.12.

Part3: parameter c is varied and a, b are fixed:

Table 6 Range of parameter c of Yang Rössler system

0.01~5.92	Periodic trajectory
5.92~7.55	Chaos
7.55~7.99	Periodic trajectory
7.99~10.25	Chaos
10.25~10.47	Periodic trajectory
10.47~11	Chaos

Table 7 Range of parameter c of Yin Rössler system

-0.01~-5.92	Periodic trajectory
-5.92~-7.55	Chaos
-7.55~-7.99	Periodic trajectory
-7.99~-10.25	Chaos
-10.25~-10.47	Periodic trajectory
-10.47~-11	Chaos

In Table 6 and 7, the behaviors of Yang and Yin Rössler system are rather similar. but not identical. Bifurcation diagram and Lyapunov exponents are shown in Fig. 5.13 and Fig. 5.14.

5.5 Summary

In this Chapter, the Yin Rössler system is firstly introduced. Via numerical simulation, the Yin Rössler system is compared with the Yang Rössler system. It is found that there are similarity and difference between history and presence. If the *Yang* parameter is one of the chaotic parameters for Yang Rössler system, then the chaotic behavior of the Yin Rössler system can be displayed by using the corresponding *Yin* parameter. Fig. 5.15 and Fig. 5.16 give the summary of similarity and difference between the Yang and Yin Rössler system by bifurcation diagram and Lyapunov exponents. This Chapter explores the importance of Yin chaos of dynamic systems. It would be an epoch-making significance in future.

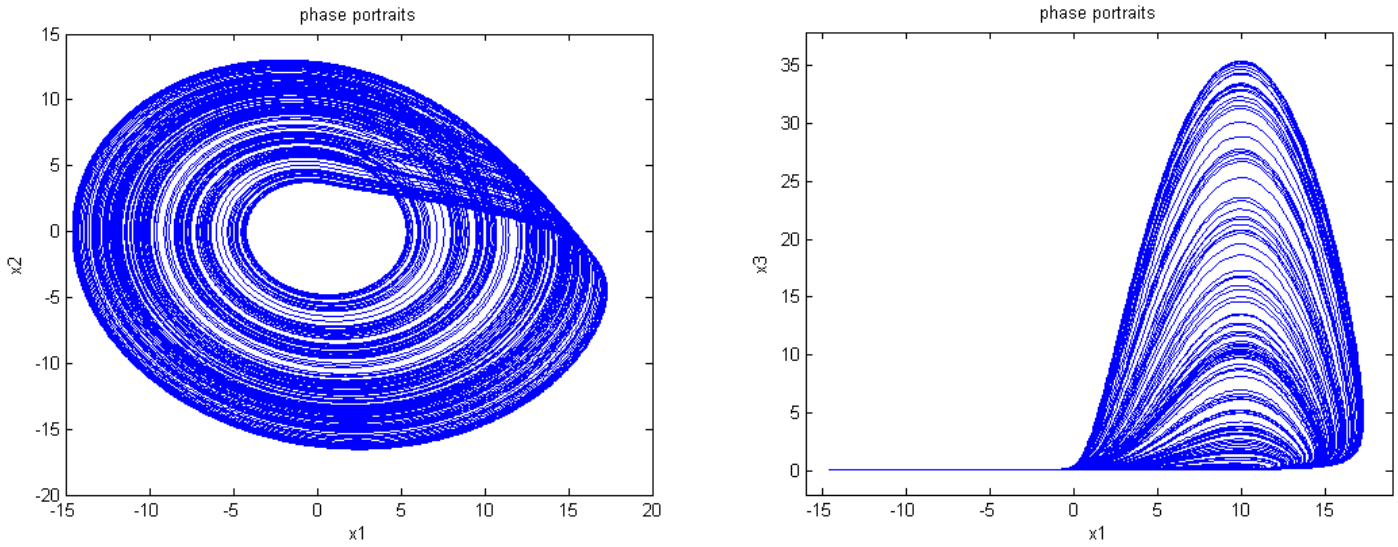

Fig. 5.1 Projections of phase portrait of chaotic Yang Rössler system with *a=0.15*, *b=0.2* and *c=10.*

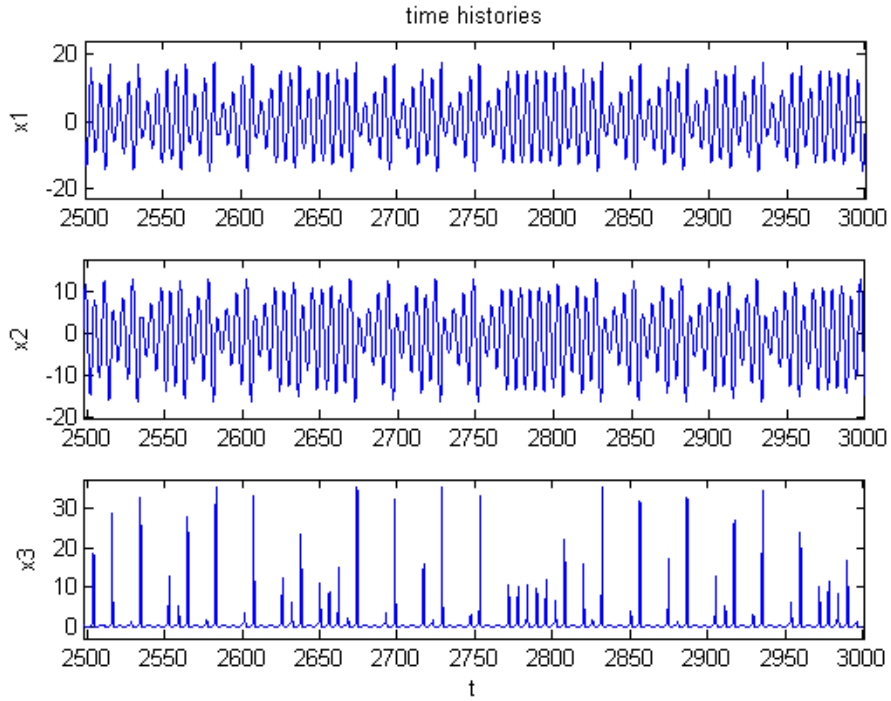

Fig. 5.2 Time histories of three states for Yang Rössler system with *a=0.15*, *b=0.2* and *c=10.*

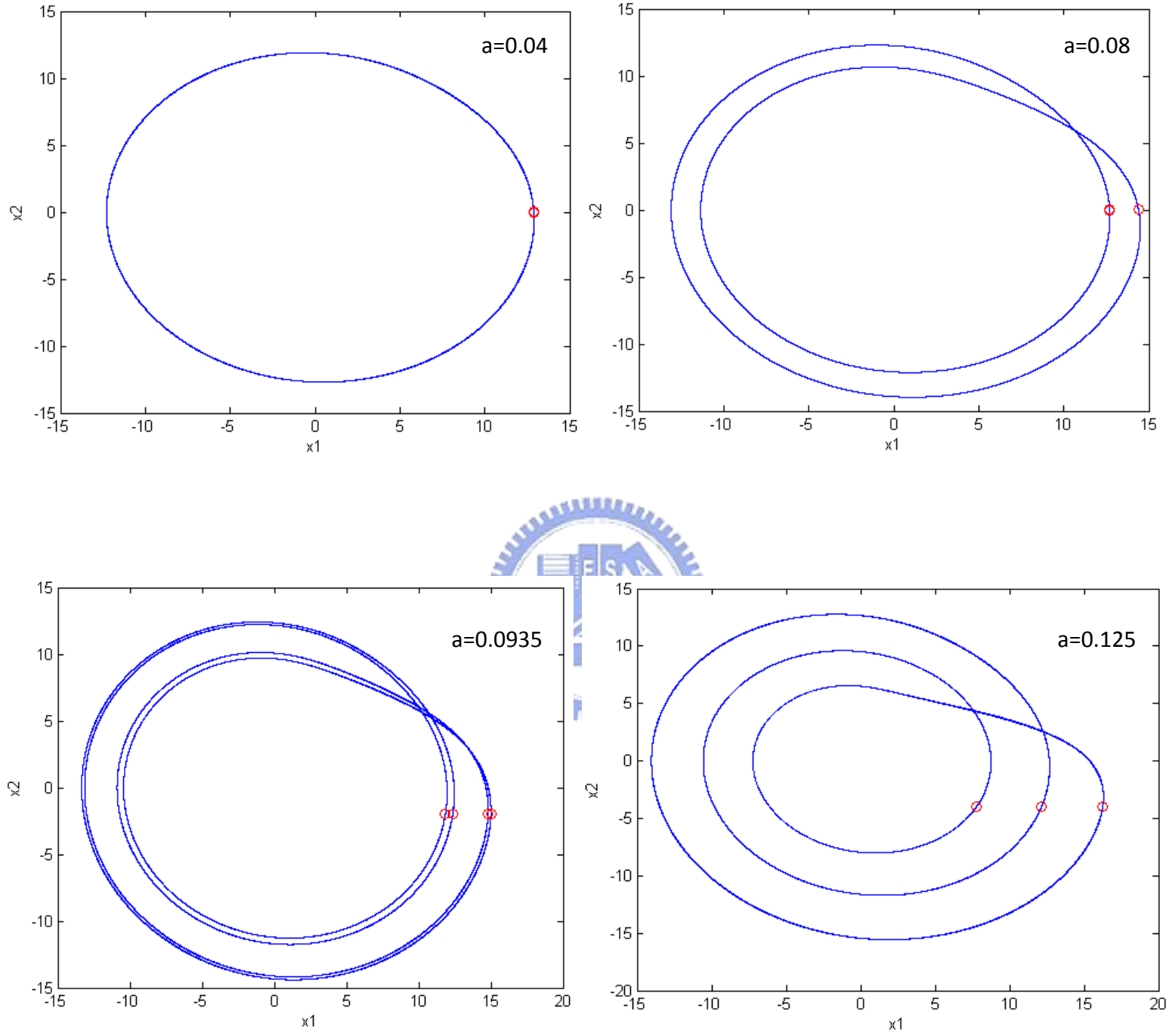

Fig. 5.3 Periodic motions of phase portraits for Yang Rössler system with parameters *b=0.2, c=10.*

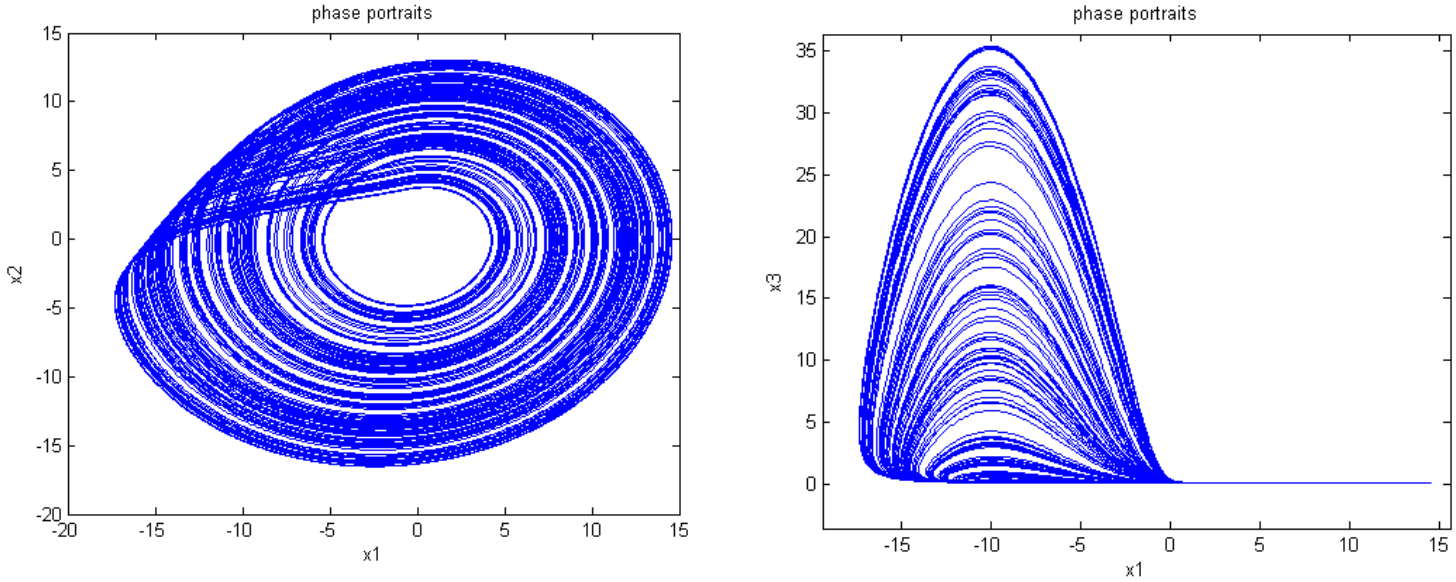

Fig. 5.4 Projections of phase portrait of chaotic Yin Rössler system with *Yin* parameters *a=-0.15, b=-0.2* and *c=-10.*

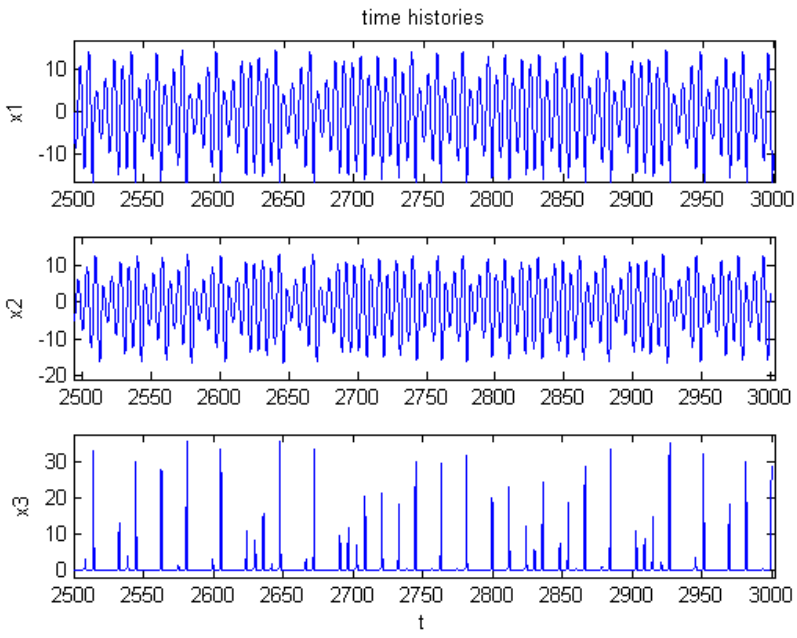

Fig. 5.5 Time histories of three states for Yin Rössler system with *a=-0.15, b=-0.2* and *c=-10.*

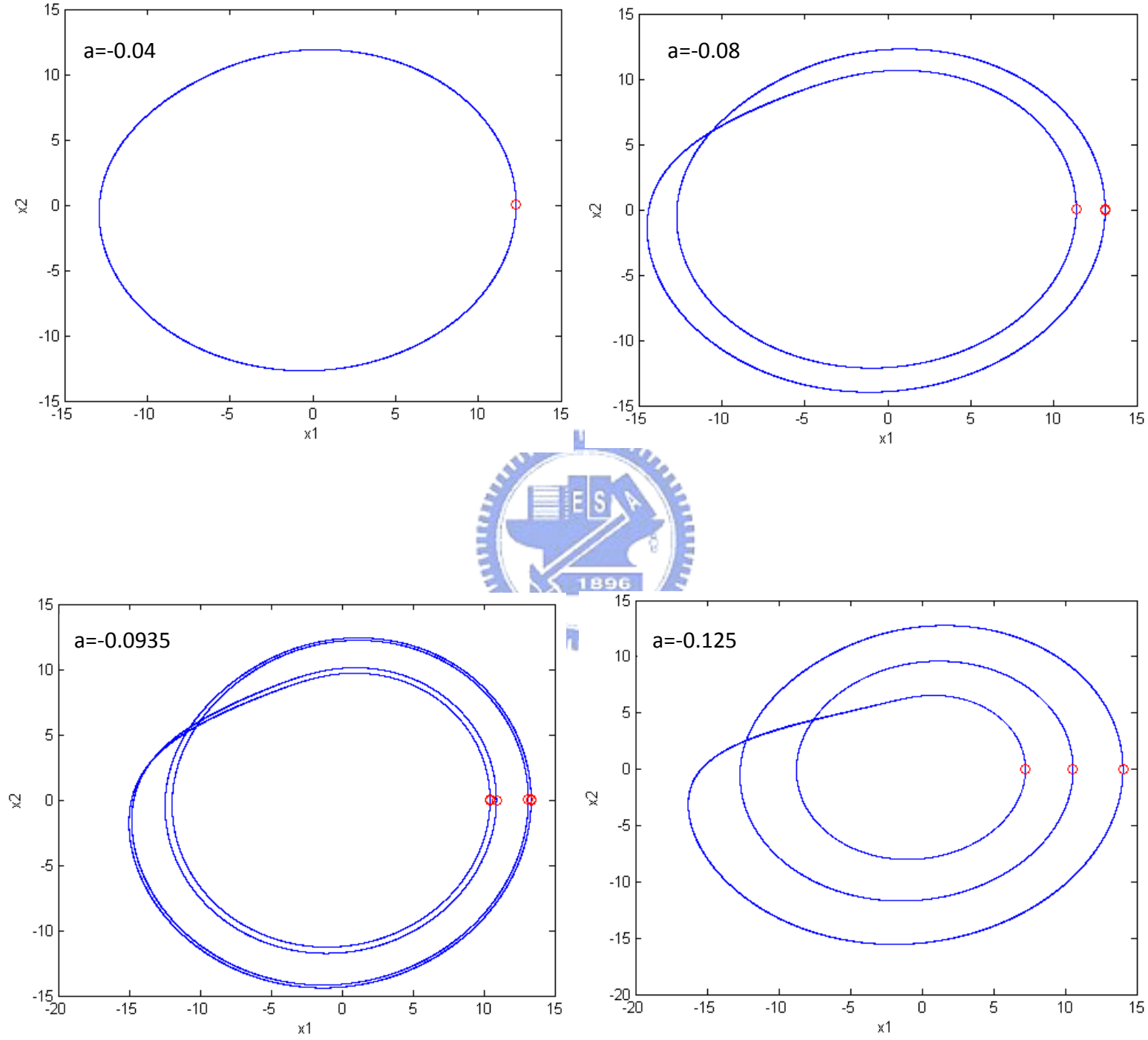

Fig. 5.6 Periodic motion of phase portraits for Yin Rössler system with parameters

b=-0.2, c=-10.

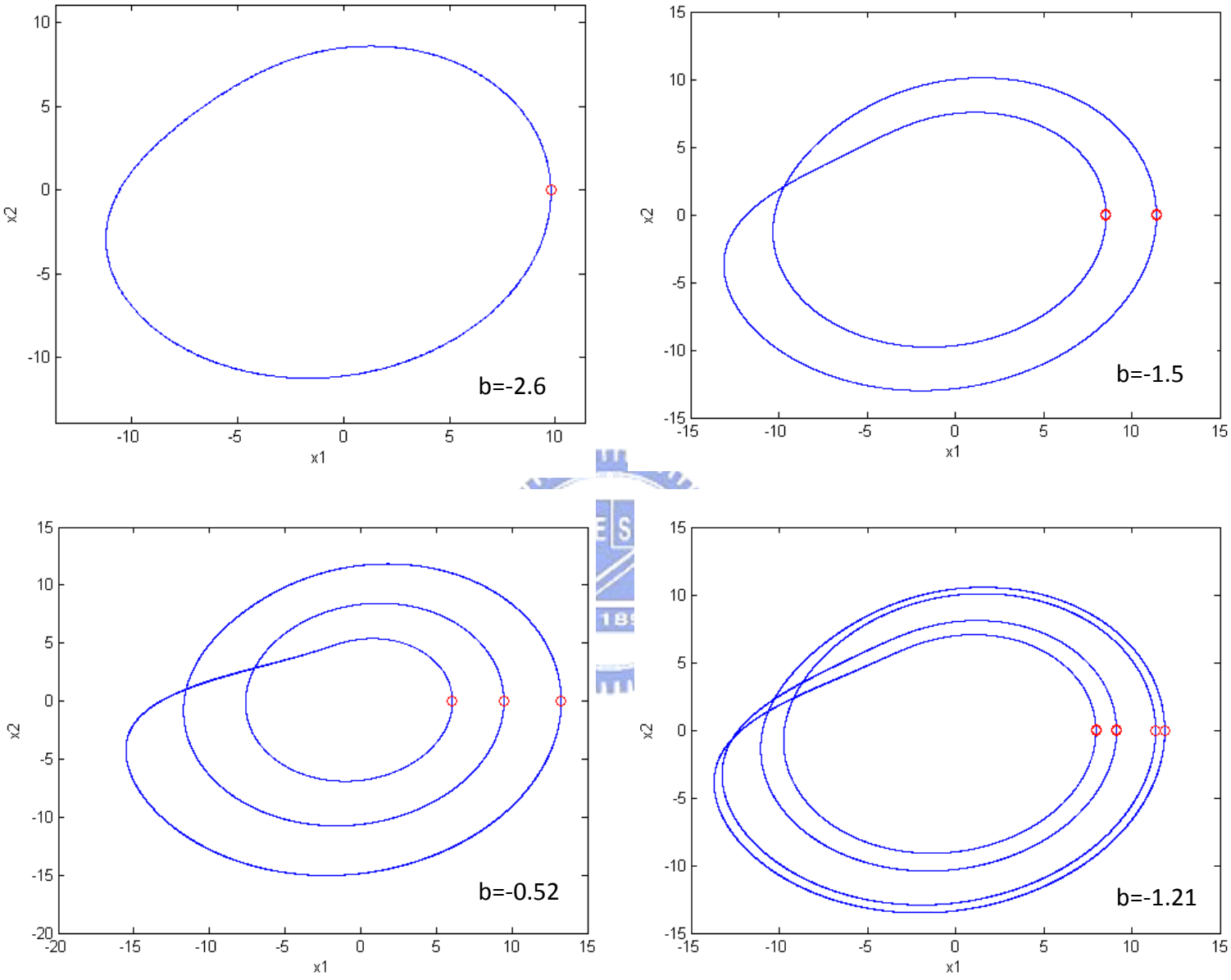

Fig. 5.7 Periodic motion of phase portraits for Yin Rössler system with parameters

a=-0.15, b=-0.2.

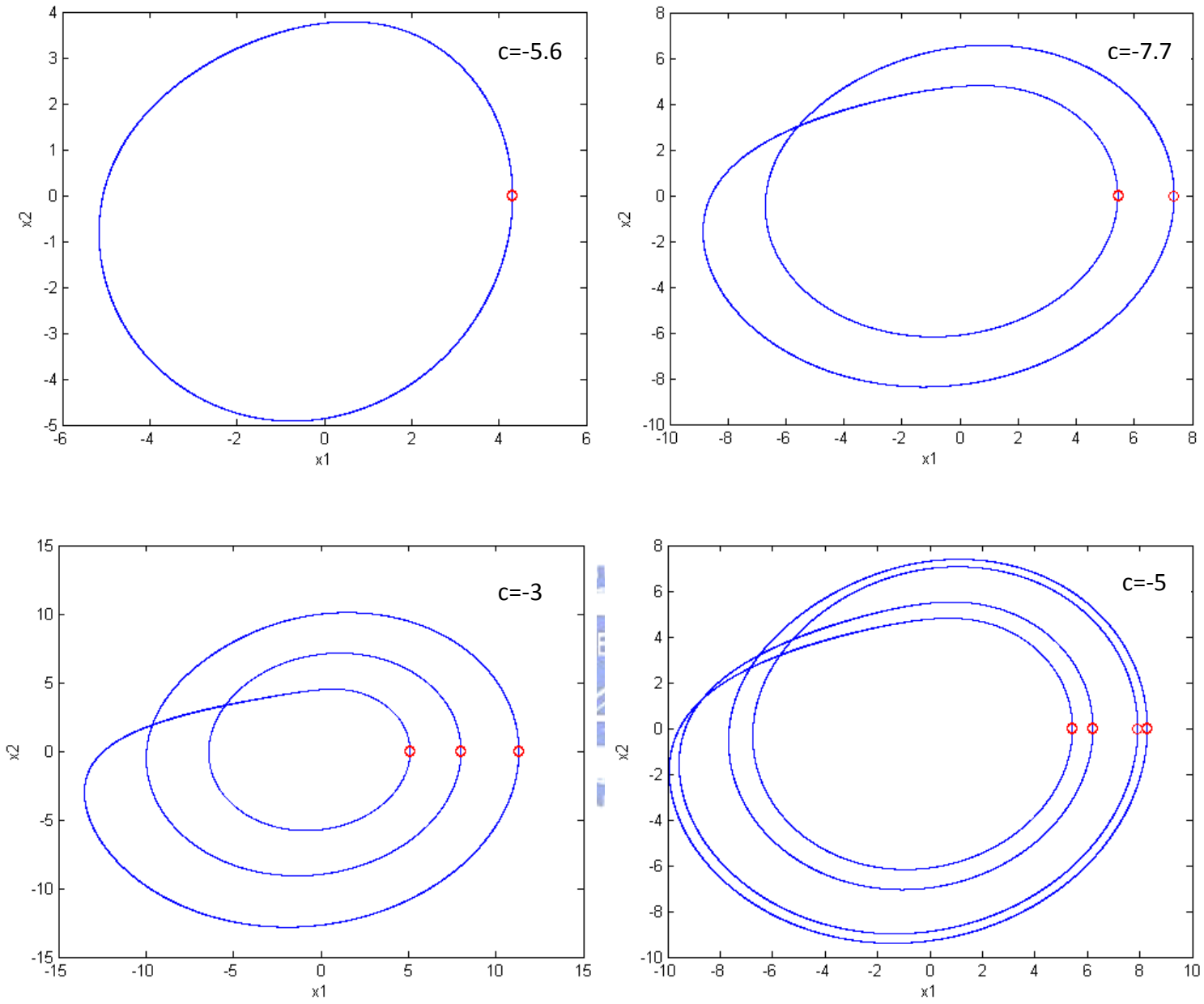

Fig. 5.8 Periodic motion of phase portraits for Yin Rössler system with parameters *a=-0.15, b=-0.2.*

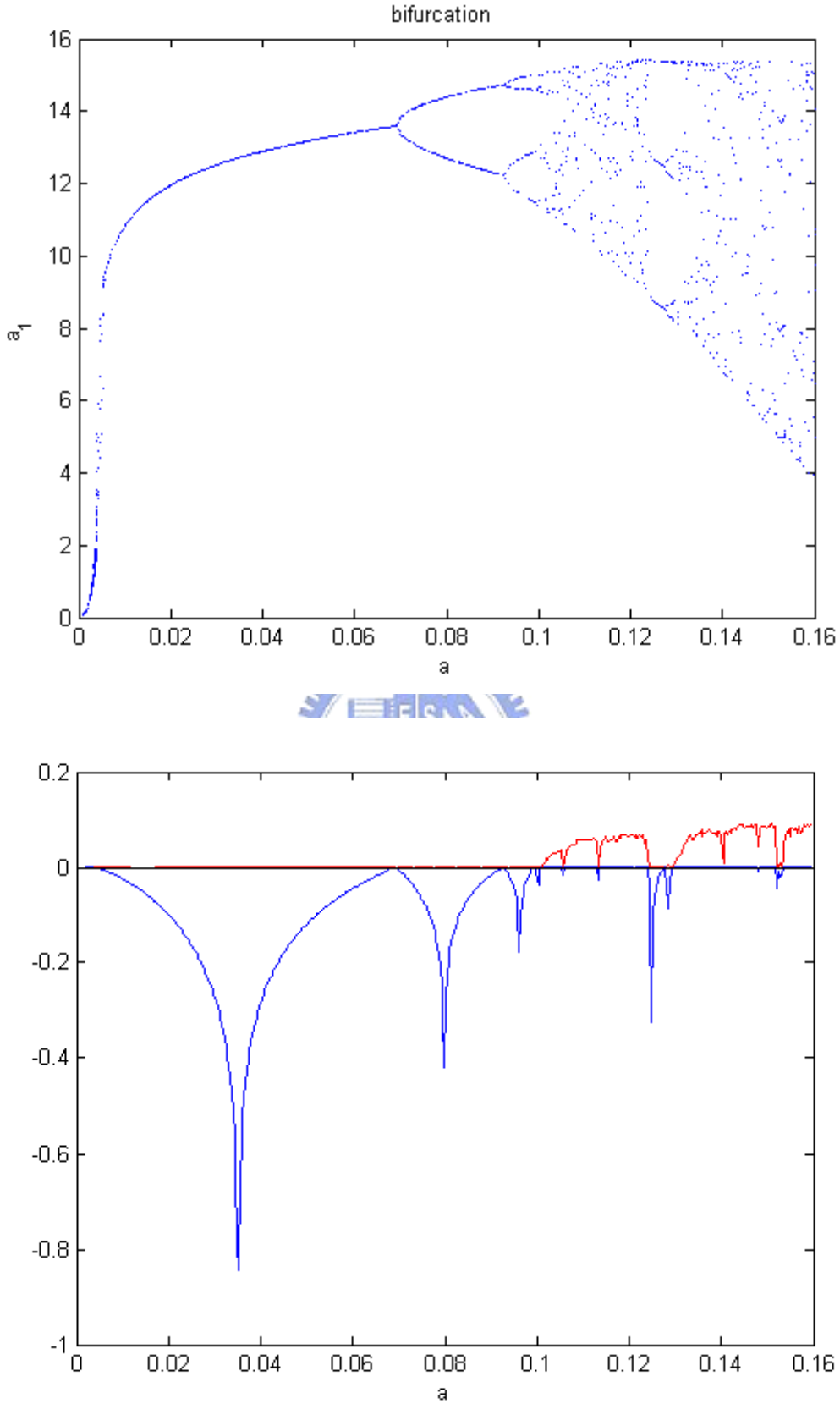

Fig. 5.9 Bifurcation diagram and Lyapunov exponents of chaotic Yang Rössler system with *b=0.2, c=10.*

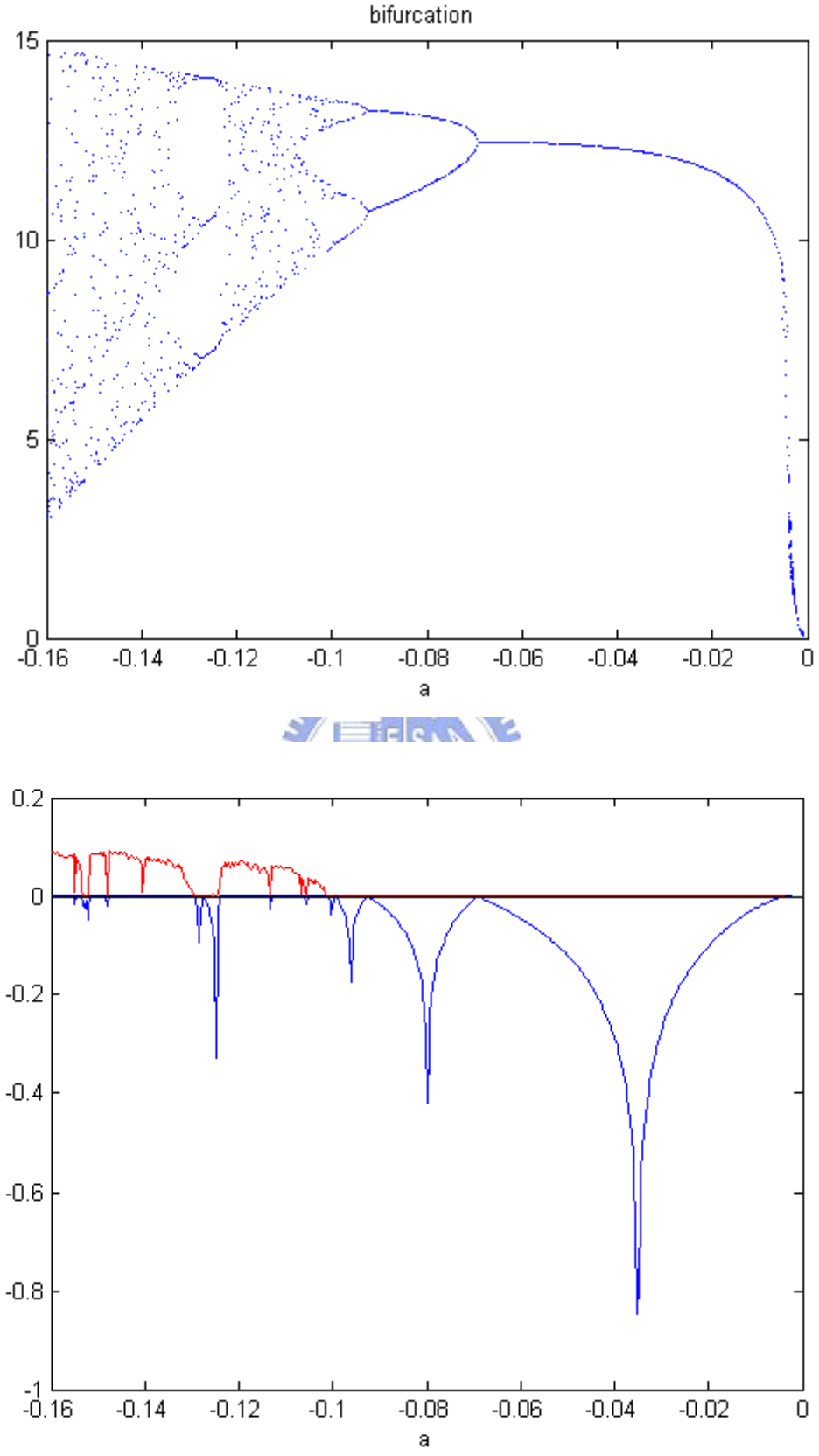

Fig. 5.10 Bifurcation diagram and Lyapunov exponents of chaotic Yang Rössler system with *b=-0.2*, *c=-10.*

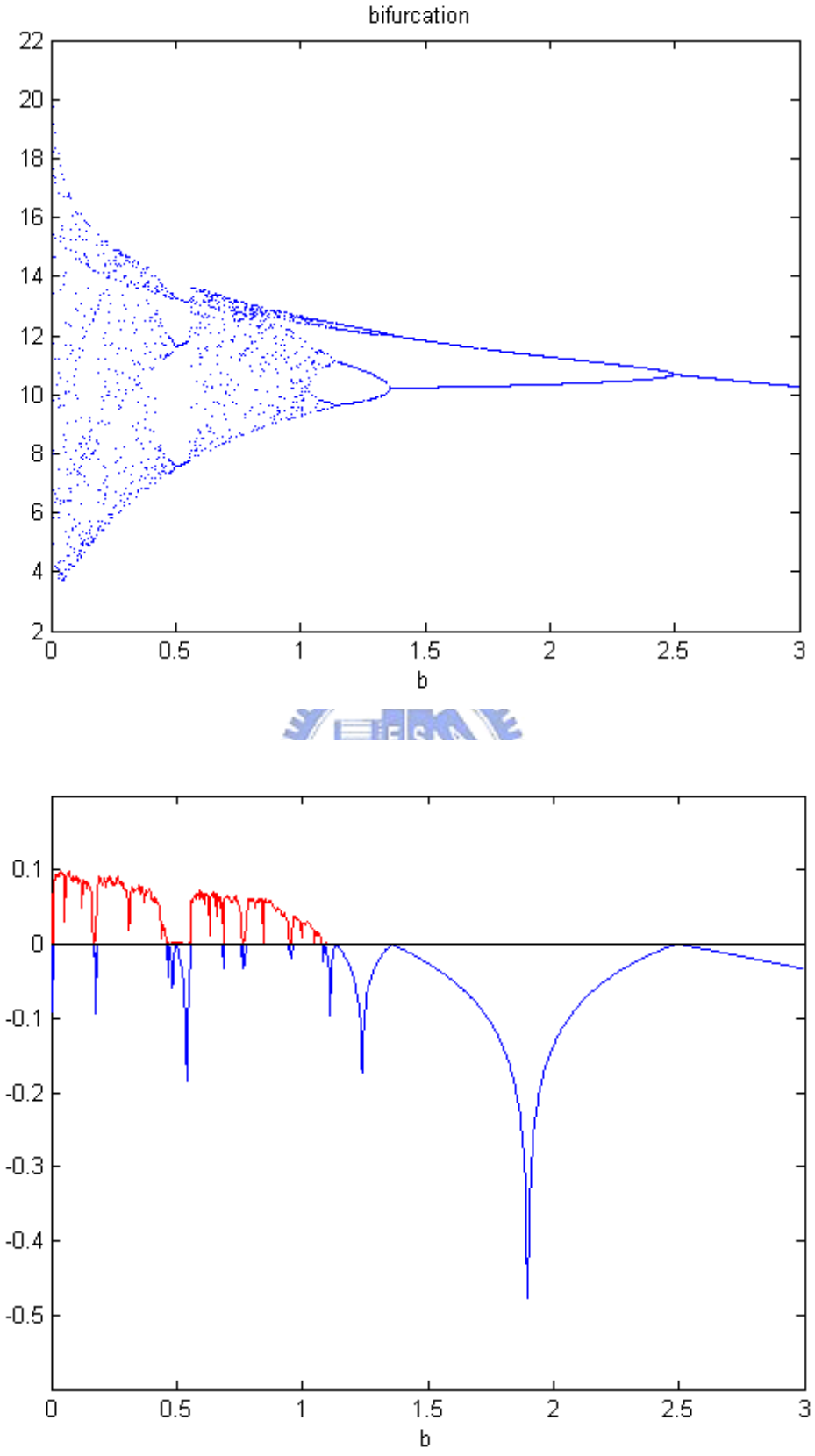

Fig. 5.11 Bifurcation diagram and Lyapunov exponents of chaotic Yang Rössler system with *a=0.15, c=10.*

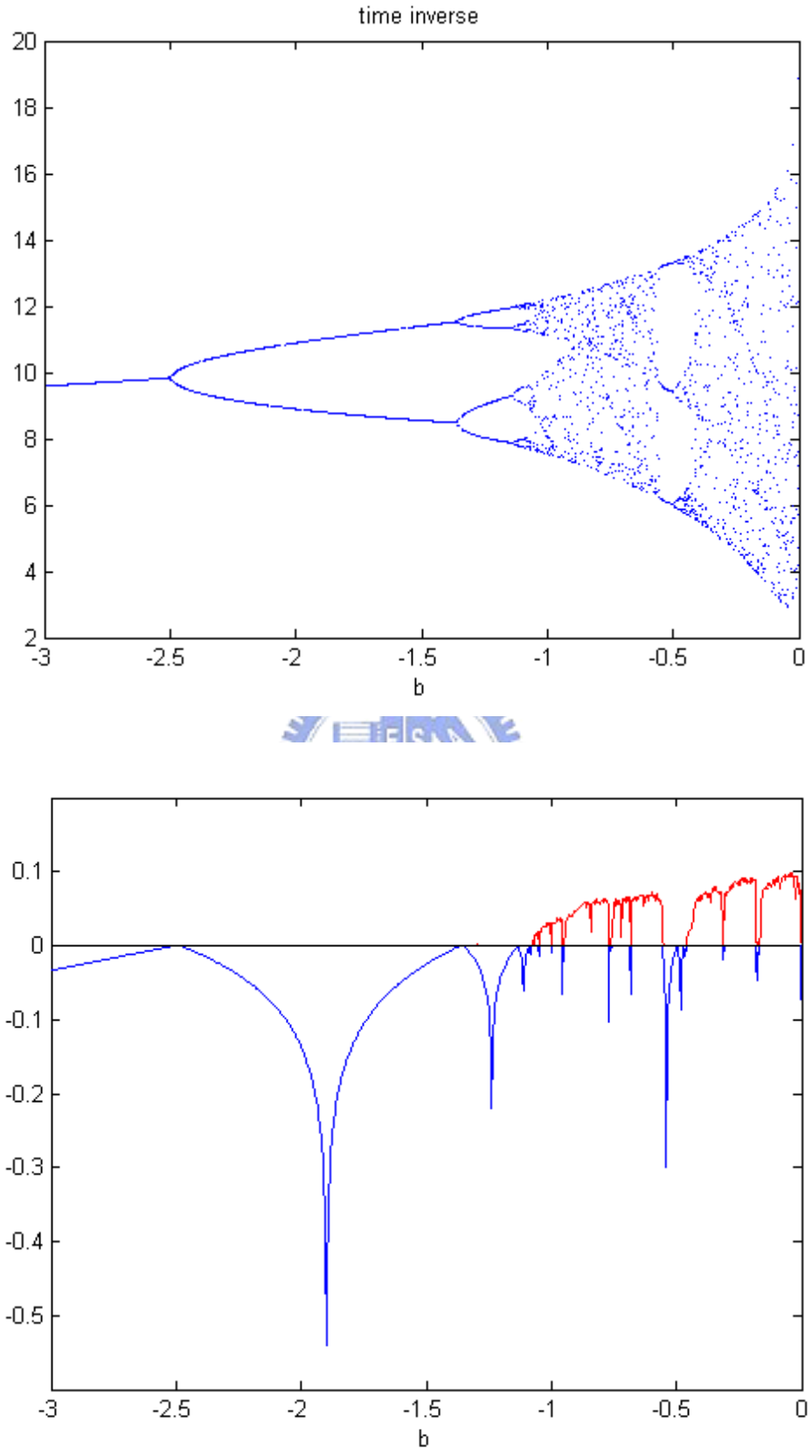

Fig. 5.12 Bifurcation diagram and Lyapunov exponents of chaotic Yang Rössler system with *a=-0.15, c=-10.*

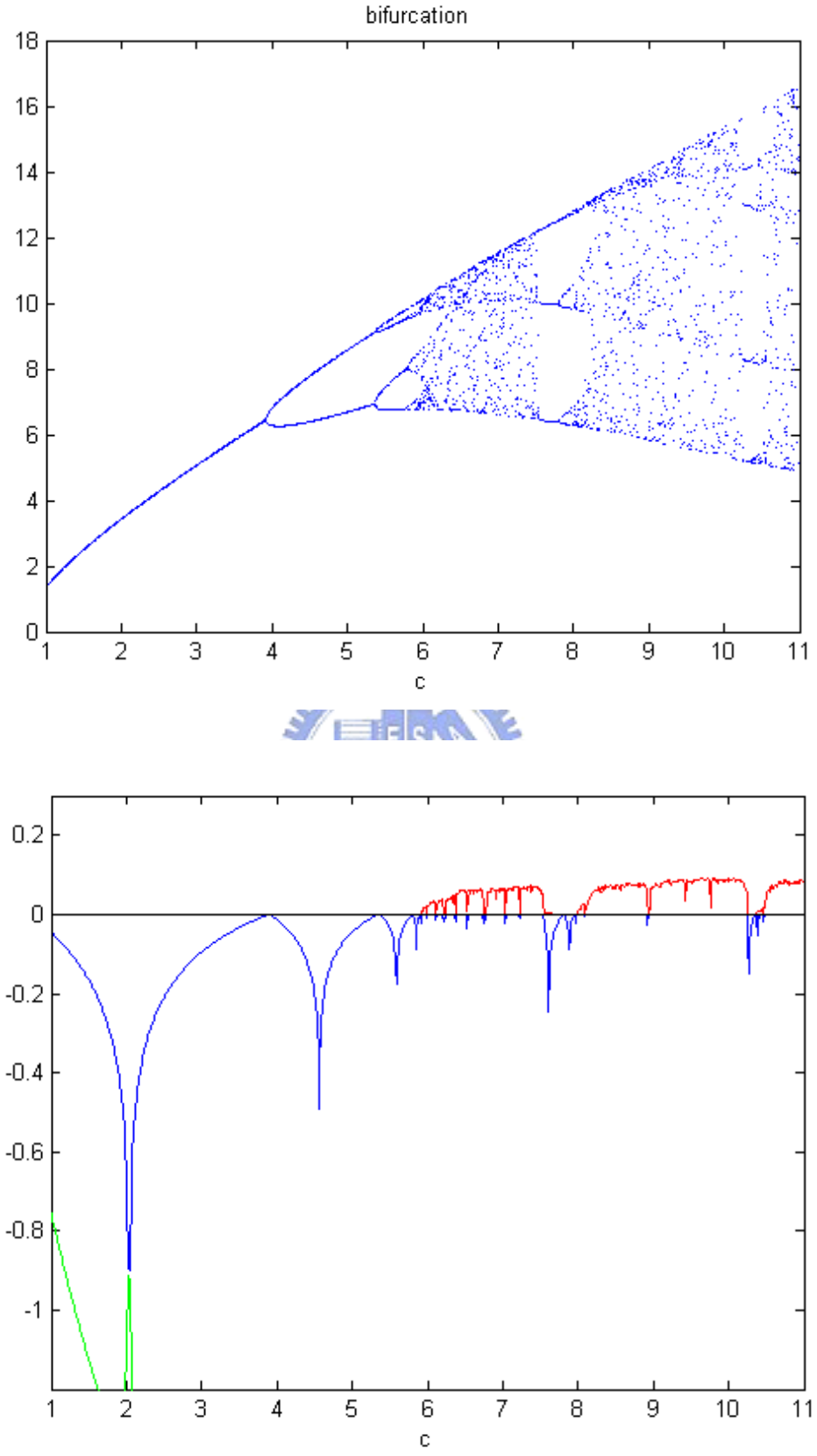

Fig. 5.13 Bifurcation diagram and Lyapunov exponents of chaotic Yang Rössler system with *a=0.15, b=0.2.*

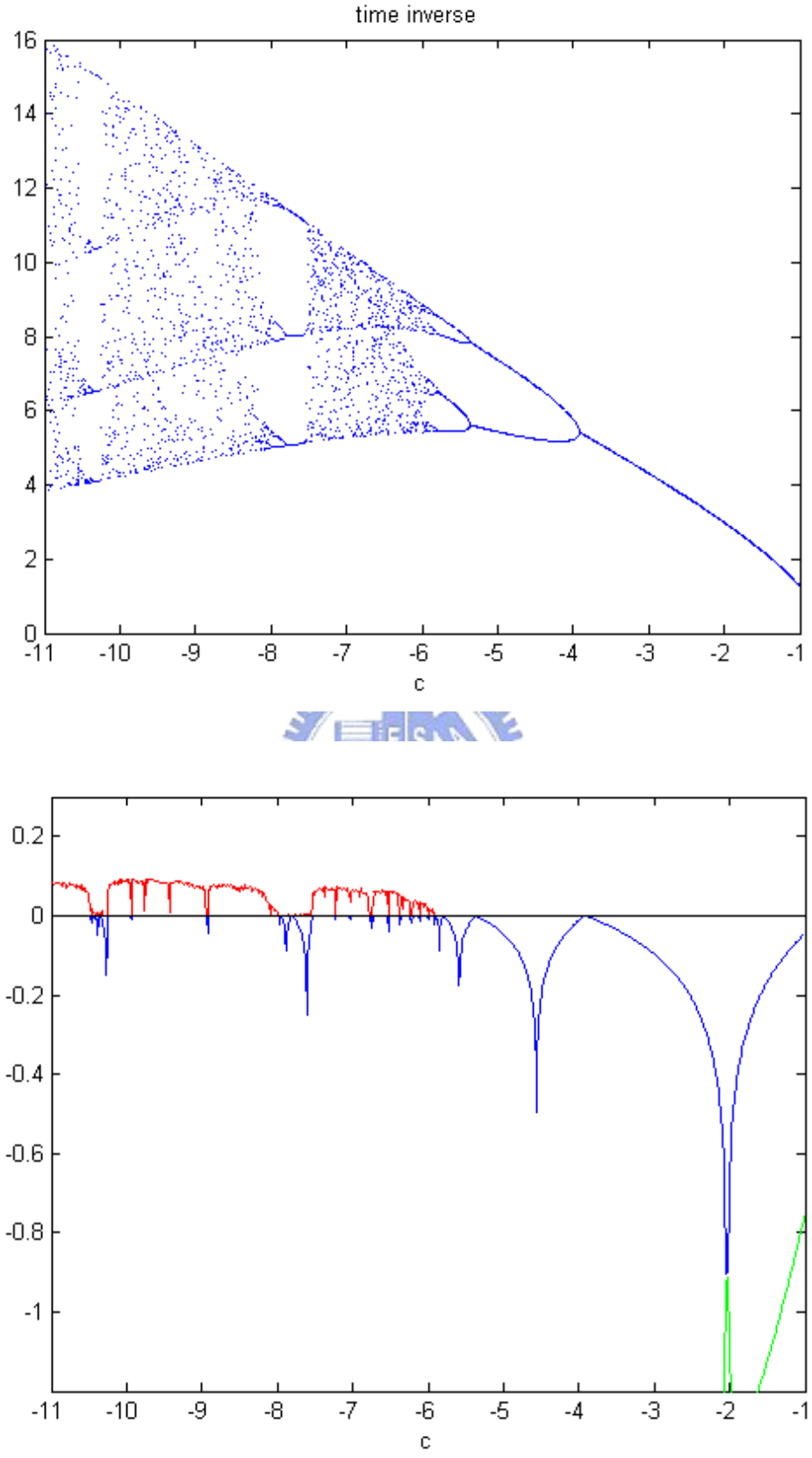

Fig. 5.14 Bifurcation diagram and Lyapunov exponents of chaotic Yang Rössler system with *a=-0.15, b=-0.2.*

Present	Past
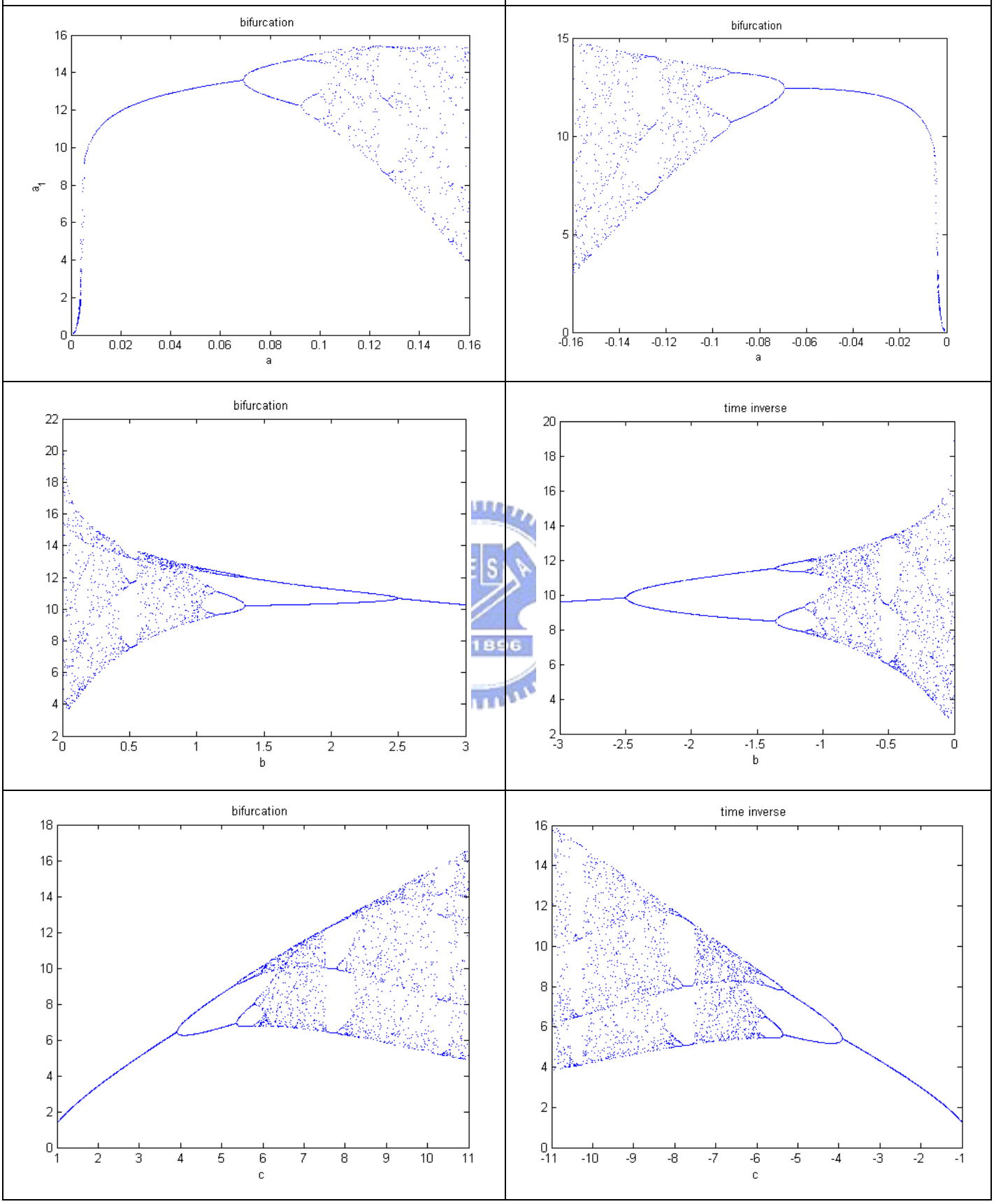	

Fig. 5.15 Comparison between the Yang and Yin Rössler system bifurcation diagrams.

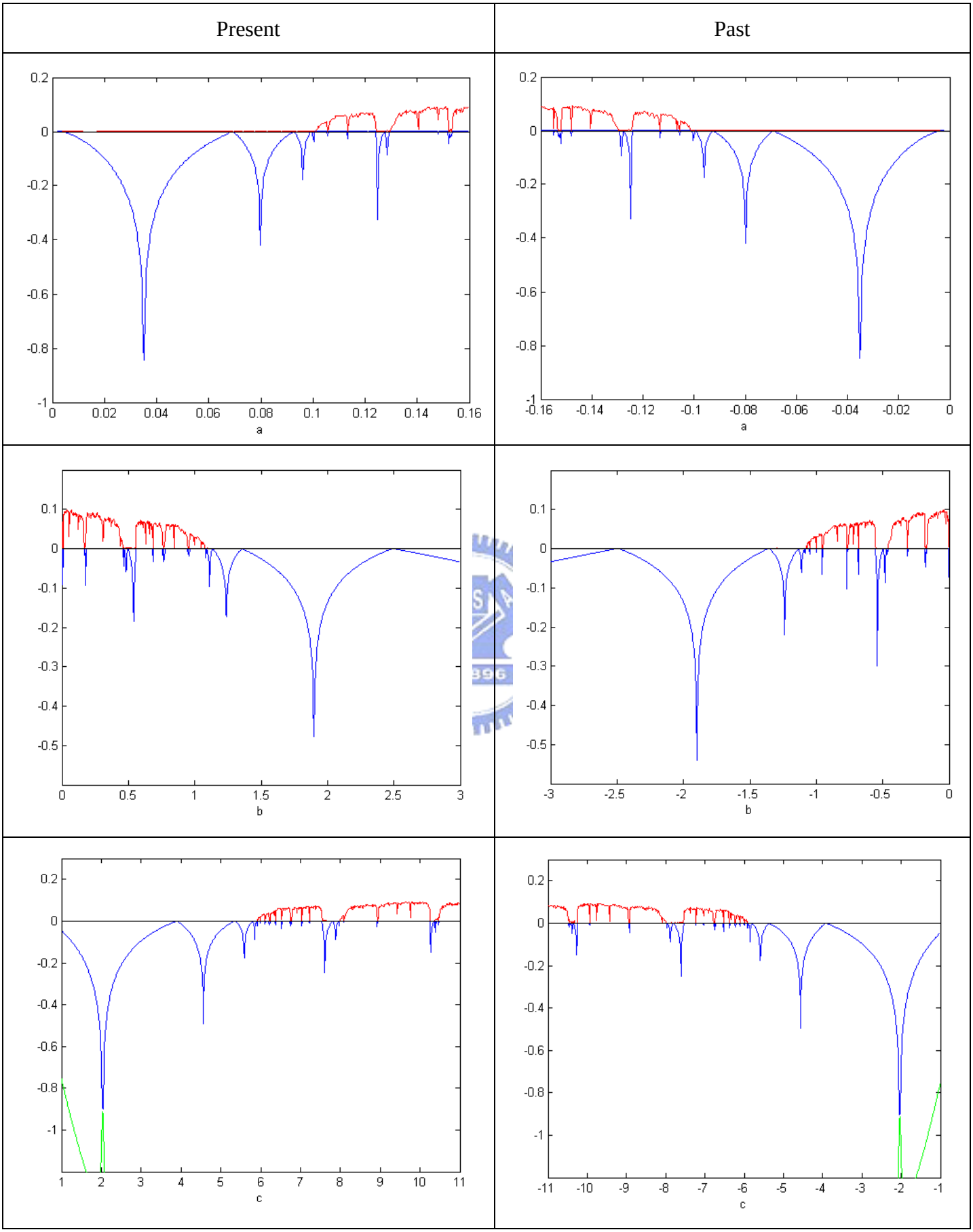

Fig. 5.16 Comparison between the Yang and Yin Rössler system Lyapunov exponents.

Chapter 6

Projective Yin-Yang Generalized Synchronization of Chaos with Uncertain Parameters by Pragmatical Asymptotically Stability Theorem

6.1 Preliminaries

In this Chapter, our study is devoted to a pragmatical hybrid projective chaotic synchronization of two chaotic systems, i.e. Yang Rössler system and Yin Rössler system. This synchronization of two identical chaotic systems of which one has uncertain parameters the another has estimated parameters, by pragmatical adaptive control, is achieved with the state vector of another hyperchaotic chaotic system as a constituent of the functional relation between master and slave. An adaptive Yin-Yang chaos synchronization of Yin and Yang Rössler systems are achieved by using pragmatical asymptotically stability theorem. Numerical simulations show the effectiveness of the scheme.

6.2 Synchronization Scheme

Among many kinds of synchronizations [21-27], the generalized synchronization is investigated [28-34]. This means that we can give a function relationship between the states of the master and slave: $y = G(x)$. In this chapter, a hybrid projective Yin-Yang generalized synchronization(HPYYGS)

$$y = G(x, z) = g\,x(t)z(t) \qquad (6\text{-}1)$$

is studied, where $x(t)$ and $y(-t)$ are state variable vectors of the Yang master and Yin slave, respectively. $z(t)$ is state vector of a third chaotic system, called

constituent system, because it is a constituent of function *G*. Since *g* is a constant vector with both positive and negative entries, hybrid projective synchronization is named.

The master system is

$$\frac{dx}{dt} = f(x) \tag{6-2}$$

where $x(t) = [x_1(t), x_2(t), ..., x_n(t)]^T \in \Re^n$ is a state vector and all parameters of Eq.(6-2) are uncertain. The slave system is

$$\frac{dy(-t)}{d(-t)} = f(y(-t)) + u(t) \tag{6-3}$$

where $y(-t) = [y_1(-t), y_2(-t), ..., y_n(-t)]^T \in \Re^n$ is a state vector of Yin chaotic system and all parameters of Eq.(6-3) are estimated, u is a controlled vector. The function system is

$$\frac{dz}{dt} = k(z) \tag{6-4}$$

where $z(t) = [z_1(t), z_2(t), ..., z_n(t)]^T \in \Re^n$ is a chaotic state vector of the constituent system and all parameters of Eq.(2-4) are known.

Let

$$h(t) = [h_1(t), h_2(t), ..., h_n(t)] = [g_1 x_1(t) z_1(t), g_2 x_2(t) z_2(t), ..., g_n x_n(t) z_n(t)] \tag{6-5}$$

where $g = [g_1, g_2, ..., g_n]$ are constant vector with positive and negative entries, i.e. hybrid entries.

Define the error of HPYYGS as

$$e(t) = h(t) - y(-t) = gx(t)z(t) - y(-t) \tag{6-6}$$

where $e(t) = [e_1, e_2, ..., e_n]^T \in \Re^n$ denotes an error vector. The controlling goal is that

$$\lim_{t \to \infty} e = 0 \tag{6-7}$$

can be accomplished on the base of pragmatical asymptotical stability theorem by adaptive control.

When our aim is

$$y(-t) = x(t) + F(z(t))$$

where F is a given function , the scheme is similar.

6.3 Adaptive Yin-Yang synchronization of Yin chaos and Yang chaos

In this Section, adaptive synchronization from Yin Rössler chaos to Yang Rössler chaos is proposed. The Yin Rössler system is considered as slave system and the Yang Rössler system is regarded as master system. These two equations are shown below:

Master system- Yang Rössler system:

$$\begin{cases} \dfrac{dx_1(t)}{dt} = -(x_2(t) + x_3(t)) \\ \dfrac{dx_2(t)}{dt} = x_1(t) + ax_2(t) \\ \dfrac{dx_3(t)}{dt} = b + x_1(t)x_3(t) - cx_3(t) \end{cases} \quad (6\text{-}8)$$

Slave system- Yin Rössler system:

$$\begin{cases} \dfrac{dy_1(-t)}{d(-t)} = -(y_2(-t) + y_3(-t)) + u_1 \\ \dfrac{dy_2(-t)}{d(-t)} = y_1(-t) + \hat{a}y_2(-t) + u_2 \\ \dfrac{dy_3(-t)}{d(-t)} = \hat{b} + y_1(-t)y_3(-t) - \hat{c}y_3(-t) + u_3 \end{cases} \quad (6\text{-}9)$$

where $x_i(t)$ stands for states variables of the master system and $y_i(-t)$ for the slave system, respectively. Parameters, a, b and c are uncertain parameters of master system.

$\hat{a}$, $\hat{b}$ and $\hat{c}$ are estimated parameters. The master system exhibits chaos when the parameters are $a = 0.15, b = 0.2$ and $c = 10$. u_1, u_2 and u_3 are nonlinear controller to synchronize the slave Rössler system to master one, i.e.,

CASE I. The synchronization error component is

$$e_i = x_i(t) - y_i(-t), \qquad i = 1,\ 2,\ 3 \tag{6-10}$$

Our goal is

$$\lim_{t\to\infty} e_i = \lim_{t\to\infty}(x_i(t) - y_i(-t)) = 0, \qquad i = 1,2,3 \tag{6-11}$$

where the error vector $e = [e_1(t)\ \ e_2(t)\ \ e_3(t)]$ and

$$\begin{cases} e_1(t) = x_1(t) - y_1(-t) \\ e_2(t) = x_2(t) - y_2(-t) \\ e_3(t) = x_3(t) - y_3(-t) \end{cases} \tag{6-12}$$

From Eq. (6-5), we have the following error dynamics:

$$\begin{cases} \dfrac{de_1(t)}{dt} = \dfrac{dx_1(t)}{dt} - \dfrac{dy_1(-t)}{dt} = \dfrac{dx_1(t)}{dt} + \dfrac{dy_1(-t)}{d(-t)} \\ \dfrac{de_2(t)}{dt} = \dfrac{dx_2(t)}{dt} - \dfrac{dy_2(-t)}{dt} = \dfrac{dx_2(t)}{dt} + \dfrac{dy_2(-t)}{d(-t)} \\ \dfrac{de_3(t)}{dt} = \dfrac{dx_3(t)}{dt} - \dfrac{dy_3(-t)}{dt} = \dfrac{dx_3(t)}{dt} + \dfrac{dy_3(-t)}{d(-t)} \end{cases} \tag{6-13}$$

$$\begin{aligned} \dot{e}_1 &= -(x_2 + x_3) - (y_2(-t) + y_3(-t)) + u_1 \\ \dot{e}_2 &= (x_1 + ax_2) + (y_1(-t) + \hat{a}y_2(-t)) + u_2 \\ \dot{e}_3 &= (b + x_1x_3 - cx_3) + (\hat{b} + y_1(-t)y_3(-t) - \hat{c}y_3(-t)) + u_3 \end{aligned} \tag{6-14}$$

The two systems will be synchronized for any initial condition by appropriate controllers and update laws for those estimated parameters. As a result, the following controllers and update laws are designed by pragmatical asymptotical stability theorem(Appendix C).

Choose Lyapunov function as:

$$V = \frac{1}{2}(e_1^2 + e_2^2 + e_3^2 + \tilde{a}^2 + \tilde{b}^2 + \tilde{c}^2) \tag{6-15}$$

where $\tilde{a} = a - \hat{a}$, $\tilde{b} = b - \hat{b}$ and $\tilde{c} = c - \hat{c}$.

Its time derivative is:

$$\begin{aligned}
\dot{V} = {} & e_1\dot{e}_1 + \dot{e}_2 e_2 + \dot{e}_3 e_3 + \tilde{a}\dot{\tilde{a}} + \tilde{b}\dot{\tilde{b}} + c\dot{c} \\
& e_1[-(x_2 + x_3) - y_2(-t) + y_3(-t) - t(+y_1)u] \\
& e_2[x_1 + (ax_2 +)y_1 - t(-)y_2 - t(+)u] \\
& e_3[b + (x_1x_3 - cx_3 +)\hat{b} + y_1(-t)y_3(-t) - \hat{c}(t)y_3c - (\\
& \tilde{a}\dot{\hat{a}} + \tilde{b}\dot{\hat{b}} - \tilde{b}(\tilde{b} + \hat{b}) - \tilde{c}\dot{\hat{c}} - \tilde{c}(\hat{c})
\end{aligned} \tag{6-16}$$

We choose the update laws for those uncertain parameters as:

$$\begin{cases}
\dot{\hat{a}} = -\dot{\tilde{a}} = \tilde{a}_2 e \\
\dot{\hat{c}} = -\dot{\tilde{c}} = \tilde{b}_3 e \\
\dot{\hat{b}} = -\dot{\tilde{b}} = \tilde{c}_3 e
\end{cases} \tag{6-17}$$

Through Eqs. (6-16) and (6-17), the appropriate controllers can be designed as:

$$\begin{cases}
u_1 = (x_2 + x_3) + (y_2(-t) + y_3(-t)) - e_1 \\
u_2 = -(x_1 + ax_2) - (y_1(-t) + \hat{a}y_2(-t)) - \tilde{a}^2 - e_2 \\
u_3 = -(b + x_1x_3 - cx_3) - (\hat{b} + y_1(-t)y_3(-t) - \hat{c}y_3(-t)) - \tilde{b}^2 - \tilde{c}^2 - e_3
\end{cases} \tag{6-18}$$

We obtain

$$\dot{V} = -e_1^2 - e_2^2 - e_3^2 < 0 \tag{6-19}$$

which is negative semi-definite function of e_1, e_2, e_3, $\hat{a}$, $\hat{b}$ and $\hat{c}$. The Lyapunov asymptotical stability theorem is not satisfied. We cannot obtain that common origin of error dynamics (6-14) and parameter dynamics (6-17) is asymptotically stable. By pragmatical asymptotically stability theorem (see Appendix), D is a 6-manifold, $n = 6$ and the number of error state variables $p = 3$. When $e_1 = e_2 = e_3 = 0$ and $\hat{a}$, $\hat{b}$, $\hat{c}$ take arbitrary values, $\dot{V} = 0$, so X is of 3 dimensions, $m = n - p = 6 - 3 = 3$, $m + 1 < n$ is satisfied. According to the pragmatical asymptotically stability theorem, error vector e approaches zero and the estimated parameters also approach the

uncertain parameters. The equilibrium point is pragmatically asymptotically stable. Under the assumption of equal probability, it is actually asymptotically stable. The simulation results are shown in Figs. 6.1~6.4.

CASE II. The generalized synchronization error component is

$$e_i = [x_i(t) + z_i(t)] - y_i(-t), \qquad i = 1,\ 2,\ 3 \tag{6-20}$$

$z = \begin{bmatrix} z_1 & z_2 & z_3 \end{bmatrix}^T$ is the chaotic state vector of a Chen-Lee system[30].

The constituent system for generalized synchronization is a Chen-Lee system

$$\begin{cases} \dfrac{dz_1(t)}{d(t)} = -z_2(t)z_3(t) + \delta_1 z_1(t) \\ \dfrac{dz_2(t)}{d(t)} = z_1(t)z_3(t) + \delta_2 z_2(t) \\ \dfrac{dz_3(t)}{d(t)} = (1/3)z_1(t)z_2(t) + \delta_3 z_3(t) \end{cases} \tag{6-21}$$

where $\delta_1 = 5, \delta_2 = -10, \delta_3 = -3.8$

Our goal is

$$\lim_{t\to\infty} e_i = \lim_{t\to\infty}(x_i(t) - y_i(-t) + z_i(t)) = 0, \qquad i = 1,2,3 \tag{6-22}$$

where the error vector $\mathrm{e} = \begin{bmatrix} \mathrm{e}_1(\mathrm{t}) & \mathrm{e}_2(\mathrm{t}) & \mathrm{e}_3(\mathrm{t}) \end{bmatrix}$ and

$$\begin{cases} e_1(t) = x_1(t) - y_1(-t) + z_1(t) \\ e_2(t) = x_2(t) - y_2(-t) + z_2(t) \\ e_3(t) = x_3(t) - y_3(-t) + z_3(t) \end{cases} \tag{6-23}$$

From Eq. (6-23), we have the following error dynamics:

$$\begin{cases} \dfrac{de_1(t)}{dt} = \dfrac{dx_1(t)}{dt} - \dfrac{dy_1(-t)}{dt} + \dfrac{dz_1(t)}{dt} = \dfrac{dx_1(t)}{dt} + \dfrac{dy_1(-t)}{d(-t)} + \dfrac{dz_1(t)}{dt} \\ \dfrac{de_2(t)}{dt} = \dfrac{dx_2(t)}{dt} - \dfrac{dy_2(-t)}{dt} + \dfrac{dz_2(t)}{dt} = \dfrac{dx_2(t)}{dt} + \dfrac{dy_2(-t)}{d(-t)} + \dfrac{dz_2(t)}{dt} \\ \dfrac{de_3(t)}{dt} = \dfrac{dx_3(t)}{dt} - \dfrac{dy_3(-t)}{dt} + \dfrac{dz_3(t)}{dt} = \dfrac{dx_3(t)}{dt} + \dfrac{dy_3(-t)}{d(-t)} + \dfrac{dz_3(t)}{dt} \end{cases} \tag{6-24}$$

$$\begin{aligned}
\dot{e}_1 &= -(x_2 + x_3) - (y_2(-t) + y_3(-t)) + u_1 + \dot{z}_1 \\
\dot{e}_2 &= (x_1 + ax_2) + (y_1(-t) + \hat{a}y_2(-t)) + u_2 + \dot{z}_2 \\
\dot{e}_3 &= (b + x_1x_3 - cx_3) + (\hat{b} + y_1(-t)y_3(-t) - \hat{c}y_3(-t)) + u_3 + \dot{z}_3
\end{aligned} \tag{6-25}$$

The three systems will be synchronized for any initial condition by appropriate controllers and update laws for those estimated parameters. As a result, the following controllers and update laws are designed by pragmatical asymptotical stability theorem as follows:

Choosing Lyapunov function as:

$$\mathrm{V} = \frac{1}{2}(\mathrm{e}_1^2 + \mathrm{e}_2^2 + \mathrm{e}_3^2 + \tilde{\mathrm{a}}^2 + \tilde{\mathrm{b}}^2 + \tilde{\mathrm{c}}^2) \tag{6-26}$$

where $\tilde{\mathrm{a}} = \mathrm{a} - \hat{\mathrm{a}}$, $\tilde{\mathrm{b}} = \mathrm{b} - \hat{\mathrm{b}}$ and $\tilde{\mathrm{c}} = \mathrm{c} - \hat{\mathrm{c}}$.

Its time derivative is:

$$\begin{aligned}
\dot{V} &= e_1\dot{e}_1 + e_2\dot{e}_2 + e_3\dot{e}_3 + \tilde{a}\dot{\tilde{a}} + \tilde{b}\dot{\tilde{b}} + \tilde{c}\dot{\tilde{c}} \\
&= e_1[-(x_2 + x_3) - (y_2(-t) + y_3(-t)) + u_1 - z_2(t)z_3(t) + \delta_1 z_1(t)] \\
&+ e_2[(x_1 + ax_2) + (y_1(-t) + \hat{a}y_2(-t)) + u_2 + z_1(t)z_3(t) + \delta_2 z_2(t)] \\
&+ e_3[(b + x_1x_3 - cx_3) + (\hat{b} + y_1(-t)y_3(-t) - \hat{c}y_3(-t)) + u_3 + (1/3)z_1(t)z_2(t) + \delta_3 z_3(t)] \\
&+ \tilde{a}(-\dot{\hat{a}}) + \tilde{b}(-\dot{\hat{b}}) + \tilde{c}(-\dot{\hat{c}})
\end{aligned} \tag{6-27}$$

We choose the update laws for those uncertain parameters as:

$$\begin{cases}
\dot{\tilde{a}} = -\dot{\hat{a}} = \tilde{a}_2 e \\
\dot{\tilde{c}} = -\dot{\hat{c}} = \tilde{b}_3 e \\
\dot{\tilde{b}} = -\dot{\hat{b}} = \tilde{c}_3 e
\end{cases} \tag{6-28}$$

Through Eqs. (6-27) and (6-28), the appropriate controllers can be designed as:

$$\begin{cases}
u_1 = (x_2 + x_3) + (y_2(-t) + y_3(-t)) - e_1 - (-z_2(t)z_3(t) + \delta_1 z_1(t)) \\
u_2 = -(x_1 + ax_2) - (y_1(-t) + \hat{a}y_2(-t)) - \tilde{a}^2 - e_2 - (z_1(t)z_3(t) + \delta_2 z_2(t)) \\
u_3 = -(b + x_1x_3 - cx_3) - (\hat{b} + y_1(-t)y_3(-t) - \hat{c}y_3(-t)) - \tilde{b}^2 - \tilde{c}^2 - e_3 - ((1/3)z_1(t)z_2(t) + \delta_3 z_3(t))
\end{cases} \tag{6-29}$$

We obtain

$$\dot{\mathrm{V}} = -\mathrm{e}_1^2 - \mathrm{e}_2^2 - \mathrm{e}_3^2 < 0 \tag{6-30}$$

The simulation results are shown in Figs. 6.5~6. 8.

CASE III. The generalized synchronization error function is

$$e_i = [x_i(t) + z_i^{\,2}(t)] - y_i(-t), \qquad i = 1,\ 2,\ 3 \tag{6-31}$$

$z = \begin{bmatrix} z_1 & z_2 & z_3 \end{bmatrix}^T$ is the state vector of a Chen-Lee system.

The goal system for generalized synchronization is a Chen-Lee system

$$\begin{cases} \dfrac{dz_1(t)}{d(t)} = -z_2(t)z_3(t) + \delta_1 z_1(t) \\ \dfrac{dz_2(t)}{d(t)} = z_1(t)z_3(t) + \delta_2 z_2(t) \\ \dfrac{dz_3(t)}{d(t)} = (1/3)z_1(t)z_2(t) + \delta_3 z_3(t) \end{cases} \tag{6-32}$$

where $\delta_1 = 5, \delta_2 = -10, \delta_3 = -3.8$

Our goal is

$$\lim_{t\to\infty} e_i = \lim_{t\to\infty}(x_i(t) - y_i(-t) + z_i^{\,2}(t)) = 0, \quad i = 1,2,3 \tag{6-33}$$

where the error vector $\mathrm{e} = \begin{bmatrix} \mathrm{e}_1(\mathrm{t}) & \mathrm{e}_2(\mathrm{t}) & \mathrm{e}_3(\mathrm{t}) \end{bmatrix}$ and

$$\begin{cases} e_1(t) = x_1(t) - y_1(-t) + z_1^{\,2}(t) \\ e_2(t) = x_2(t) - y_2(-t) + z_2^{\,2}(t) \\ e_3(t) = x_3(t) - y_3(-t) + z_3^{\,2}(t) \end{cases} \tag{6-34}$$

From Eq. (6-27), we have the following error dynamics:

$$\begin{cases} \dfrac{de_1(t)}{dt} = \dfrac{dx_1(t)}{dt} - \dfrac{dy_1(-t)}{d(t)} + \dfrac{dz_1^{\,2}(t)}{dt} = \dfrac{dx_1(t)}{dt} + \dfrac{dy_1(-t)}{d(-t)} + 2z_1(t)\dfrac{dz_1(t)}{dt} \\ \dfrac{de_2(t)}{dt} = \dfrac{dx_2(t)}{dt} - \dfrac{dy_2(-t)}{d(t)} + \dfrac{dz_2^{\,2}(t)}{dt} = \dfrac{dx_2(t)}{dt} + \dfrac{dy_2(-t)}{d(-t)} + 2z_2(t)\dfrac{dz_2(t)}{dt} \\ \dfrac{de_3(t)}{dt} = \dfrac{dx_3(t)}{dt} - \dfrac{dy_3(-t)}{d(t)} + \dfrac{dz_3^{\,2}(t)}{dt} = \dfrac{dx_3(t)}{dt} + \dfrac{dy_3(-t)}{d(-t)} + 2z_3(t)\dfrac{dz_3(t)}{dt} \end{cases} \tag{6-35}$$

$$\begin{aligned}
\dot{e}_1 &= -(x_2 + x_3) - (y_2(-t) + y_3(-t)) + u_1 + 2z_1\dot{z}_1 \\
\dot{e}_2 &= (x_1 + ax_2) + (y_1(-t) + \hat{a}y_2(-t)) + u_2 + 2z_2\dot{z}_2 \\
\dot{e}_3 &= (b + x_1x_3 - cx_3) + (\hat{b} + y_1(-t)y_3(-t) - \hat{c}y_3(-t)) + u_3 + 2z_3\dot{z}_3
\end{aligned} \tag{6-36}$$

The three systems will be synchronized for any initial condition by appropriate controllers and update laws for those estimated parameters. As a result, the following controllers and update laws are designed by pragmatical asymptotical stability theorem as follows:

Choosing Lyapunov function as:

$$\mathrm{V} = \frac{1}{2}(\mathrm{e}_1^2 + \mathrm{e}_2^2 + \mathrm{e}_3^2 + \tilde{\mathrm{a}}^2 + \tilde{\mathrm{b}}^2 + \tilde{\mathrm{c}}^2) \tag{6-37}$$

where $\tilde{\mathrm{a}} = \mathrm{a} - \hat{\mathrm{a}}$, $\tilde{\mathrm{b}} = \mathrm{b} - \hat{\mathrm{b}}$ and $\tilde{\mathrm{c}} = \mathrm{c} - \hat{\mathrm{c}}$.

Its time derivative is:

$$\begin{aligned}
\dot{V} &= e_1\dot{e}_1 + e_2\dot{e}_2 + e_3\dot{e}_3 + \tilde{a}\dot{\tilde{a}} + \tilde{b}\dot{\tilde{b}} + \tilde{c}\dot{\tilde{c}} \\
&= e_1[-(x_2 + x_3) - (y_2(-t) + y_3(-t)) + u_1 + 2z_1(-z_2(t)z_3(t) + \delta_1 z_1(t))] \\
&+ e_2[(x_1 + ax_2) + (y_1(-t) + \hat{a}y_2(-t)) + u_2 + 2z_2(z_1(t)z_3(t) + \delta_2 z_2(t))] \\
&+ e_3[(b + x_1x_3 - cx_3) + (\hat{b} + y_1(-t)y_3(-t) - \hat{c}y_3(-t)) + u_3 + 2z_3((1/3)z_1(t)z_2(t) + \delta_3 z_3(t))] \\
&+ \tilde{a}(-\dot{\hat{a}}) + \tilde{b}(-\dot{\hat{b}}) + \tilde{c}(-\dot{\hat{c}})
\end{aligned} \tag{6-38}$$

We choose the update laws for those uncertain parameters as:

$$\begin{cases}
\dot{\tilde{a}} = -\dot{\hat{a}} = \tilde{a}_2 e \\
\dot{\tilde{c}} = -\dot{\hat{c}} = \tilde{b}_3 e \\
\dot{\tilde{b}} = -\dot{\hat{b}} = \tilde{c}_3 e
\end{cases} \tag{6-39}$$

Through Eqs. (6-38) and (6-39), the appropriate controllers can be designed as:

$$\begin{cases}
u_1 = (x_2 + x_3) + (y_2(-t) + y_3(-t)) - e_1 - 2z_1(-z_2(t)z_3(t) + \delta_1 z_1(t)) \\
u_2 = -(x_1 + ax_2) - (y_1(-t) + \hat{a}y_2(-t)) - \tilde{a}^2 - e_2 - 2z_2(z_1(t)z_3(t) + \delta_2 z_2(t)) \\
u_3 = -(b + x_1x_3 - cx_3) - (\hat{b} + y_1(-t)y_3(-t) - \hat{c}y_3(-t)) - \tilde{b}^2 - \tilde{c}^2 - e_3 - 2z_3((1/3)z_1(t)z_2(t) + \delta_3 z_3(t))
\end{cases} \tag{6-40}$$

We obtain

$$\dot{\mathrm{V}} = -\mathrm{e}_1^2 - \mathrm{e}_2^2 - \mathrm{e}_3^2 < 0 \tag{6-41}$$

The simulation results are shown in Figs. 6.9~6.12.

CASE IV. The generalized synchronization error function is

$$e_i = g_i x_i(t) z_i(t) - y_i(-t), \qquad i = 1,\ 2,\ 3 \tag{6-42}$$

$z = \begin{bmatrix} z_1 & z_2 & z_3 \end{bmatrix}^T$ is the state vector of a Lorenz system.

The goal system for generalized synchronization is a Lorenz system

$$\begin{cases} \dfrac{dz_1(t)}{dt} = \delta_1(z_2(t) - z_1(t)) \\ \dfrac{dz_2(t)}{dt} = \delta_2 z_1(t) - z_1(t) z_3(t) - z_2(t) \\ \dfrac{dz_3(t)}{dt} = z_1(t) z_2(t) - \delta_3 z_3(t) \end{cases} \tag{6-43}$$

where $\delta_1 = 10, \delta_2 = 28, \delta_3 = 8/3$

Our goal is

$$\lim_{t\to\infty} e_i = \lim_{t\to\infty} (y_i(-t) - g_i x_i(t) z_i(t)) = 0, \qquad i = 1, 2, 3 \tag{6-44}$$

where the error vector $e = \begin{bmatrix} e_1(t) & e_2(t) & e_3(t) \end{bmatrix}$ and

$$\begin{cases} e_1 = g_1 x_1(t) z_1(t) - y_1(-t) \\ e_2 = g_2 x_2(t) z_2(t) - y_2(-t) \\ e_3 = g_3 x_3(t) z_3(t) - y_3(-t) \end{cases} \tag{6-45}$$

From Eq. (6-38), we have the following error dynamics:

$$\begin{cases} \dfrac{de_1(t)}{dt} = g_1 z_1(t) \dfrac{dx_1(t)}{dt} + g_1 x_1(t) \dfrac{dz_1(t)}{dt} - \dfrac{dy_1(-t)}{d(t)} - = g_1 z_1(t) \dfrac{dx_1(t)}{dt} + g_1 x_1(t) \dfrac{dz_1(t)}{dt} + \dfrac{dy_1(-t)}{d(-t)} \\ \dfrac{de_2(t)}{dt} = g_2 z_2(t) \dfrac{dx_2(t)}{dt} + g_2 x_2(t) \dfrac{dz_2(t)}{dt} - \dfrac{dy_2(-t)}{d(t)} = g_2 z_2(t) \dfrac{dx_2(t)}{dt} + g_2 x_2(t) \dfrac{dz_2(t)}{dt} + \dfrac{dy_2(-t)}{d(-t)} \\ \dfrac{de_3(t)}{dt} = g_3 z_3(t) \dfrac{dx_3(t)}{dt} + g_3 x_3(t) \dfrac{dz_3(t)}{dt} - \dfrac{dy_3(-t)}{d(t)} = g_3 z_3(t) \dfrac{dx_3(t)}{dt} + g_3 x_3(t) \dfrac{dz_3(t)}{dt} + \dfrac{dy_3(-t)}{d(-t)} \end{cases} \tag{6-46}$$

$$\begin{aligned} \dot{e}_1 &= g_1(-(x_2 + x_3)) z_1 + g_1 x_1(\delta_1(z_2 - z_1)) - (y_2(-t) + y_3(-t)) + u_1 \\ \dot{e}_2 &= g_2(x_1 + a x_2) z_2 + g_2 x_2(\delta_2 z_1 - z_1 z_3 - z_2) + (y_1(-t) + \hat{a} y_2(-t)) + u_2 \\ \dot{e}_3 &= g_3(b + x_1 x_3 - c x_3) z_3 + g_3 x_3(z_1 z_2 - \delta_3 z_3) + (\hat{b} + y_1(-t) y_3(-t) - \hat{c} y_3(-t)) + u_3 \end{aligned} \tag{6-47}$$

The three systems will be synchronized for any initial condition by appropriate controllers and update laws for those estimated parameters. As a result, the following

controllers and update laws are designed by pragmatical asymptotical stability theorem as follows:

Choosing Lyapunov function as:

$$V = \frac{1}{2}(e_1^2 + e_2^2 + e_3^2 + \tilde{a}^2 + \tilde{b}^2 + \tilde{c}^2) \tag{6-48}$$

where $\tilde{a} = a - \hat{a}$, $\tilde{b} = b - \hat{b}$ and $\tilde{c} = c - \hat{c}$.

Its time derivative is:

$$\begin{aligned}
\dot{V} &= e_1\dot{e}_1 + e_2\dot{e}_2 + e_3\dot{e}_3 + \tilde{a}\dot{\tilde{a}} + \tilde{b}\dot{\tilde{b}} + \tilde{c}\dot{\tilde{c}} \\
&= e_1[g_1(-(x_2 + x_3))z_1 + g_1x_1(\delta_1(z_2 - z_1)) - (y_2(-t) + y_3(-t)) + u_1] \\
&+ e_2[g_2(x_1 + ax_2)z_2 + g_2x_2(\delta_2z_1 - z_1z_3 - z_2) + (y_1(-t) + \hat{a}y_2(-t)) + u_2] \\
&+ e_3[g_3(b + x_1x_3 - cx_3)z_3 + g_3x_3(z_1z_2 - \delta_3z_3) + (\hat{b} + y_1(-t)y_3(-t) - \hat{c}y_3(-t)) + u_3] \\
&+ \tilde{a}(-\dot{\hat{a}}) + \tilde{b}(-\dot{\hat{b}}) + \tilde{c}(-\dot{\hat{c}})
\end{aligned} \tag{6-49}$$

We choose the update laws for those uncertain parameters as:

$$\begin{cases}
\dot{\tilde{a}} = -\dot{\hat{a}} = \tilde{a}_2e \\
\dot{\tilde{c}} = -\dot{\hat{c}} = \tilde{b}_3e \\
\dot{\tilde{b}} = -\dot{\hat{b}} = \tilde{c}_3e
\end{cases} \tag{6-50}$$

Through Eqs. (6-49) and (6-50), the appropriate controllers can be designed as:

$$\begin{cases}
u_1 = (y_2(-t) + y_3(-t)) - g_1(-(x_2 + x_3))z_1 - g_1x_1(\delta_1(z_2 - z_1)) - e_1 \\
u_2 = -(y_1(-t) + \hat{a}y_2(-t)) - g_2(x_1 + ax_2)z_2 - g_2x_2(\delta_2z_1 - z_1z_3 - z_2) - e_2 - \tilde{a}^2 \\
u_3 = -(\hat{b} + y_1(-t)y_3(-t) - \hat{c}y_3(-t)) - g_3(b + x_1x_3 - cx_3)z_3 - g_3x_3(z_1z_2 - \delta_3z_3) - e_3 - \tilde{b}^2 - \tilde{c}^2
\end{cases} \tag{6-51}$$

We obtain

$$\dot{V} = -e_1^2 - e_2^2 - e_3^2 < 0 \tag{6-52}$$

The simulation results are shown in Figs. 6.13~6.16.

6.4 Summary

In this Chapter, PYYGS of Yang Rössler and Yin Rössler system is obtained by adaptive control based on pragmetical asymptotical stability theory. This Chapter explores the another half battle field for chaos study, would be proved to have epoch-making significance in the future.

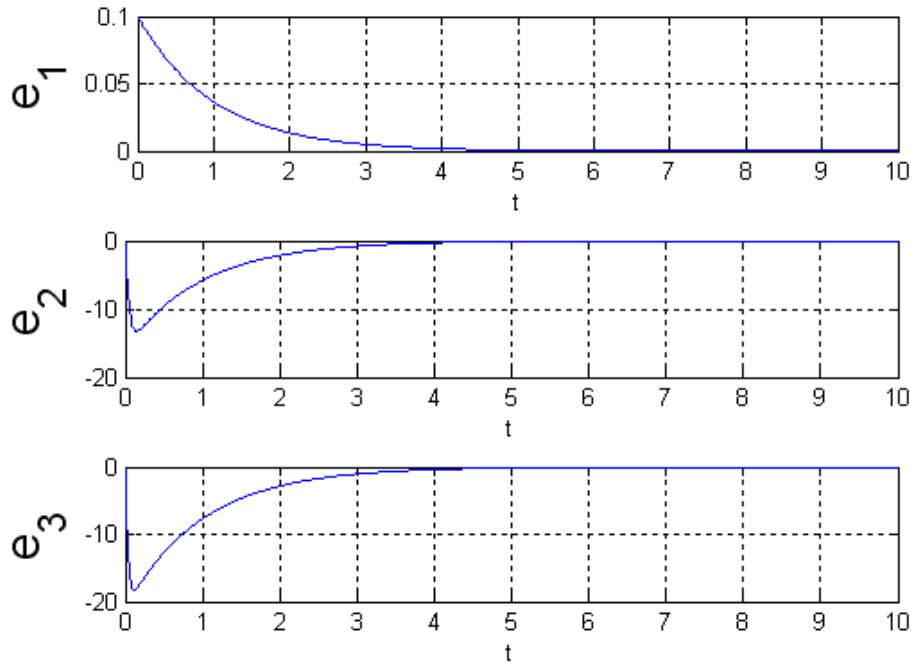

Fig. 6.1 Time histories of state errors for Yin and Yang Rössler chaotic systems for Case I.

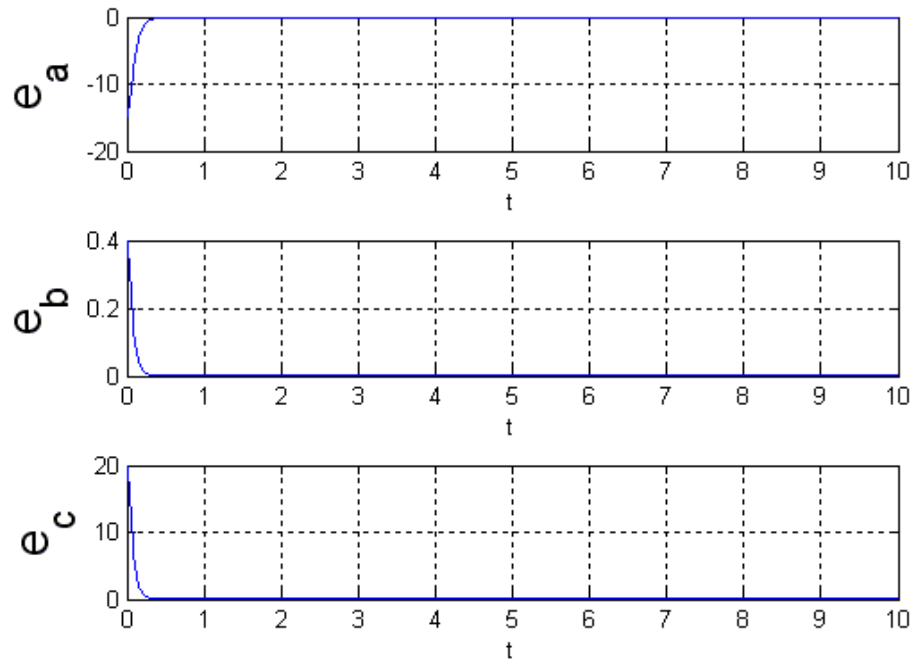

Fig. 6.2 Time histories of parameter errors for Yin and Yang Rössler chaotic systems for Case I.

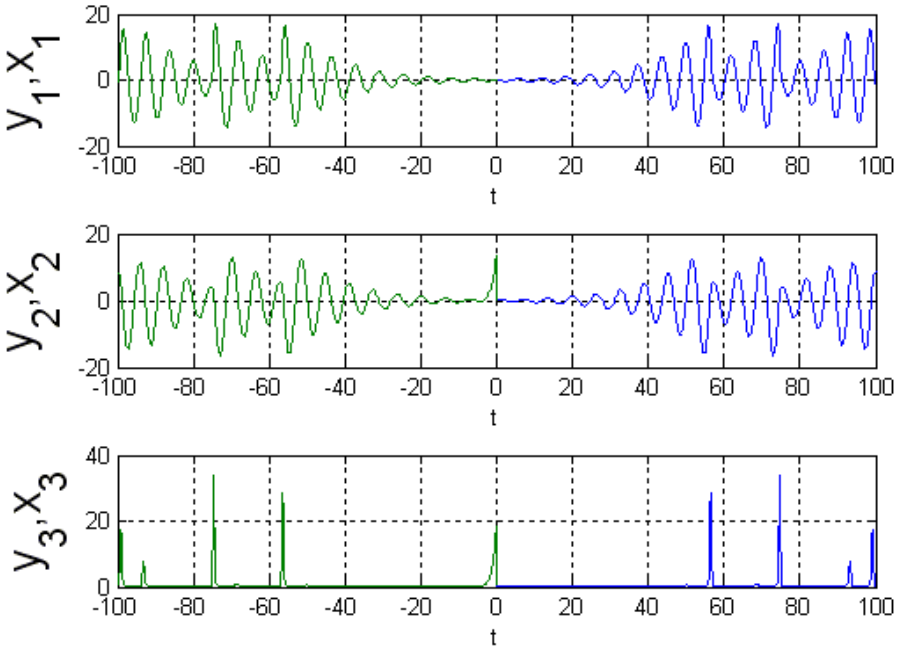

Fig. 6.3 Time histories of $x_i(t)$ and $y_i(-t)$ for Case I.

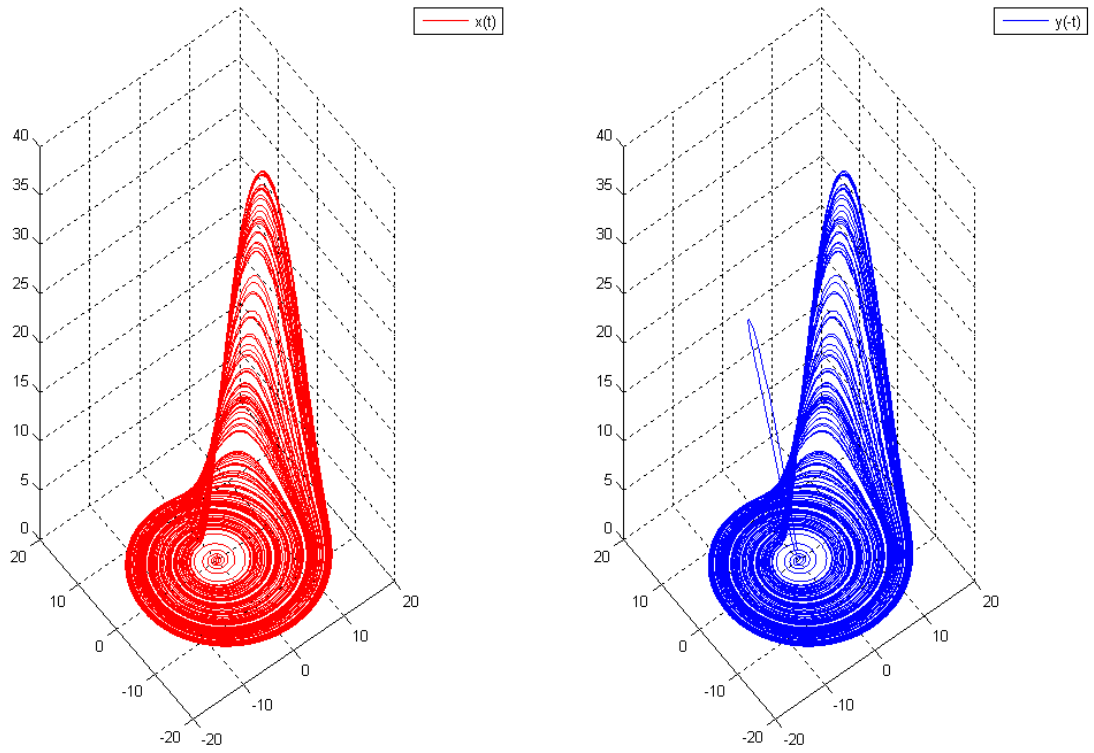

Fig. 6.4 Phase portraits of $x_i(t)$ and $y_i(-t)$ for Case I.

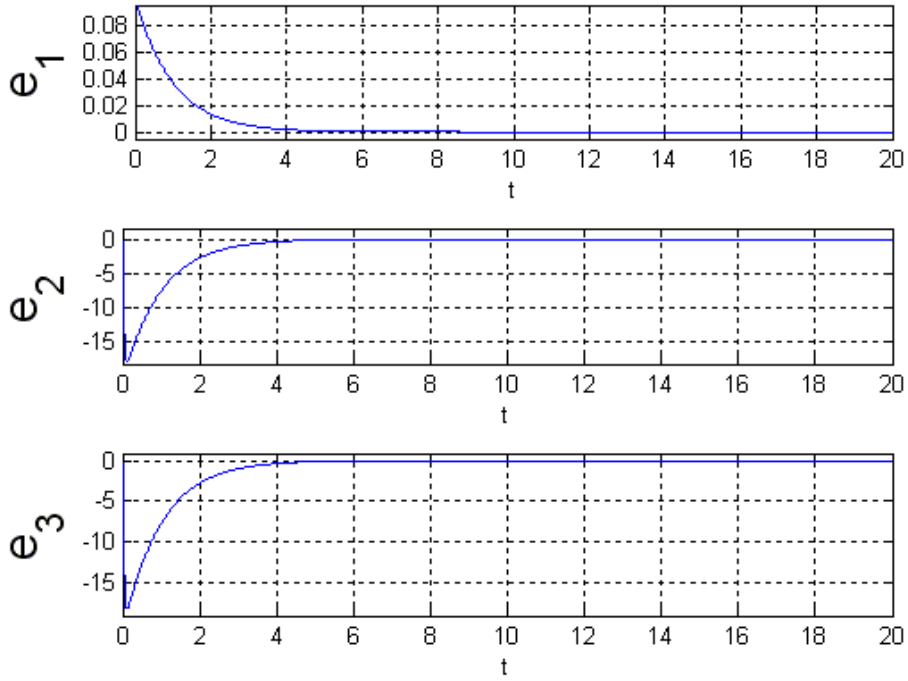

Fig. 6.5 Time histories of state errors for Yin and Yang Rössler chaotic systems for Case II.

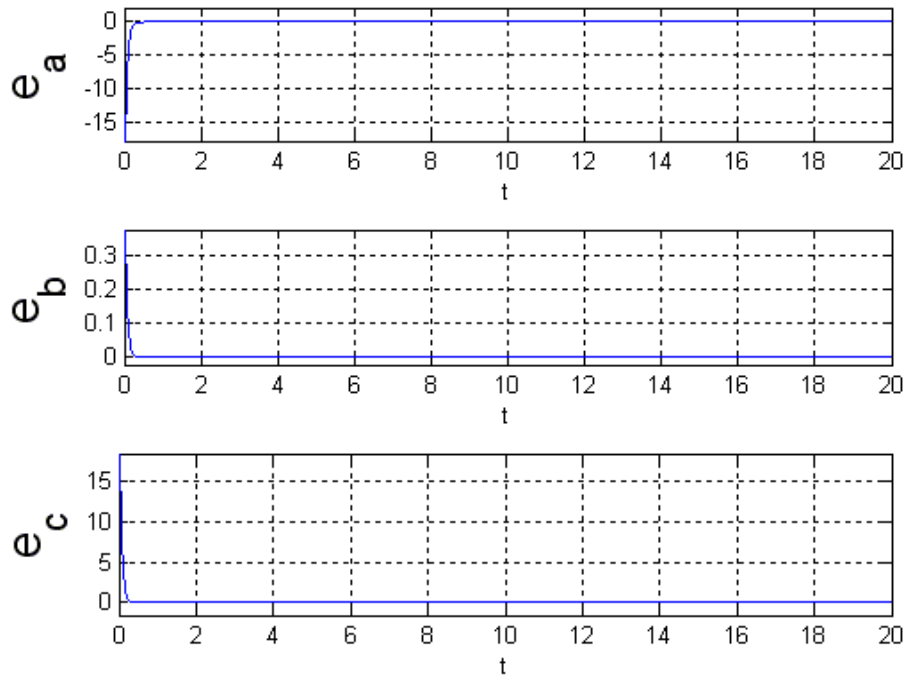

Fig. 6.6 Time histories of parameter errors for Yin and Yang Rössler chaotic systems for Case II.

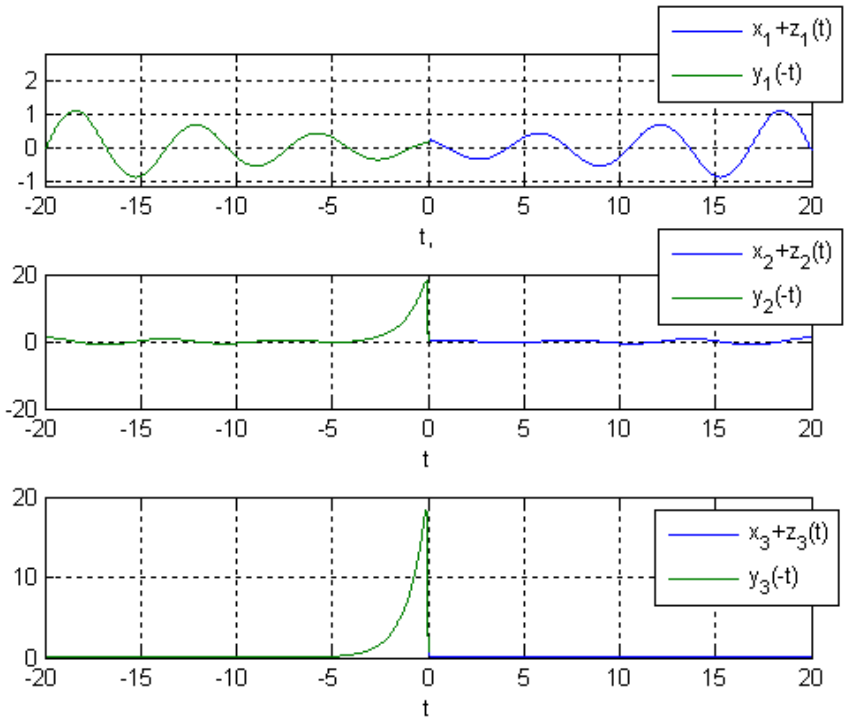

Fig. 6.7 Time histories of $x_i(t)+z_i(t)$ and $y_i(-t)$ for Case II.

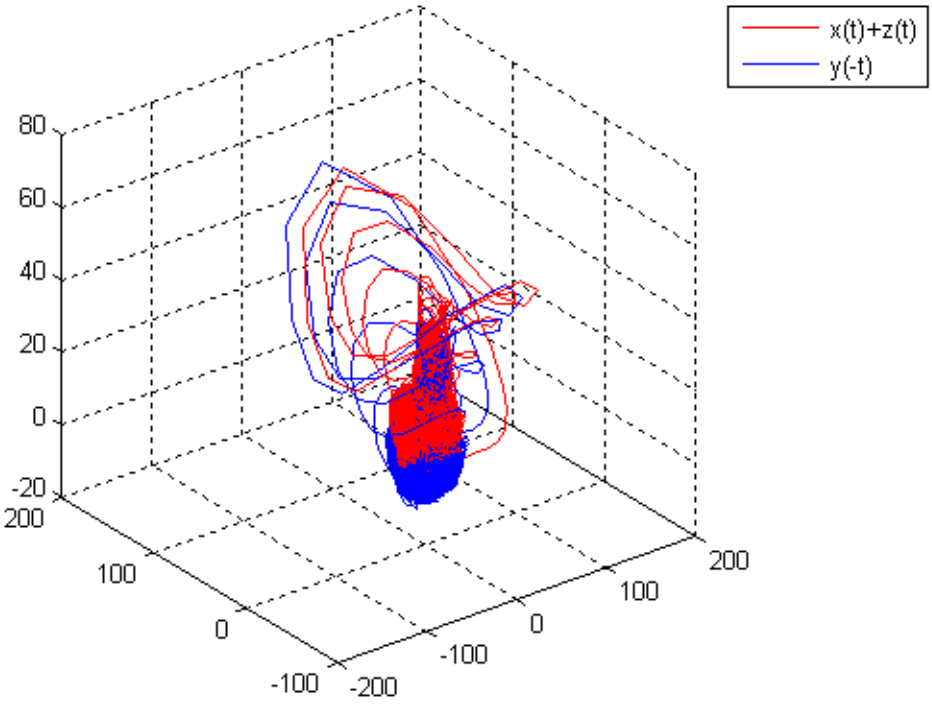

Fig. 6.8 Phase portraits of $x_i(t)+z_i(t)$ and $y_i(-t)$ for Case II.

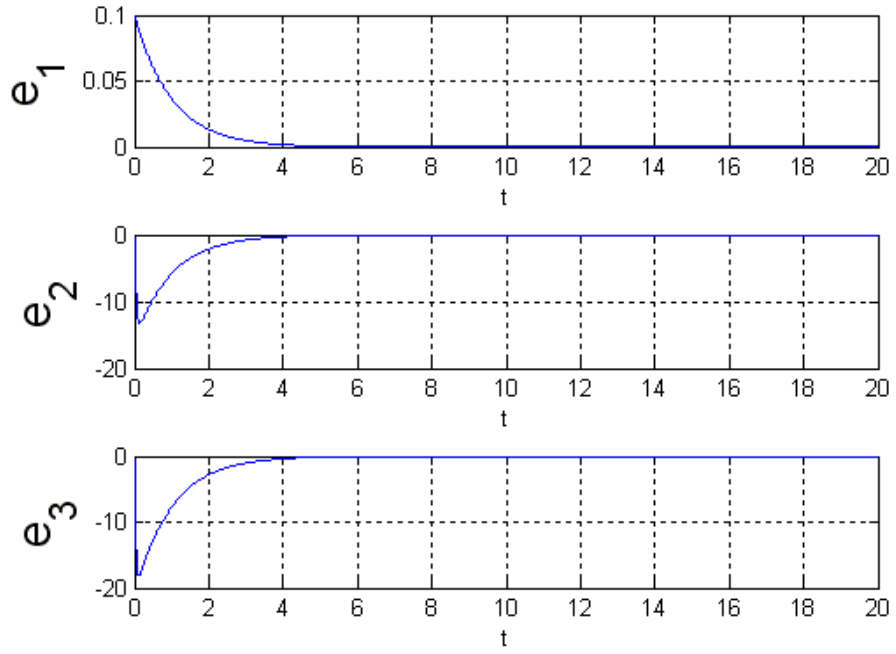

Fig. 6.9 Time histories of state errors for Yin and Yang Rössler chaotic systems for Case III.

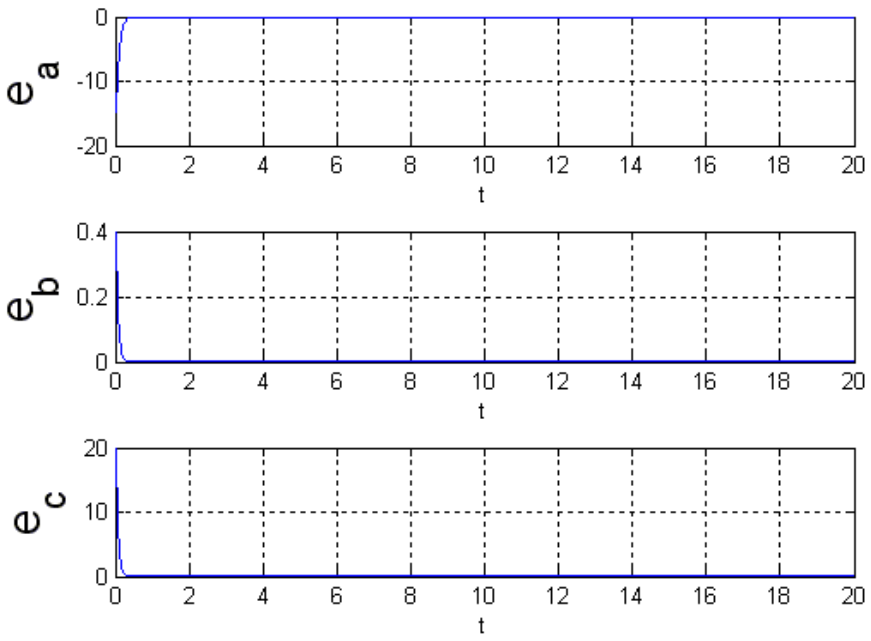

Fig. 6.10 Time histories of parameter errors for Yin and Yang Rössler chaotic systems for Case III.

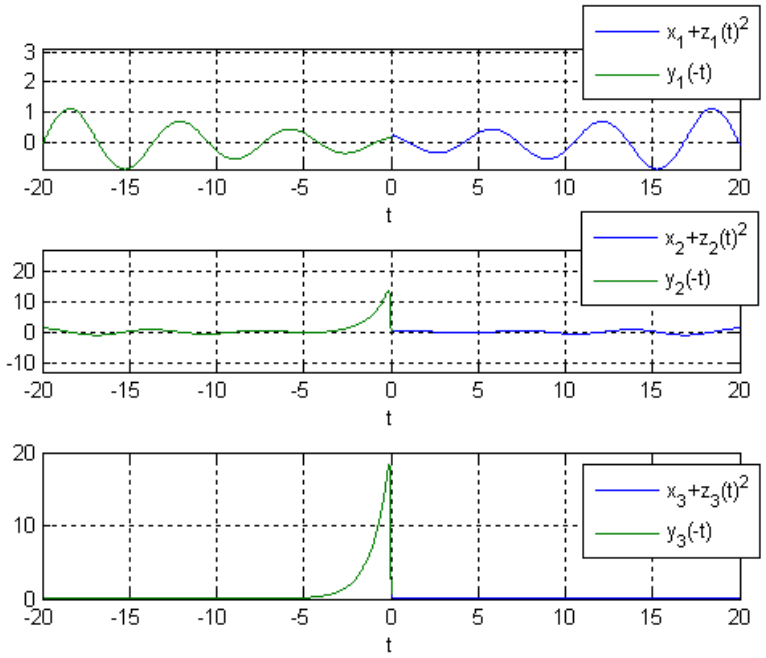

Fig. 6.11 Time histories of $x_i(t)+z_i^2(t)$ and $y_i(-t)$ for Case III.

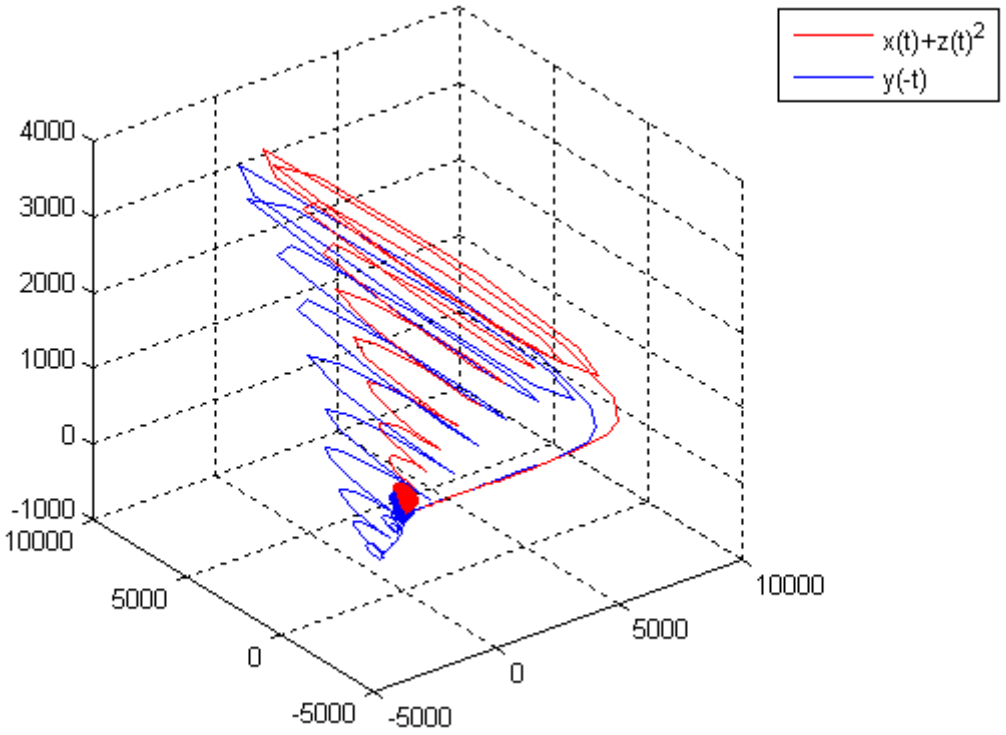

Fig. 6.12 Phase portraits of $x_i(t)+z_i^2(t)$ and $y_i(-t)$ for Case III.

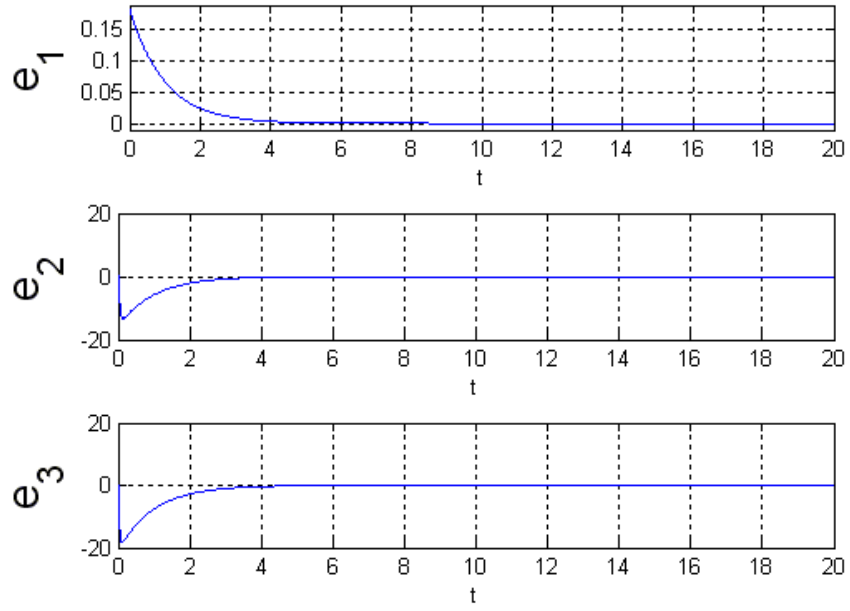

Fig. 6.13 Time histories of state errors for Yin and Yang Rössler chaotic systems for Case IV.

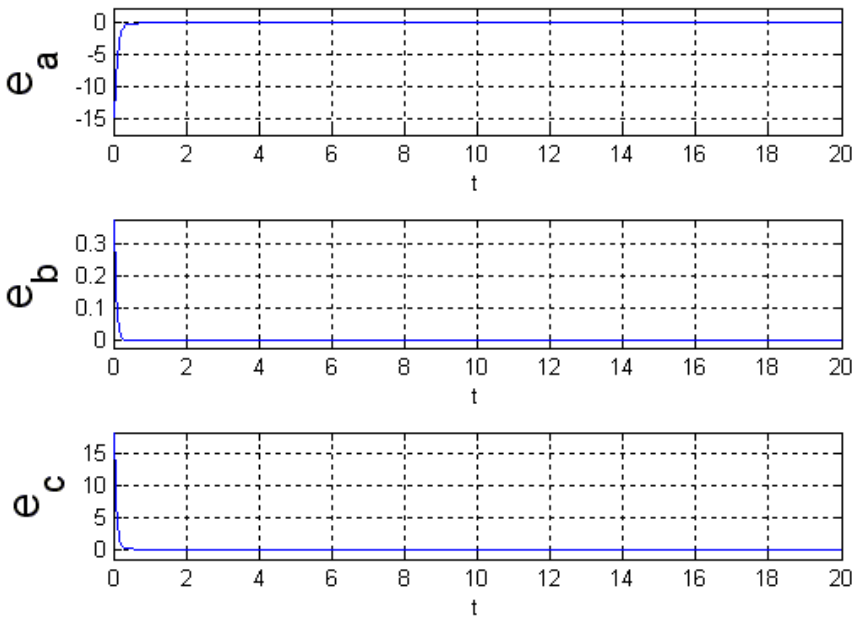

Fig. 6.14 Time histories of errors for Yin and Yang Rössler chaotic systems for Case IV.

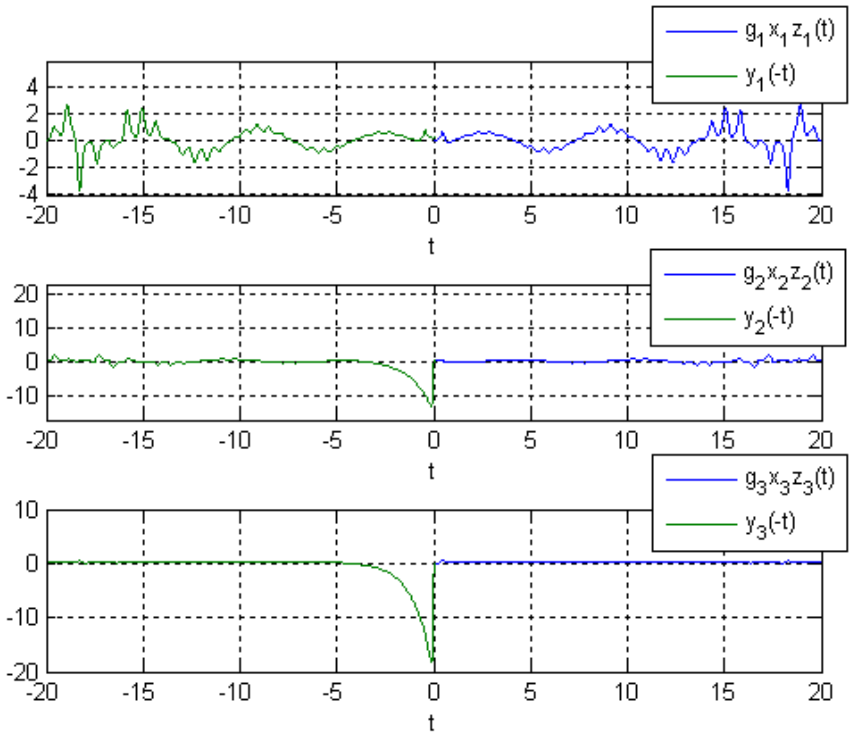

Fig. 6.15 Time histories of $g_i x_i(t) z_i(t)$ and $y_i(-t)$ for Case IV.

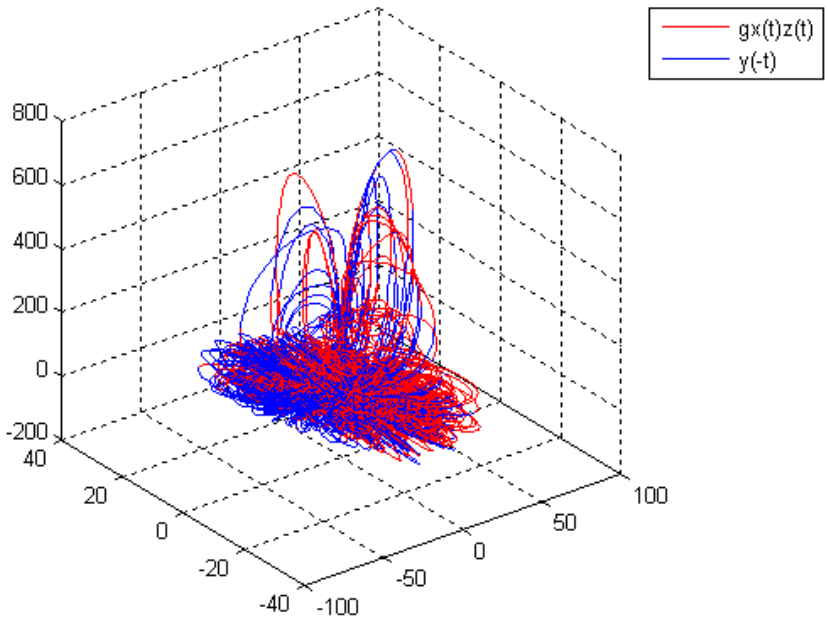

Fig. 6.16 Phase portraits of $g_i x_i(t) z_i(t)$ and $y_i(-t)$ for Case IV.

Chapter 7

Conclusions

In this thesis, the chaotic behavior in a New Froude-Duffing system is studied by phase portraits, time history, Poincaré maps, Lyapunov exponent, and bifurcation diagrams.

A new chaos generalized synchronization method, using GYC partial region stability theory is proposed, and generalized Lorenz system are used as one of four simulation examples which verify the effectiveness of the proposed scheme in Chapter 2. Moreover, we also study the chaos control by using the GYC partial region stability theory in Chapter 3. By using this theory, the controllers are of lower degree than that of controllers by using traditional Lyapunov asymptotical stability theorem. The simple linear homogeneous Lyapunov function of error states makes that the controllers are simpler and introduce less simulation error.

In Chapter 4, the chaotic behaviors of Rössler system with Bessel function parameters is studied firstly. The results are verified by time histories of states, phase portraits, Poincaré maps, bifurcation diagram, Lyapunov exponents and parametric diagram. Abundant hyperchaos is found for this system, which gives potential in various applications, particularly in secret communication.

In Chapter 5, the Yin Rössler system is firstly introduced. Via numerical simulation, the Yin Rössler system is compared with the Yang Rössler system and we find out there are similarity and difference between history and presence. In Chapter 6, (PYYGS) of Yang Rössler and Yin Rössler system is obtained by adaptive control based on pragmetical asymptotical stability theory. This thesis explores the another half battle field for chaos study, would be proved to have epoch-making significance in the future.

Appendix A

GYC Partial Region Stability Theory

Consider the differential equations of disturbed motion of a nonautonomous system in the normal form

$$\frac{dx_s}{dt} = X_s(t, x_1, \cdots, x_n), \qquad (s = 1, \cdots, n) \tag{A-1}$$

where the function X_s is defined on the intersection of the partial region Ω (shown in Fig. A-1) and

$$\sum_s x_s^2 \le H \tag{A-2}$$

and $t > t_0$, where t_0 and H are certain positive constants. X_s which vanishes when the variables x_s are all zero, is a real valued function of t, $x_1, \cdots, x_n$. It is assumed that X_s is smooth enough to ensure the existence, uniqueness of the solution of the initial value problem. When X_s does not contain t explicitly, the system is autonomous.

Obviously, $x_s = 0 \quad (s = 1, \cdots n)$ is a solution of Eq.(A-1). We are interested to the asymptotical stability of this zero solution on partial region Ω (including the boundary) of the neighborhood of the origin which in general may consist of several subregions (Fig. A.1).

Definition 1:

For any given number $\varepsilon > 0$, if there exists a $\delta > 0$, such that on the closed given partial region Ω when

$$\sum_s x_{s0}^2 \le \delta, \quad (s = 1, \cdots, n) \tag{A-3}$$

for all $t \ge t_0$, the inequality

$$\sum_s x_s^2 < \varepsilon, \quad (s = 1, \cdots, n) \tag{A-4}$$

is satisfied for the solutions of Eq.(A-27) on Ω, then the disturbed motion $x_s = 0 \quad (s = 1, \cdots n)$ is stable on the partial region Ω.

Definition 2:

If the undisturbed motion is stable on the partial region Ω, and there exists a $\delta' > 0$, so that on the given partial region Ω when

$$\sum_s x_{s0}^2 \le \delta', \quad (s = 1, \cdots, n) \tag{A-5}$$

The equality

$$\lim_{t \to \infty} \left(\sum_s x_s^2 \right) = 0 \tag{A-6}$$

is satisfied for the solutions of Eq.(A-1) on Ω, then the undisturbed motion $x_s = 0 \quad (s = 1, \cdots n)$ is asymptotically stable on the partial region Ω.

The intersection of Ω and region defined by Eq.(A-2) is called the region of attraction.

Definition of Functions $V(t, x_1, \cdots, x_n)$:

Let us consider the functions $V(t, x_1, \cdots, x_n)$ given on the intersection Ω_1 of the partial region Ω and the region

$$\sum_s x_s^2 \le h, \quad (s = 1, \cdots, n) \tag{A-7}$$

for $t \ge t_0 > 0$, where t_0 and h are positive constants. We suppose that the functions are single-valued and have continuous partial derivatives and become zero when $x_1 = \cdots = x_n = 0$.

Definition 3:

If there exists $t_0 > 0$ and a sufficiently small $h > 0$, so that on partial region Ω_1 and $t \geq t_0$, $V \geq 0$ (or ≤ 0), then V is a positive (or negative) semidefinite, in general semidefinite, function on the Ω_1 and $t \geq t_0$.

Definition 4:

If there exists a positive (negative) definitive function $W(x_1 \ldots x_n)$ on Ω_1, so that on the partial region Ω_1 and $t \geq t_0$

$$V - W \geq 0 \, (or \, -V - W \geq 0), \tag{A-8}$$

then $V(t, x_1, \ldots, x_n)$ is a positive definite function on the partial region Ω_1 and $t \geq t_0$.

Definition 5:

If $V(t, x_1, \ldots, x_n)$ is neither definite nor semidefinite on Ω_1 and $t \geq t_0$, then $V(t, x_1, \ldots, x_n)$ is an indefinite function on partial region Ω_1 and $t \geq t_0$. That is, for any small $h > 0$ and any large $t_0 > 0$, $V(t, x_1, \ldots, x_n)$ can take either positive or negative value on the partial region Ω_1 and $t \geq t_0$.

Definition 6: Bounded function V

If there exist $t_0 > 0$, $h > 0$, so that on the partial region Ω_1, we have

$$\left| V(t, x_1, \ldots, x_n) \right| < L \tag{B.9}$$

where L is a positive constant, then V is said to be bounded on Ω_1.

Definition 7: Function with infinitesimal upper bound

If V is bounded, and for any $\lambda > 0$, there exists $\mu > 0$, so that on Ω_1 when

$\sum_s x_s^2 \le \mu$, and $t \ge t_0$, we have

$$|V(t, x_1, \ldots, x_n)| \le \lambda \tag{A-10}$$

then *V* admits an infinitesimal upper bound on Ω_1.

Theorem 1 [22, 23]

If there can be found for the differential equations of the disturbed motion (Eq.(A-27)) a definite function $V(t, x_1, \ldots, x_n)$ on the partial region, and for which the derivative with respect to time based on these equations as given by the following :

$$\frac{dV}{dt} = \frac{\partial V}{\partial t} + \sum_{s=1}^{n} \frac{\partial V}{\partial x_s} X_s \tag{A-11}$$

is a semidefinite function on the paritial region whose sense is opposite to that of V, or if it becomes zero identically, then the undisturbed motion is stable on the partial region.

Proof:

Let us assume for the sake of definiteness that *V* is a positive definite function. Consequently, there exists a sufficiently large number t_0 and a sufficiently small number $h < H$, such that on the intersection Ω_1 of partial region Ω and

$$\sum_s x_s^2 \le h, \quad (s = 1, \ldots, n) \tag{A-12}$$

and $t \ge t_0$, the following inequality is satisfied

$$V(t, x_1, \ldots, x_n) \ge W(x_1, \ldots, x_n) \tag{A-13}$$

where *W* is a certain positive definite function which does not depend on *t*. Besides that, Eq. (A-7) may assume only negative or zero value in this region.

Let ε be an arbitrarily small positive number. We shall suppose that in any case $\varepsilon < h$. Let us consider the aggregation of all possible values of the quantities

$x_1,\ldots,x_n$, which are on the intersection ω_2 of Ω_1 and

$$\sum_s x_s^2 = \varepsilon, \tag{A-14}$$

and let us designate by $l>0$ the precise lower limit of the function W under this condition. by virtue of Eq. (B.5), we shall have

$$V(t,x_1,\ldots,x_n)\geq l \quad \text{for} \quad (x_1,\ldots,x_n) \quad \text{on} \quad \omega_2 . \tag{A-15}$$

We shall now consider the quantities x_s as functions of time which satisfy the differential equations of disturbed motion. We shall assume that the initial values x_{s0} of these functions for $t=t_0$ lie on the intersection Ω_2 of Ω_1 and the region

$$\sum_s x_s^2 \leq \delta, \tag{A-16}$$

where δ is so small that

$$V(t_0,x_{10},\ldots,x_{n0})<l \tag{A-17}$$

By virtue of the fact that $V(t_0,0,\ldots,0)=0$, such a selection of the number δ is obviously possible. We shall suppose that in any case the number δ is smaller than ε .Then the inequality

$$\sum_s x_s^2 < \varepsilon, \tag{A-18}$$

being satisfied at the initial instant will be satisfied, in the very least, for a sufficiently small $t-t_0$, since the functions $x_s(t)$ very continuously with time. We shall show that these inequalities will be satisfied for all values $t>t_0$. Indeed, if these inequalities were not satisfied at some time, there would have to exist such an instant $t=T$ for which this inequality would become an equality. In other words, we would have

$$\sum_s x_s^2(T) = \varepsilon, \tag{A-19}$$

and consequently, on the basis of Eq. (A-9)

$$V(T, x_1(T), \ldots, x_n(T)) \geq l \tag{A-20}$$

On the other hand, since $\varepsilon < h$, the inequality (Eq.(A-4)) is satisfied in the entire interval of time [t_0, T], and consequently, in this entire time interval $\frac{dV}{dt} \leq 0$. This yields

$$V(T, x_1(T), \ldots, x_n(T)) \leq V(t_0, x_{10}, \ldots, x_{n0}), \tag{A-21}$$

which contradicts Eq. (A-12) on the basis of Eq. (A-11). Thus, the inequality (Eq.(A-1)) must be satisfied for all values of $t > t_0$, hence follows that the motion is stable.

Finally, we must point out that from the view-point of mathenatics, the stability on partial region in general does not be related logically to the stability on whole region. If an undisturbed solution is stable on a partial region, it may be either stable or unstable on the whole region and vice versa. From the viewpoint of dynamics, we wre not interesting to the solution starting from Ω_2 and going out of Ω.

Theorem 2 [22, 23]

If in satisfying the conditions of theorem 1, the derivative $\frac{dV}{dt}$ is a definite function on the partial region with opposite sign to that of V and the function V itself permits an infinitesimal upper limit, then the undisturbed motion is asymptotically stable on the partial region.

Proof:

Let us suppose that V is a positive definite function on the partial region and that consequently, $\frac{dV}{dt}$ is negative definite. Thus on the intersection Ω_1 of Ω and the

region defined by Eq. (A-4) and $t \geq t_0$ there will be satisfied not only the inequality (Eq.(A-5)), but the following inequality as will:

$$\frac{dV}{dt} \leq -W_1(x_1, \ldots x_n), \tag{A-22}$$

where W_1 is a positive definite function on the partial region independent of t.

Let us consider the quantities x_s as functions of time which satisfy the differential equations of disturbed motion assuming that the initial values $x_{s0} = x_s(t_0)$ of these quantities satisfy the inequalities (Eq. (A-10)). Since the undisturbed motion is stable in any case, the magnitude δ may be selected so small that for all values of $t \geq t_0$ the quantities x_s remain within Ω_1. Then, on the basis of Eq. (A-13) the derivative of function $V(t, x_1(t), \ldots, x_n(t))$ will be negative at all times and, consequently, this function will approach a certain limit, as *t* increases without limit, remaining larger than this limit at all times. We shall show that this limit is equal to some positive quantity different from zero. Then for all values of $t \geq t_0$ the following inequality will be satisfied:

$$V(t, x_1(t), \ldots, x_n(t)) > \alpha \tag{A-23}$$

where $\alpha > 0$.

Since *V* permits an infinitesimal upper limit, it follows from this inequality that

$$\sum_s x_s^2(t) \geq \lambda, \quad (s = 1, \ldots, n), \tag{B.24}$$

where λ is a certain sufficiently small positive number. Indeed, if such a number λ did not exist, that is , if the quantity $\sum_s x_s(t)$ were smaller than any preassigned number no matter how small, then the magnitude $V(t, x_1(t), \ldots, x_n(t))$, as follows from the definition of an infinitesimal upper limit, would also be arbitrarily small,

which contradicts (A-14).

If for all values of $t \geq t_0$ the inequality (Eq. (A-15)) is satisfied, then Eq. (A-13) shows that the following inequality will be satisfied at all times:

$$\frac{dV}{dt} \leq -l_1, \tag{A-25}$$

where l_1 is positive number different from zero which constitutes the precise lower limit of the function $W_1(t, x_1(t), \ldots, x_n(t))$ under condition (Eq. (A-15)). Consequently, for all values of $t \geq t_0$ we shall have:

$$V(t, x_1(t), \ldots, x_n(t)) = V(t_0, x_{10}, \ldots, x_{n0}) + \int_{t_0}^{t} \frac{dV}{dt} dt \leq V(t_0, x_{10}, \ldots, x_{n0}) - l_1(t - t_0),$$

which is, obviously, in contradiction with Eq.(A-14). The contradiction thus obtained shows that the function $V(t, x_1(t), \ldots, x_n(t))$ approached zero as *t* increase without limit. Consequently, the same will be true for the function $W(x_1(t), \ldots, x_n(t))$ as well, from which it follows directly that

$$\lim_{t \to \infty} x_s(t) = 0, \quad (s = 1, \ldots, n), \tag{A-26}$$

which proves the theorem.

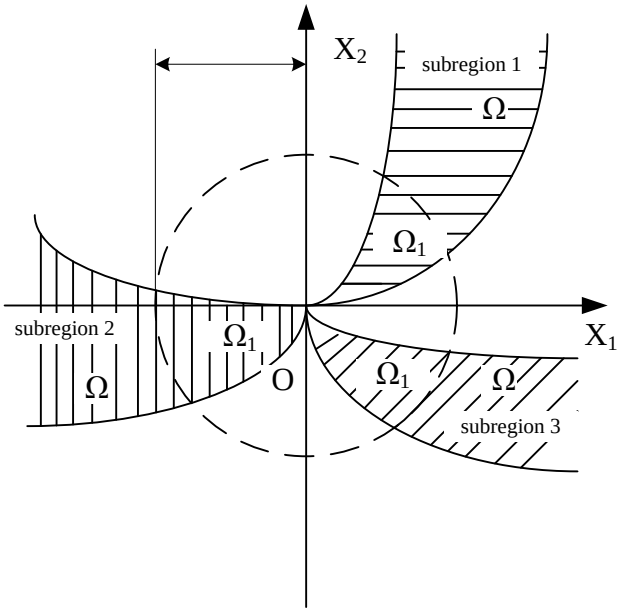

Fig. A.1 Partial regions Ω and Ω_1.

Appendix B

Systems of Positive States

B.1 Three species prey-predator system

The three species prey-predator system which consists of two competing preys and one predator can be described by the following set of nonlinear differential equations:

$$\begin{cases} \dfrac{dx}{dt} = r_1(1-k_1^{-1}x-k_1^{-1}c_2y)-\Phi_1(x,y)z \\ \dfrac{dy}{dt} = r_2(1-k_2^{-1}c_1x-k_2^{-1}y)-\Phi_2(x,y)z \\ \dfrac{dz}{dt} = e_1\Phi_1(x,y)z+e_2\Phi_2(x,y)z-\alpha z \end{cases} \quad \text{(B.1)}$$

where α, r_i, k_i, e_i and c_i, $i=1,2$ are the model parameters assuming only positive values, and the functions $\Phi_i(x,y)$, $i=1,2$ represent the densities of the two prey species and z represents the density of the predator species. The predator z consumes the preys x, y according to the response functions [71]:

$$\Phi_1(x,y)=\frac{a_1x}{1+b_1x+b_2y}, \quad \Phi_2(x,y)=\frac{a_2x}{1+b_1x+b_2y} \quad \text{(B.2)}$$

where a_i, $i=1,2$ are the search rates of a predator for the preys x, y respectively, while $b_i=h_ia_i$, $i=1,2$ where h_i, $i=1,2$ are the expected handing times spent with the preys x, y respectively. The parameters e_1 and e_2 represent, the conversion rates of the preys x, y to predator z. Obviously, when b_1 and b_2 are very small the functional of response Φ_i, ($i=1,2$) become linear response see Volttera functional response [72]. In the other hand as one of both b_1 and b_2 tends to zero the system approaches to hyperbolic Holling type II [73]. The prescribed model characterized by nonlinear response since amount of food consumed by predator per unit time depends upon the available food

sources from the two preys *x* and *y*.

B.2 Double Mackey-Glass systems

We consider two double Mackey-Glass systems which consist of two coupled Mackey-Glass equations [74]:

$$\begin{cases} \dot{x}_1 = \dfrac{bx_{1\tau}}{1+x_{1\tau}^n} - rx_1 \\ \dot{x}_2 = \dfrac{bx_{2\tau}}{1+x_{2\tau}^n} - rx_2 - x_1 \end{cases} \tag{B.3}$$

The system is a model of blood production of patients with leukemia. The variables x_1, x_2 are the concentration of the mature blood cells in the blood, and $x_{1\tau}$, $x_{2\tau}$ are presented the request of the cells which is made after τ seconds, i.e. $x_{i\tau} = x_i(t-\tau), (i=1,2)$. The time delay τ indicates the difference between the time of cellular production in the bone marrow and of the release of mature cells into the blood. According to the observations, the time τ is large in the patients with leukemia and the concentration of the blood cells becomes oscillatory. In this study, the delay time fixed in 20 second ($\tau = 20$) and the parameters are shown as follow: $b = 0.2$, $r = 0.1$, and $n = 10$.

B.3 Energy communication system in biological research

The so-call static state in life sciences means that the system of life is approach to a stable condition. Moreover, the relation of energy communication among the elements in a system of life is called arrangement of static state. The energy communication of elements in a system of life in static state can be divided into two forms:

(1) Independent form:

All the elements in a system of life can communicate energy individually with

other energy systems out of theirs. The mathematics form is as fallow:

$$\begin{cases} \dfrac{du_1}{dt} = -A_1u_1^2 + B_1u_1 + (C_{12} - D_{12}u_1)u_2 - \varphi_1 \\ \dfrac{du_2}{dt} = -A_2u_2^2 + B_2u_2 + (C_{21} - D_{21}u_2)u_1 - \varphi_2 \end{cases} \tag{B.5}$$

where A_i, B_i, C_{ij} and D_{ij} ($i,j=1, 2, \ldots, n$)are parameters, u_1 and u_2 are two different elements in a system of life and φ_1, φ_2 are modified terms. The term $(-A_iu_i^2 + B_iu_i)$ represents the energy communicated with other energy systems, and the term $(C_{ij} - D_{ij}u_i)u_j$ represents the energy communicated with the elements in the system of themselves. As a result, independent form can be $(-A_iu_i^2 + B_iu_i) \neq 0$, ($i=1, 2, \ldots, n$) and $(C_{ij} - D_{ij}u_i)u_j$,($i,j=1, 2, \ldots, n$) are very small in general. If the natural medium is change, such as the lack of food or the limit of living space, $(C_{ij} - D_{ij}u_i)u_j$ may be rising.

(2) Dependent form:

There are two different parts of elements in these systems of life. The first part of elements can communicate energy individually with other energy systems out of theirs. The mathematics form is the same to (Eq. (B.5)). The second part of elements can not communicate energy individually with other energy systems out of theirs, they have to be provided the energy by the first part of elements. The mathematics form is as fallow:

$$\begin{cases} \dfrac{du_i}{dt} = -A_iu_i^2 + B_iu_i + \sum_{j=k+1}^{n}(C_{ij} - D_{ij}u_i)u_j - \varphi_i \\ \dfrac{du_j}{dt} = \sum_{h=1}^{m_j}(C_{jh} - D_{jh}u_j)u_h - \varphi_j \end{cases} \tag{B.6}$$

$(i \in k, j \in n-k)$

where k represents the number of the first part elements and m_j represents the number

of the second part elements.

In further studies, the system of food chain with three states can be described by the mathematical model as follow:

$$\begin{cases} \dfrac{du_1}{dt} = A_1 u_1^2 + B_1 u_1 + (C_{12} - D_{12} u_1) u_2 - \varphi_1 \\ \dfrac{du_2}{dt} = (C_{21} - D_{21} u_2) u_1 + (C_{23} - D_{23} u_2) u_3 - \varphi_2 \\ \dfrac{du_3}{dt} = (C_{32} - D_{32} u_3) u_2 - \varphi_3 \end{cases} \tag{B.7}$$

B.4 Virus-immune system

A mathematical model of the virus-immune system consisting of the following three nonlinear differential equations is considered in this study:

$$\begin{cases} \dfrac{dT}{dt} = s - \mu_1 T + rT\left[1 - \dfrac{T+I}{\Gamma}\right] - kVT \\ \dfrac{dI}{dt} = kVT - \mu_2 I \\ \dfrac{dV}{dt} = \mu_3 NI - k\,V\,T - \mu_4 V \end{cases} \tag{B.5}$$

where T, I and V represent the population concentrations of uninfected, infected target cells and virus respectively. We denote by the s constant supply of target cells from its precursor. These cells have a finite life time and μ_1 represents the average death rates of these cells. These target cells are assumed to grow logistically with specific growth rate r and carrying capacity Γ. In the presence of virus, the target cells become infected. Since virus must meet the cells in order to infect them, a mass action term is used to model infection with k as the infection rate. μ_2 denote the natural death rate of infected cells. All infected cells are assumed to be capable of producing virus. It is assumed that N virion are released by each infected cell during its lifetime. μ_3 represents the death rate of infected cells due to lysis. μ_4 is the death rate of free virus.

Appendix C

Pragmatical Asymptotical Stability Theory

The stability for many problems in real dynamical systems is actual asymptotical stability, although may not be mathematical asymptotical stability. The mathematical asymptotical stability demands that trajectories from all initial states in the neighborhood of zero solution must approach the origin as $t \to \infty$. If there are only a small part or even a few of the initial states from which the trajectories do not approach the origin as $t \to \infty$, the zero solution is not mathematically asymptotically stable. However, when the probability of occurrence of an event is zero, it means the event does not occur actually. If the probability of occurrence of the event that the trajectries from the initial states are that they do not approach zero when $t \to \infty$, is zero, the stability of zero solution is actual asymptotical stability though it is not mathematical asymptotical stability. In order to analyze the asymptotical stability of the equilibrium point of such systems, the pragmatical asymptotical stability theorem is used.

Let X and Y be two manifolds of dimensions m and n ($m<n$), respectively, and φ be a differentiable map from X to Y, then $\varphi(X)$ is subset of Lebesque measure 0 of Y [75]. For an autonomous system

$$\frac{dx}{dt} = f(x_1, \cdots, x_n) \tag{A-1}$$

where $x = [x_1, \cdots, x_n]^T$ is a state vector, the function $f = [f_1, \cdots, f_n]^T$ is defined on $D \subset R^n$ and $\|x\| \le H > 0$. Let x=0 be an equilibrium point for the system (A-1). Then

$$f(0) = 0 \tag{A-2}$$

For a nonautonomous systems,

$$\dot{x} = f(x_1, ..., x_{n+1}) \tag{A-3}$$

where $x = [x_1, ..., x_{n+1}]^T$, the function $f = [f_1, ..., f_n]^T$ is define on $D \subset R^n \times R_+$,here $t = x_{n+1} \subset R_+$. The equilibrium point is

$$f(0 x_{n+1} \ni \quad . \tag{A-4}$$

Definition The equilibrium point for the system (A-1) is pragmatically asymptotically stable provided that with initial points on *C* which is a subset of Lebesque measure 0 of *D*, the behaviors of the corresponding trajectories cannot be determined, while with initial points on $D-C$, the corresponding trajectories behave as that agree with traditional asymptotical stability [76, 77].

Theorem Let $V = [x_1, \cdots, x_n]^T : D \rightarrow R_+$ be positive definite and analytic on *D*, where $x_1, x_2, ..., x_n$ are all space coordinates such that the derivative of *V* through Eq. (A-1)or(A-3), $\dot{V}$, is negative semi-definite of $[x_1, x_2, \cdots, x_n]^T$.

For autonomous system, Let *X* be the m-manifold consisted of point set for which $\forall x \neq 0$, $\dot{V}(x) = 0$ and *D* is a n-manifold. If *m*+1<*n*, then the equilibrium point of the system is pragmatically asymptotically stable.

For nonautonomous system, let X be the $m+1$-manifold consisting of point set of which $\forall x \neq 0, \dot{V}(x_1, x_2, ..., x_n) = 0$ and D is $n+1$-manifold. If $m+1+1 < n+1$, i.e. $m+1 < n$ then the equilibrium point of the system is pragmatically asymptotically stable. Therefore, for both autonomous and nonautonomous system the formula $m+1 < n$ is universal. So the following proof is only for autonomous system. The proof for nonautonomous system is similar.

Proof Since every point of *X* can be passed by a trajectory of Eq. (A-1), which

is one- dimensional, the collection of these trajectories, *A*, is a (*m*+1)-manifold [76, 77].

If $m+1 < n$, then the collection *C* is a subset of Lebesque measure 0 of *D*. By the above definition, the equilibrium point of the system is pragmatically asymptotically stable.

If an initial point is ergodicly chosen in *D*, *the probability of that the initial point falls on the collection C is zero. Here, equal probability is assumed for every point chosen as an initial point in the neighborhood of the equilibrium point.* Hence, the event that the initial point is chosen from collection *C does not occur actually*. Therefore, under the equal probability assumption, pragmatical asymptotical stability becomes actual asymptotical stability. When the initial point falls on $D-C$, $\dot{V}(x) < 0$, the corresponding trajectories behave as that agree with traditional asymptotical stability because by the existence and uniqueness of the solution of initial-value problem, these trajectories never meet *C*.

In Eq. *V* is a positive definite function of *n* variables, i.e. *p* error state variables and *n*-*p*=*m* differences between unknown and estimated parameters, while $\dot{V} = e^T Ce$ is a negative semi-definite function of *n* variables. Since the number of error state variables is always more than one, *p*>1, *m*+1<*n* is always satisfied, by pragmatical asymptotical stability theorem we have

$$\lim_{t\to\infty} e = 0 \qquad \text{(A-5)}$$

and the estimated parameters approach the uncertain parameters. The pragmatical adaptive control theorem is obtained. Therefore, the equilibrium point of the system is pragmatically asymptotically stable. Under the equal probability assumption, it is actually asymptotically stable for both error state variables and parameter variables.

References

1. Moon F. C., *Chaotic Vibrations： An Introduction for Applied for Scientists and Engineer*, Wiley, New York, 2004.
2. Thompson J. M. T. and Stewart H. B., *Nonlinear Dynamics and Chaos* ,2nd edition, New York Wiley, 2002.
3. Brockett T. W. ,“On Conditions Leading to Chaos in Feedback System”, Proc. IEEE 21st conf. Decision and Control, (1982)932.
4. Holems P. ,“Bifurcation and Chaos is a Simple Feedback Control System”, proc. IEEE 22st conf. Decision and Control, (1983) 365.
5. Huber A.W., “Adaptive control of chaotic system”, Helv Acta, 62 (1989) 343.
6. Fuh C.C. and Tung P.C., ‘‘Controlling chaos using differential geometric method’’, Phys Rev Lett **75** (1995) 2952.
7. Ge Z.-M. and Cheng, J.-W., ‘‘Chaos synchronization and parameter identification of three time scales brushless DC motor system’’, Chaos, Solitons and Fractals 24 (2005) 597-616.
8. Ge Z.-M. and Chen C.-C., ‘‘Phase Synchronization of Coupled Chaotic Multiple Time Scales Systems’’, Chaos, Solitons and Fractals 20 (2004) 639-647.
9. Ge Z.-M. and, Cheng, J.-W., ‘‘Chaos synchronization and parameter identification of three time scales brushless DC motor system’’, Chaos, Solitons and Fractals 24 (2005) 597-616.
10. Huang L.-L., Feng R.-P. and Wang M., “Synchronization of chaotic systems via nonlinear control”, Phys Lett A 320(4) (2004) 271.
11. Shahverdiev E.M., Sivaprakasam S. and Shore K.A., “Lag synchronization in time-delayed systems”, Phys Lett A 292 (2002) 320.
12. Li Guo-Hui and Zhou Shi-Ping, “An observer-based anti-synchronization”,

Chaos, Solitons and Fractals 29 (2006) 495.

13. Chen H.-K. and Sheu L.-J., “The transient ladder synchronization of chaotic systems”, Phys Lett A 355 (2006) 207.
14. Chen G., Dong X., *From chaos to order: methodologies, perspectives and applications*, Singapore: World Scientific; 1998.
15. Chen G., Dong X. , ‘‘On feedback control of chaotic continuous time systems’’, IEEE Trans Circ Syst I, (1993) 591.
16. Yassen M.T., “Chaos synchronization between two different chaotic system using active control”, Chaos, Solitons & Fractals **23** (2005) 131.
17. Keiji K., Michio H., Hideki K., ‘‘Sliding mode control for a class of chaotic systems’’, Phys Lett A, 245 (1998) 511.
18. Fuh C., Tung, P., ‘‘Robust control for a class of nonlinear oscillators with chaotic attractors’’, Phys Lett A, 218 (1996) 240.
19. Yu Y., Zhang, S., ‘‘Controlling uncertain Lu system using backstepping design’’, Chaos, Solitons and Fractals, 15 (2003) 897.
20. Moez F., ‘‘An adaptive feedback control of linearizable chaotic systems’’, Chaos, Solitons & Fractals, 15 (2003) 883.
21. Ge Z.-M., Leu W.-Y. ,“Anti-control of chaos of two-degrees-of- freedom louderspeaker system and chaos synchronization of different order systems”, Chaos, Solitons and Fractals 20 (2004) 503.
22. Tang Fang, Wang Ling, “An adaptive active control for the modified Chua’s circuit”, Physics Letters A, 346 (2005) 342.
23. Kapitaniak T. , “Continuous control and synchronization in chaotic systems”, Chaos Solitons Fractals 6 (3) (1995) 237.
24. Femat R. and Perales G. S., “On the chaos synchronization phenomenon”, Phys Lett A 262(1999)50.

25. Lu J., Wu X., Lu J. , “Synchronization of a unified chaotic system and the application in secure communication”, Phys Lett A 305 (2002)365.
26. Han S.K., Kurrer C., Kuramoto Y., “Dephasing and bursting in coupled neural oscillators”, Phys. Rev. Lett. 75 (1995) 3190.
27. Blasius B., Huppert A., Stone L., “Complex dynamics and phase synchronization in spatially extended ecological systems”, Nature 399 (1999) 354.
28. Wang C. and Ge S. S., “Adaptive synchronization of uncertain chaotic systems via backstepping design”, Chaos, Solitons and Fractals, 12, pp. 1199-1206, 2001.
29. Femat R., Ramirez J. A. and Anaya G. F., “Adaptive synchronization of high-order chaotic systems: A feedback with low-order parameterization”, Physica D, 139, pp. 231-246, 2000.
30. Mei Sun, Lixin Tian and Shumin Jiang, Jun Xu , “Feedback control and adaptive control of the energy resource chaotic system”, Chaos, Solitons and Fractals, pp. 1725-1734, 2007.
31. Femat R. and Perales G. S., “On the chaos synchronization phenomenon”, Phys., letters A,262, pp. 50-60, 1999.
32. Abarbaned H. D. I., Rulkov, N. F. and Sushchik, M. M., “Generalized synchronization of chaos: The auxiliary systems”, Phy. Rev E,53, pp. 4528-4535, 1996.
33. Yang S. S. and Duan, C. K., “Generalized synchronization in chaotic systems”, Chaos, Solitons and Fractals, 9, pp. 1703-1707, 1998.
34. Yang X. S., “Concepts of synchronization in dynamic systems”, Phys., letters A, 260, pp. 340-344, 1999.
35. Smith Richard J., *Fathoming the Cosmos and Ordering the World: The Yijing (I Ching or Classic of Changes) and Its Evolution in China.* University of Virginia Press. ISBN 978-0813927053 , 2008.
36. Karcher Stephen, *I Ching: The Classic Chinese Oracle of Change: The First*

Complete Translation with Concordance. London: Vega Books. ISBN 1-84333-003-2, 2002.

37. Marshall S. J., *The Mandate of Heaven: Hidden History in the I Ching*. Columbia University Press, ISBN 0-231-12299-3, 2001.
38. Rössler O.E., "An equation for hyperchaos ", Physics Letters A, 71 (1979) 155.
39. Letellier C., Dutertre P. & Maheu B., "Unstable periodic orbits and templates of the Rössler system: toward a systematic topological characterization", *Chaos*, (1995) , 5 (1), 271.
40. Gilmore R., Lefranc M., *The topology of chaos*, Wiley, (2002).
41. Ge Z.-M. and Li Shih-Yu "Yin Chaos" submitted to Journal of Computational and Applied Mathematics. (SCI, Impact Factor: 0.943)
42. Ge Z.-M., Yao C.-W., Chen H.-K., "Stability on partial region in dynamics", Journal of Chinese Society of Mechanical Engineer 15 (1994) 140.
43. Ge Z.-M., Chen H.-K., "Three asymptotical stability theorems on partial region with applications", Japanse Journal of Applied Physics 37 (1998) 2762.
44. Ge Z.-M., "Necessary and sufficient conditions for the stability of a sleeping top described by three forms of dynamic equations" Phys. Rev. E77 (2008) 046606 .
45. Rössler O.E., "An equation for hyperchaos ", Physics Letters A, 71 (1979) 155.
46. Matsumoto T., Chua L.O., Kobaiashi K., "Hyperchaos: Laboratory experiments and numerical confirmation", IEEE Trans. Circuits Syst. CAS-33, (1986) 1143.
47. Thamilmaran K., Lakshmanan M., Venkatesan A. " Hyperchaos in a modified canonical Chua's circuit", Int. J. Bifurcation and Chaos,14 (2004) 221.
48. Li Y., Tang W.K.S., Chen G., "Generating hyperchaos via state feedback control", Int. J. Bifurcation and Chaos,15 (2005) 3367.
49. Barboza R., "Dynamics of a hyperchaotic Lorenz system", Int. J. Bifurcation and Chaos,Vol.17 No.12 (2007) 4285.

50. Elabbasy E.M., Agiza, H.N., El-Dessoky, M.M., “Adaptive synchronization of a hyperchaotic system with uncertain parameter Chaos”, Chaos, Solitons & Fractals, 30, PP 1133-1142, 2006.
51. Wang Y.W., Wen C., Soh Y. C., Xiao, J.W., “Adaptive control and synchronization for a class of nonlinear chaotic systems using partial system states”, Physics Letters A, 351, 79, 2006.
52. Fotsin H., Bowong Samuel., “Adaptive control and synchronization of chaotic systems consisting of Van der Pol oscillators coupled to linear oscillators”, Chaos, Solitons & Fractals, 27, PP 822-835, 2006.
53. Lu J., Wu X., Han X., Lu J., “Adaptive feedback synchronization of a unified chaotic system”, Physics Letters A, 329, PP 327-333, 2004.
54. Ge Z.-M and Yang C.-H., “Pragmatical generalized synchronization of chaotic systems with uncertain parameters by adaptive control”, Physica D: Nonlinear Phenomena 231(2) , 87-94, 2007.
55. Ge Z.-M, Li S.-C., Li S.-Y. and Chang C.-M., “Pragmatical adaptive chaos control from a new double van der Pol system to a new double Duffing system”, Applied Mathematics and Computation, In Press, Available online, 2008.
56. Minorsky N., Nonlinear oscillations Van Nostrand Princeton NJ (1962).
57. Ge Z.-M. and Chang C.-M.,”Chaos synchronization and parameters identification of single time scale brushless DC motors”, Chaos, Solitons and Fractals 20, pp. 883-903, 2004.
58. Ge Z.-M. and Chen C.-C. ”Phase synchronization of coupled chaotic multiple time scales systems”, Chaos, Solitons and Fractals 20, pp. 639-647, 2004.
59. Ge Z.-M. and Leu W.-Y., “Chaos synchronization and parameter identification for identical system”, Chaos, Solitons and Fractals, 21, pp.1231-1247, 2004.
60. Ge Z.-M. Ge and Le W.-Y., “Anti-control of chaos of two-degrees-of- freedom

louderspeaker system and chaos synchronization of different order systems", Chaos, Solitons and Fractals 20, pp. 503-521, 2004.

61. Ge Z.-M. and Yang C.-H., "Pragmatical generalized synchronization of chaotic systems with uncertain parameters by adaptive control", Physica D 231 , pp. 87-94, 2007.
62. Liu F., Ren Y., Shan X., Qiu Z., "A linear feedback synchronization theorem for a class of chaotic systems", Chaos, Solitons and Fractals, 13(4), pp. 723-730, 2002.
63. Krawiecki A and Sukiennicki A., "Generalizations of the concept of marginal synchronization of chaos", Chaos, Solitons and Fractals, 11(9), pp. 1445–1458, 2000.
64. Yang X.-S. and Chen, G. , "Some observer-based criteria for discrete-time generalized chaos synchronization", Chaos, Solitons and Fractals, 13, pp. 1303-1308, 2002.
65. Terry J. R., VanWiggeren G. D. , "Chaotic communication using generalized synchronization", Chaos, Solitons and Fractals, 12, pp. 145-152, 2001.
66. Ge Z.-M. and Yang, C.-H., "Synchronization of complex chaotic systems in series expansion form," accepted by Chaos, Solitons, and Fractals, 2006.
67. Ge Z.-M., Yang C.-H., Chen H.-H., and Lee S.-C., "Non-linear dynamics and chaos control of a physical pendulum with vibrating and rotation support" , Journal of Sound and Vibration, 242 (2), pp.247-264, 2001.
68. Lü J., Zhou T., Zhang S., "Chaos synchronization between linearly coupled chaotic systems", Chaos, Solitons and Fractals, 14(4), pp. 529-541, 2002.
69. Lu J. and Xi Y., "Linear generalized synchronization of continuous-time chaotic systems", Chaos, Solitons and Fractals, 17, pp. 825-831, 2003.
70. Tam LM, SiTou WM., "Parametric study of the fractional order Chen–Lee

System", Chaos, Solitons & Fractals, 37,817–26, 2008.

71. Kuang Y., "Basic properties of mathematical population models", Biomathematics ,17 ,pp129-142, 2002.
72. EI-Gohary A. and Yassen M., "Optimal control and synchronization of Lotka-Volterra model", Chaos, Solitions & Fractals, 12, pp2087-2093, 2001.
73. Sugie J. and Katayama M., "Global asymptotic stability of a predator-prey system of Holling type", Nonlinear Analysis 160 ,pp105-121, 1999.
74. Mackey M. C. and Glass L., "Oscillation and chaos in physiological control systems", Science 197(4300), pp287-289,1977.
75. Atsushima Y.M., *Differentiable Manifolds,* Marcel Dekker, City, 1972.
76. Ge Z.-M., Yu J.K. and Chen Y.T., "Pragmatical asymptotical stability theorem with application to satellite system", Jpn. J. Appl. Phys.,38 (1999) 6178.
77. Ge Z.-M. and Yu J. K., "Pragmatical asymptotical stability theorem partial region and for partial variable with applications to gyroscopic systems", The Chinese Journal of Mechanics, 16 (2000) 179.